

00140001-16

IRF--213

**Auroral Tomography Workshop
Proceedings**

edited by
Åke Steen

IRF Scientific Report 213
August 1993

ISSN 0284-1703

INSTITUTET FÖR RYMDFYSIK
Swedish Institute of Space Physics

Kiruna, Sweden

**Proceedings
of the
Auroral Tomography Workshop**

Kiruna, Sweden, March 9-11, 1993

edited by

Åke Steen

*Swedish Institute of Space Physics
P.O. Box 812, S-981 28 Kiruna, Sweden*

IRF Scientific Report 213
August 1993

Printed in Sweden
Swedish Institute of Space Physics
Kiruna 1993
ISSN 0284-1703

WORKSHOP PROCEEDINGS

TABLE OF CONTENTS

Preface	v
Workshop Program	vii
Maximum entropy methods for reconstructing physical distributions <i>T. Oscarsson</i>	1
Experimental physics inverse problems at the P.L. Kapitza Institute for Physical Problems <i>E.L. Kosarev</i>	3
Report on the ALIS-project <i>U. Brändström, and Å. Steen</i>	5
Plans for auroral tomography in Finland <i>K. Kaila</i>	7
A study of feasible tomographic inversion techniques for ALIS <i>B. Gustavsson</i>	11
Studies of natural and artificial irregularities in the near space by optic tomography methods <i>V.V. Alpatov</i>	13
A note on the computed auroral tomography by the MART method <i>T. Aso, K. Muguruina, T. Yabu, T. Hashimoto, M. Abe, and M. Ejiri</i> (paper presented by B. Gustavsson)	23
Informational analysis of auroral tomograph <i>V.V. Alpatov, V.V. Pickalov, and A.V. Lihachov</i>	35
Imaging ionospheric electron density with tomographic techniques <i>G. Fehmers</i>	47
Software for deconvolution recovery and its application <i>E.L. Kosarev</i> (no manuscript received)	
Spectrotomography - a new method of studying the internal structure of the polychromatic objects <i>G.G. Levin, F.V. Bulygin, and V.V. Alpatov</i>	49
Test of auroral tomography methods for the ALIS project <i>V.S. Davydov, and V.V. Pivovarov</i> (presented by S. Chernouss)	59
Possibilities of calibration of auroral tomography methods by direct rocket measurements <i>V.S. Davydov, V.V. Pivovarov, and S.A. Chernouss</i>	63
Feasibility study of ionospheric tomography with radio telescopes <i>G. Fehmers</i>	69
Prospects for 3-D visualisation <i>Å. Steen</i>	81
Aurora as a subject of tomography <i>V. Tagirov</i> (no manuscript received)	
Tomography reconstruction of a 3-D auroral luminosity distribution <i>M.I. Pudovkin, V.N. Troyan, and G.A. Ryzhikov</i>	83
LIST OF PARTICIPANTS AND ADDRESSES	103

Preface

In ionospheric and atmospheric physics the importance of multi-station imaging has grown as a consequence of the availability of scientific grade CCD cameras with digital output and affordable massive computing power. Tomographic inversion techniques are used in many different areas, e.g. medicine, plasma research and space physics. The tomography workshop was announced to gather a limited group of people interested in auroral tomography or tomographic inversion methods in general.

ALIS (Auroral Large Imaging System) is a multi-station ground-based system developed primarily for three-dimensional auroral imaging, however other non-auroral objects can be studied with ALIS, e.g. stratospheric clouds. Several of the contributions in the workshop dealt with problems related to geometries similar to the ALIS-configuration.

The workshop started on Tuesday noon, March 9, and ended Thursday noon, March 11, 1993. The workshop was attended by 14 persons and 17 papers were presented in oral form. A few of the papers were presented by colleagues of the author(s) since some of the registered participants could not make it to Kiruna due to difficulties with the travel arrangements.

The Proceedings contain written contributions received either in abstract form or as full papers. The Proceedings also contain contributions intended for the Workshop but not presented due to the absence of the speaker.

The organising committee at IRF sincerely expresses its gratitude to the meeting participants and to the authors for their contributions. We hope that this type of workshop can be repeated in the future, perhaps when ALIS starts to produce scientific data.

Kiruna, August, 1993

Åke Steen

FINAL PROGRAM TOMOGRAPHY WORKSHOP

KIRUNA, SWEDEN, MARCH 9-11, 1993

Tuesday March 9

- 1300 **OPENING OF WORKSHOP**
Åke Steen
Introduction
- 1315 - 1400 **Tord Oscarsson**
Maximum entropy methods for reconstructing physical distributions
- 1400 - 1445 **Evgeny Kosarev**
Experimental physics inverse problems at the P. I. Kapitza Institute for Physical Problems
- 1445 - 1515 **Urban Brändström**
Report on the ALIS project
- 1515 - 1545 **COFFEE BREAK**
coffee is served at the Optical Lab.
- 1545 - 1630 **Kari Kalla**
Preparations to auroral tomography in Finland
- 1630 - 1700 **Björn Gustavsson**
A study of tomography methods for ALIS
- 1900 **GET-ACQUAINTED-BEER-PARTY**
(IRT lunch room)

Wednesday March 10

- 0900 - 0940 **Victor Alpatov**
Studies of natural and artificial irregularities in the near space by optical tomography methods
- 0940 - 1010 **Takehiko Aso**
(presented by B. Gustavsson)
A note on the computed auroral tomography by the MARI method
- 1010 - 1040 **COFFEE BREAK**
- 1040 - 1120 **Victor Alpatov**
Synchrotronography - a new method of studying the internal structure of the polychromatic objects
- 1120 - 1200 **Gijs Fehmers**
Mapping ionospheric electron density using tomographic techniques
- 1200 - 1400 **LUNCH**
- 1400 - 1445 **Evgeny Kosarev**
Software for deconvolution recovery and its applications
- 1445 - 1515 **COFFEE BREAK**
- 1515 - 1600 **Victor Alpatov**
Information analysis in creating of auroral tomography
- 1600 - 1630 **Vladimir Pivovarov**
(presented by S. Chernouss)
Test of auroral tomography methods for the ALIS project
- 1630 - 1700 **Sergey Chernouss**
Possibilities of calibration of auroral tomography methods by direct rocket measurements
- 1900 **DINNER** (IRT lunch room)

Thursday March 11

- 0900 - 0930 **Gijs Fehmers**
Feasibility study of ionospheric tomography with radio telescopes
- 0930 - 1000 **COFFEE BREAK**
- 1000 - 1030 **Åke Steen**
Prospects for 3-D visualisation
- 1030 - 1100 **Vartan Tagirov**
Aurora as a subject of tomography
- 1100 - 1200 **Conclusions**
- 1200 **END OF WORKSHOP**

Maximum Entropy methods for reconstructing physical distributions

TORD OSCARSSON

Swedish Institute of Space Physics, University of Umeå, Umeå, Sweden

Abstract

The use of Maximum-Entropy methods for resolving underdetermined inverse problems is discussed. In particular, we study regularization of ill-posed problems involving distributions with unknown normalization, which is the case relevant to auroral tomography. A generalized entropy functional is introduced, which automatically takes into account unknown normalization. To demonstrate that our entropy functional is a useful tool, we present a newly developed method for reconstructing wave distribution functions in space plasmas. Our method is based on the generalized entropy functional, and employs χ^2 -statistics to define a set of feasible solutions. Applications to synthetic and real satellite data are presented.

References

Oscarsson, T. E., Dual principles in Maximum Entropy Reconstruction of the Wave Distribution Function, *subm. to J. Comput. Phys.*, 1992.

Experimental Physics Inverse Problems at the P.L.Kapitza Institute for Physical Problems

E.L.Kosarev
Moscow 117334, Russia *

Abstract

This is essentially a publication list with short comments to some publications.

The papers [1-3] are concerned with the Abel integral equation to plasma diagnostics, physical electronics and astronomy. The paper [4] is a review paper. The optimal Wiener filtering of 'noisy' data, developed in paper [5], could be also applied to data compression. Maximum likelihood approach to soft X-ray detectors is described in paper [6]. Papers [7-8] are devoted to fundamental limit in signal restoration based on the Shannon theorem from information theory. Papers [9-10] are detailed description of the RECOVERY package for deconvolution.

Applications of the RECOVERY are expanding to photo-electron spectroscopy, X-ray powder diffractometry, 1D and 2D X-ray detectors, digital angiography with synchrotron radiation, different kind of tomography, including optical, X-ray, NMR and neutron tomography.

References

- [1] E.L.Kosarev. The numerical solution of Abel's integral equation *USSR Computational Mathematics and Mathematical Physics*, v.13, No.6, pp.271-277, 1973
- [2] E.L.Kosarev. The measurements of the cathod losses in microtron *Zh. Tech. Phys.*, v.42, No.4, pp.841-843, 1972 (in Russian)
- [3] E.L.Kosarev. A new method for recovering the space distribution of globular-cluster stars, applied to flare stars in the Pleades *Sov.Astron.Lett.*, v.6 (4), pp.226-229, 1980

*E-mail: kosarev @ magnit.msk.su

- [4] E.L.Kosarev. Application of integral equations of the first kind in experimental physics *Computer Physics Communications*, v.20, No.1, pp.69-75, 1980
- [5] E.L.Kosarev and E.Pantos. Optimal smoothing of 'noisy' data by fast Fourier transform *J.Phys. E: Sci.Instrum.*, v.16, pp.537-543, 1983
- [6] E.L.Kosarev, V.D.Peskov and E.R.Podolyak. High resolution soft X-ray spectrum reconstruction by MWPC attenuation measurements *Nucl.Instrum. and Methods*, v.208, pp.637-645, 1983
- [7] E.L.Kosarev. Superresolution limit for signal recovery *J.Skilling (ed.), Maximum Entropy and Bayesian Methods*, pp.475-480, Kluwer Academic Publishers, Dordrecht, 1989
- [8] E.L.Kosarev. Shanon's superresolution limit for signal recovery *Inverse Problems*, v.6, pp.55-76, 1990
- [9] V.I.Gelfgat, E.L.Kosarev, E.R.Podolyak. Programs for signal recovery from noisy data using the maximum likelihood principle. I. General description. *Computer Physics Communications*, v.74, No.3, pp.335-348, 1993
- [10] V.I.Gelfgat, E.L.Kosarev, E.R.Podolyak. Programs for signal recovery from noisy data using the maximum likelihood principle. II. Program implementation. *Computer Physics Communications*, v.74, No.3, pp.349-357, 1993

REPORT ON THE ALIS PROJECT

Urban Brändström
and
Åke Steen
Swedish Institute of Space Physics
Box 812, S-981 28 Kiruna, Sweden

ABSTRACT

In northern Scandinavia, a new multi-station technique for ground-based auroral imaging measurements is developed. ALIS (*Auroral Large Imaging System*) is based on modern CCD imaging technology, powerful computers and high-speed data transfer. The aurora is simultaneously imaged from 14 stations in the northern part of Sweden (Swe-ALIS). It is proposed that ALIS is expanded into the surrounding countries: Norway, Finland and Russia so that the total coverage is increased. The stations are synchronised by GPS-clocks, and record image data with moderate FoV, 60 degrees. The distances between the stations are on the average 50km which is used to apply tomographic inversion methods by using the overlapping fields of view. For discrete auroral structures a three-dimensional estimate of the auroral signal can be derived. The complete system is controlled and operated from a Control Centre (CC). At CC experimental files can be written and transferred to the computers in the stations. The station computers is responsible for operating the imager(s) and sending alarms to CC if something unexpected happens in the unmanned measurement houses. The first auroral data from ALIS will be available in the fall of 1992. The principles of operations is illustrated by simulated data.

Plans for auroral tomography in Finland

Kari Kaila

University of Oulu, Department of Physics
SF-90570 Oulu, Finland

Abstract

It is the aim of the Department of Physics, University of Oulu to get three manned optical stations with a high quality photometer and TV-camera in operation within a couple of years. Automatic measurements of high temporal resolution will be made during several winter months. Some coordinated campaigns with radar and other instruments will be made. Such measurements will be the input data to the auroral model, from which several emissions and other ionospheric parameters can be derived. The same parameters will be measured in an independent way and the results are compared to get a better understanding of the ionospheric response to precipitating particle fluxes.

The present situation

Optical instruments used for auroral research in Finland are 4-5 all-sky cameras, 3 photometers, a spectrometer and a TV-camera. The temporal resolution of the all-sky camera is of the order of a minute and for the other instruments it is a fraction of a second. In principle, the data of these cameras could be used for tomographic determination of auroras. However, the data has mainly been used for 2- and 3-dimensional mapping of auroral positions over Scandinavia. The TV-camera has been used in combination with a photometer and the data has been used for determination of the energy of auroral particles. A new photometer is now under construction.

Future plans

It is planned to dismantle the old all-sky cameras, which take pictures on color films. The instruments are 20 years old and it is more and more difficult and expensive to obtain film for them. New CCD-based all-sky cameras are being designed at the Finnish Meteorological Institute, Helsinki and they will replace the old cameras within a couple of years. The new cameras will operate in the same principle as the old cameras. They will store a frame in a minute or so.

Our plan at the University of Oulu is to have three high quality scanning photometers and CCD-cameras along a line (maybe from Muonio to Kilpisjärvi) to make measurements of auroras automatically during several winter months (Fig 1.). The chain will continue to Ramfjordmoen, to the EISCAT transmitter site. These optical stations will give data of good quality for tomographic inversion. The photometers give data at 3-5 different wavelengths with a high dynamic range. The cameras are used to identify the auroral activity and weather condition.

Optical stations

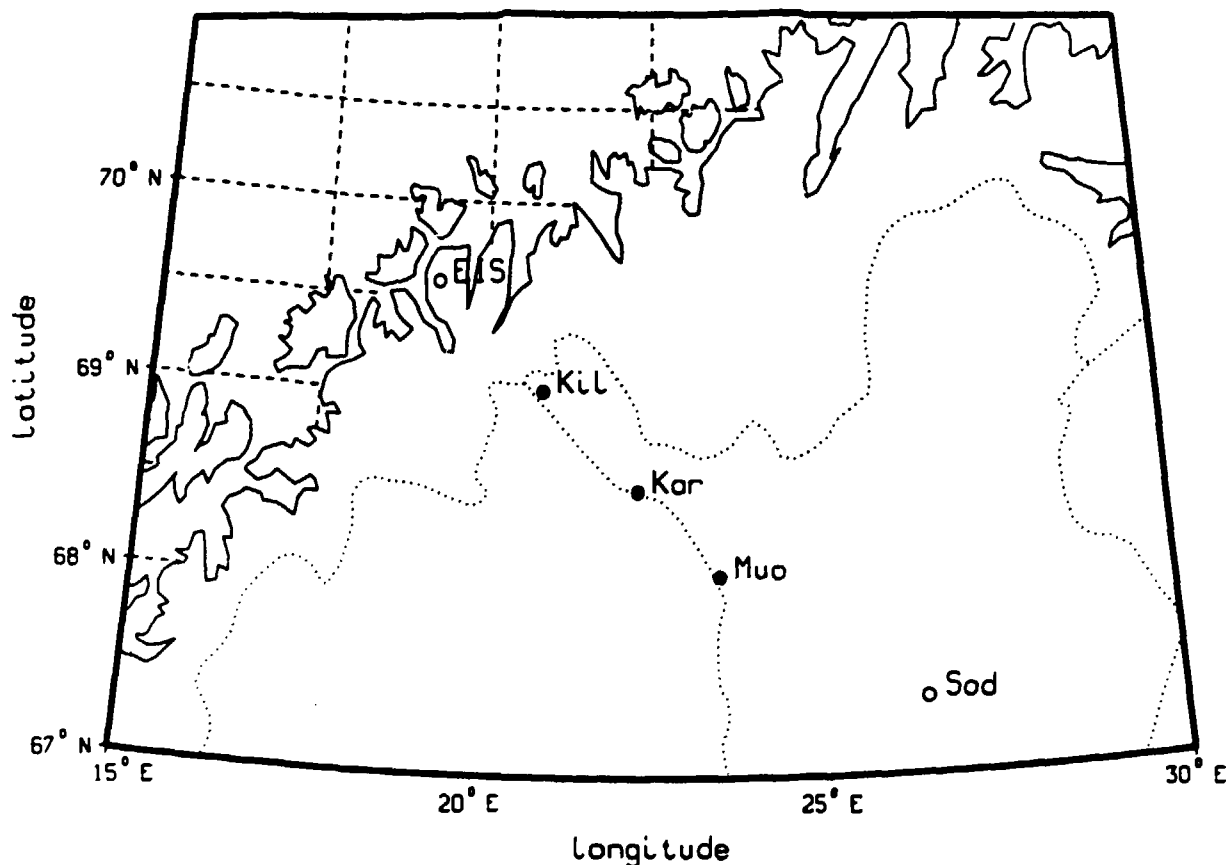


Fig 1. The locations of three optical stations (filled circles) as compared with EISCAT station and Sodankylä Observatory (open circles). Each station will have a multichannel photometer and a CCD-camera.

Two multichannel photometers have been built so far. The first device dependent photometer was built in 1984-86. It has 5 parallel channels and it can measure with a sampling rate of 10 Hz. It has both scanning and filter tilting capability. New technologies are now available and this photometer will be modernized within a year. The next generation photometer is a modular and device independent one. It can have 1-5 channels and it can measure up to 50 Hz. The size of the photometer has also been reduced. All these photometers use narrow band (1 nm) interference filters which can be tilted for the background measurements. Every photometer will have a scanning system with the absolute angle encoder. The data will be collected by a counter card, which is located inside PC. The fields of view will be of the order of 1 degree, but it can be easily changed. The scanning

speed may be selected from 60s/180° to 5s/180°. The timing will be made by the satellite clock GPS. The photometers will be very automatic, because program can read the start and stop times and the measurement parameters from premade files. Also different photometers can run synchronously according to the measurement files. It is possible to select different integration times for different channels.

It is somewhat difficult to align the photometers in the same meridian plane but it can be made by using the star locations. It is also difficult to synchronize the measurements at several stations. To avoid these difficulties one could use monochromatic CCD-cameras. They have some advantages and some disadvantages when compared to the photometers. TV-cameras cover a wide field at a time and they are easily mounted. The data flow in images is huge as compared to photometer measurements if the cameras take several frames/minute and if the auroral images are stored with a wide dynamical range.

Future aims

We have made some combined high temporal resolution optical and EISCAT measurements. The very bad statistics for clear weather in Tromso makes it difficult to make simultaneous optical measurements with EISCAT radar during clear night sky and auroral activity. That is a reason, why we try to make automatic measurements over a long time interval. We have modelled electron densities based optical measurements and compared them with radar measurements. It seems that the emission ratios for estimating the energy of auroral electrons must be applied carefully. The auroral emissions should be modelled better. The auroral tomography at several wavelengths could be an answer to some problems. Without tomographic inversion the thicknesses, horizontal and vertical profiles of auroral emissions are very uncertain. If they are known, the electron energy and electron density profiles can be estimated. More reliable emission ratios could also be found.

An extended model of auroral parameters has been made at the University of Alaska. This "Auroral model" has been improved at the University of Southampton. This will be tested in a 2-dimensional plane, where the photometric measurements are made. The 2-dimensional tomographic measurements of N⁺ emissions will give the 2-dimensional electron flux data. It can be transformed to the ionization rate profiles. By radar measurements these profiles can be checked and corrected. By using the Auroral model, several emissions and other auroral parameters can be calculated. These values can be compared with direct measurements by photometer and/or spectrometer.

A STUDY OF FEASIBLE TOMOGRAPHIC INVERSION TECHNIQUES FOR ALIS

Björn Gustavsson¹⁾

Institutet för rymdfysik, Box 812, S-981 28 Kiruna, Sweden

ALIS (Auroral Large Imaging System) is a ground-based optical system for measurements of the aurora. It is composed of a grid of stations with about 50 km separation and should in the final stage be located in the northern parts of Sweden, Norway, Finland and the USSR. Auroral imaging from the ground and from space are two complementary techniques. During nights with favourable weather conditions the ground-based technique provides the possibility to make continuous measurements with high temporal and spatial resolution. The Swedish part of ALIS is planned to consist of 14 imaging stations and a control center. Each station transfers the image data to the control center, where either a grand image or a three dimensional image is presented. The three dimensional auroral distribution is reconstructed with tomographic inversion techniques. There are a large number of different methods and techniques to recover the three dimensional structure of an object, in this paper some methods are presented. Four of these methods were tested on a simple model in a simulated ALIS system.

Keywords: Auroral Imaging, 3-D Distribution of Auroral Emissions, Tomographic Inversion.

V.V.Alpatov
Institute of applied geophysics, Moscow, Russia.

Abstract

The paper presents some evaluations of possibility to use the optical tomographic methods for investigations of natural and artificial irregularities in the near earth space. Results obtained at research of artificial irregularities are described.

1. Introduction

Recently great of interest has been expressed to apply new methods to investigate of natural and artificial optical irregularities in the near earth environment, atmosphere and near space(NS). We consider as natural the auroral structures, tropical arcs and similar objects. When active experiments in NS are carried out one can observe artificial optical irregularities such as artificial clouds, artificial auroras etc. The optical irregularities investigations may give important information on natural physical processes in NS and the ones, which cause NS pollution by the human activity. Optical irregularity studies may effectively use optical tomography methods and there are now conditions for the appearance of special tomographic systems intended for such objects. In spite of large variety of such irregularities they have some common features. The basic are:

- large spatial scales
- limited number of observation points and observation angles range
- necessity for three-dimensional different physical parameters distributions obtained from two-dimensional projections-images
- initial data obtained by different devices; TV, photo cameras, CCD-matrixes and rulers, spectrographs and spectrometers and so on.
- high cost of establishing every additive observation point.

An IAG active experiment program studied a possibility to use optic tomography methods for natural and artificial objects internal structure reconstruction.

In our opinion, the results of specific investigations in this area may be applied for a wide range of optical near space problems decision.

The paper considers some results of research in this direction. The objectives of the work were:

- 1) to study optic tomography methods possible application to determine near space natural and artificial optical large scale irregularities inner structure ;
- 2) in case of a positive answer to develop technology to design local and global tomographic systems intended for near space optical irregularities investigations.

The problem was resolved in the some integrated stages:

- analysis of probing radiation propagation in the environment(object)
- selection of the equation describing the relationship between the measured parameters within the object and radiation parameters
- search for the methods of projection inversion
- analysis of possible detecting schemes
- informational analysis
- selection of reconstructional algorithms,routines and processor for their realization
- simulation of reconstruction objects, testing of algorithms using model objects
- development of the reconstruction procedure for data obtained in field experiments
- analysis of reconstruction results
- development of tomographic systems structure.

Each stage displayed problems of different complexity and, apparently, the process is specific for every new object. The results of one series of studies may help to develop technology, facilitate studies of similar objects and provide an experience in the application of such technology.

Let us briefly show some results obtained during every stage for such objects as artificial structures(AS) usually created in active experiments[Alpatov et.al.,1985,Alpatov et.al.,1986,Alpatov et.al.,1989,Alpatov et.al.,1991].

2. Results of research

1. For different AS classes radiation within them is absorbed, scattered and reemitted by internal environment. Relation between measured radiation and physical parameters may be described by radiation transport equation(RTE).

2. The form of the equation depends on AS development stages which can be characterized by such an integral parameter as optical thickness. Therefore different types of AS in different development stages were analyzed using of experimental results and different models for this integral parameter evaluation.

3. For AS types and development stages, with optical thickness $\tau < 1$, there are well known project inversion methods, that principally allow to get decision. When $\tau > 1$, there is no decision in a general case, because it is necessary to apply partial methods or to design them specially. For example, for optically thick barium clouds special method of "couple lines" may be applied, based on the fact, that during barium clouds luminosity there are two connected spectral lines, one of which is optically thick and the other one is optically thin. Fig.1 shows an example of evaluative calculations, made for artificial barium clouds. Calculations are shown for mixture of injective masses up 1 to 10 kg, at extreme values of parameters, defined AS development.

4. Some versions of schemes were analyzed for transmission, emission tomography and tomography of scattering environments. The merits and faults, were evaluated and their application classified. Fig.2 shows table, obtained after different AS types and stages analysis. The table provides a number of conclusions as to which tomographic schemes and inversion methods are preferable or exclusively possible for various types of AS and their development stages.

5. An important stage of investigation consisted in informational analysis, which is especially important for studying such objects as AS and nature irregularities in NS. The informational analysis includes evaluations of the following parameters influence on the accuracy reconstruction :

- required number of projections and amount of data in each projection
- complexity of the studied object
- possibility to use the a priori data
- informativity of different projections(obtained from various directions)
- the effects of noise
- the minimum intensity of informative signal
- required exposition period and minimum available scales for the reconstruction of of irregularities within the object

The informational analysis revealed requirements to registration devices and to an experiment schemes, and provided data to create an object model for computer reconstruction simulation. Fig.3 shows, for example, calculated variations of barium structures luminosity intensities as a function of development period. There are two characteristic thresholds to compare these curves: sensor sensitive threshold and quantum noise essential influence threshold, below which any inversion algorithms will work worse. This threshold was calculated by simulation of different objects for required signal to noise ratio.

6. Informational analysis also showed that the problem of tomographic reconstruction of AS inner distributions belongs to the class of low view and ultra low views tomographic problems. The study also ascertained a possibility to use a priori data on the inner AS parameter distributions, which is especially important at low views tomography. We consider that best reconstruction algorithms for such tasks are ART, GP, Ment, maximum likelihood algorithms and others in this classes. They are partially realized in TOPAS-MICRO package, developed by Pickalov team.

7. An AS model was developed for computer simulation, which imitates the stratified stage of AS progress on the basis of a set of different parameter gaussians. Fig.4 presents model form. Test reconstruction has been made with modified ART and GP algorithms assistance. Several tasks were solved in the simulation.

There were evaluated, for example the influence on reconstruction quality of:

- model parameters
- number and disposition of projections
- noises of different intensity

Fig.5 presents reconstruction errors dependencies on iteration number for various number of projections and their total informativity. One can see that for the set of 19 projections the reconstruction error in several times better, than for the set of 3 projections. One can see essential reconstruction error decreasing when using projection sets with high total informativity for 5 and 3 projection sets. For more explicit presentation, of mean error percents, fig.6 shows slices in the same cross-sections of model and reconstruction by planes, which are perpendicular to one of coordinate axis. One can see, that even at 3 projections and reconstruction error 80 % distribution structure reconstructs rather well, though signal amplitude decreases and artifacts appear. If one

introduces noise in initial projections, the reconstruction depends on their values and on the presence or absence of preliminary filtration. In case of effective filtration acceptable results may be obtained even at 50-60 % noises, but without filtration at 50 % noise for 5-7 projections the reconstruction is absolutely unacceptable. In general, simulation results show a principal possibility to reconstruct inner structure of AS-like objects using ART and GP algorithms on 3-5 views, when one can choose the most informative of them and provide suitable noise filtration.

8. The research showed the necessity to develop a procedure for object reconstruction on data obtained in field experiments. The following problems were solved :

- input projection images into computer. Projections were initially registered on video- and photo films.
- removal of geometrical and brightness distortions
- geometrical fastening of projections to a common point in space
- images brightness calibration
- geometrical and brightness normalization of images (fastening to the same scale and absolute energetic values).

Solution of these complex and difficult problems resulted in a possibility to get images, which one can call tomographic projections from experimental images obtained by various devices. Such tomographic projections may be used in reconstructive routines. The procedure described above was applied to 3 images of barium cloud, obtained in one of the middle latitude experiments at 170 km. Unfortunately, the projection set was uninformative on informativity criterion used in our works: only one projection was situated in high informativity zone. Images corresponded to optically thin AS development stage, emission tomography scheme was used. Spatial luminosity distribution was reconstructed, that for given AS development stage is proportional to a spatial distribution of barium ion concentration. Marked convergence of iteration process was noted.

9. The purpose of reconstruction analysis was to check the conformity of the distribution obtained after reconstruction to a priori data and physical concepts of it, and also to formulate some additional requirements to experimental conditions, to algorithms and routines of reconstruction and visualization of its results.

Fig.7 show initial projections and the ones, obtained after reconstruction. One can see, that the general structure features are preserved, although, as was supposed after simulating the intensity of weaker details essentially decreases. One of the good tests in this case is to determinate post-reconstruction orientation of "invisible" inner details in respect to vertical z axis. The point is that it follows from a priori data that at a given AS development stage there exist some structures named "stratas", which are oriented preferably along the local magnetic field vector. These stratas are similar to some structures in aurora glow. In the experiment carried out it forms 24 degrees to the vertical axis. Fig.8 shows the form of the inner structure at 50% of the maximum intensity (it is invisible inner structure) in the plane, passing across the vertical axis and this structure. One can see that the angle between the vertical axis and this structure, which is similar to strata, is approximately 21 degrees, which in our opinion, rather well agrees with a priori data and physical presentations. At the same time the analysis of results has shown that it is perfectly insufficient to do reconstruction on grid 64x64x64 voxels to obtain spatial accuracy required in most physical applications.

10. The work allowed to formulate requirements to devices and experimental methodology including collection of necessary attending information. A version of tomographic system structure was also developed. Such a system could solve the problem of parameter spatial distribution for natural and artificial optical irregularities in near space. Its form is shown in fig.9. The basic elements of such a system are stationary and mobile observation and data registration subsystems. They have basic and extended set of different devices, including high sensitivity TV-devices and less sensitive compact TV-cameras based on image intensifier; photo cameras with image intensifier, photometers for fitting to absolute energetic values, low-light spectrographs, standard light sources, calibrate tabulars. Absolute flows are recently being measured with photometer for small flows, provided with built in radiation source for calibration and allowing measurements in narrow spectral integrals with filters with half width 0.2 nm, which can replace each other. Besides, there is a very important device to obtain spectral information - low-light spectrograph. In the basic device scheme dispersion region is 400-700 nm and spectral resolution is 2-5 nm. Registration may be by photo- and TV cameras. The major part of the apparatus is situated on a special rotate device to ensure automatic control and spatial orientation. Fig.10 presents some apparatus technical data. Such complexes may collect many attending information on the object, which is important for low view tomography, and they are mobile and can be put even on airplanes and scientific research vessels.

For successful function of the system it is necessary to provide observation subsystems with relevant means of information transmission. With these means projection data and attending information, including spatial orientation and time synchronization data, are transmitted to a central

point of collection and treatment. Depending on system purposes, a relevant calculate power processor should be selected. The experience of large scale geophysical irregularity structure reconstruction shows that the visualization subsystem is a very important subsystem, because possibility to interpretative reconstruction results and usage very much depends on this subsystem. Some possibilities for it there are in TOPAS_MICRO package. For example there is a possibility to rotate the object and to take off envelopes from it, penetrating to inner structure.

Thus, research carried out, allowed to develop a technology for local and global tomographic systems intended for inner structure reconstruction of different natural and artificial optical irregularities in the near space. This technology was tested on different kinds of artificial objects and allowed to get useful results at inner structure reconstruction of barium cloud from 3 projection images.

In conclusion one may add that such tomographic project was carried out by a group of specialists, working in different directions and scientific institutes, and they united to solve this large problem. In future it is supposed to apply these developments to create various regional and global systems for inner structure reconstruction of geophysical optical irregularities by optical tomography methods.

4. Acknowledgments.

The author gratefully acknowledge the help of Dr. Romanovsky Yu.A., Dr. Pickalov V.V., Dr. Levin G.G. in various research stages.

5. References.

- V.V. Alpatov, V. Yu. Gaydukov, G.P. Milinevsky and Yu.A. Romanovsky, "About methodic of the artificial clouds parameters determination in ionosphere at AC computer image processing", *Abstracts of reports of V All-USSR of Workshop in dynamic processes researches in upper atmosphere of Earth*, Obninsk, 1985, p. 127 (in Russian).
- V.V. Alpatov, M.B. Belotserkovsky, A.N. Evtushevsky, G.P. Milinevsky and Yu.A. Romanovsky, "Optical Observations of Phenomena During the Expansion of Alkali Metal Hot Clouds in the Earth's Upper Atmosphere", *XXVI COSPAR*, Toulouse, France, 1986, 30 June-12 July.
- V.V. Alpatov, F.V. Bulygin, G.G. Levin, V.V. Pickalov and Yu.A. Romanovsky, "About possibility of artificial ionospheric structures researchers by optic tomography methods", *Poster report in IV All-USSR computer tomography symposium*, Tashkent, 1989, (in Russian).
- Alpatov V.V., Levin G.G., Pickalov V.V., Romanovsky Yu.A., "Optical tomography techniques to study geophysical artificial structures", *SPIE Vol. 1843 Analytical Methods for Optical Tomography*, 1991, pp. 297-311.

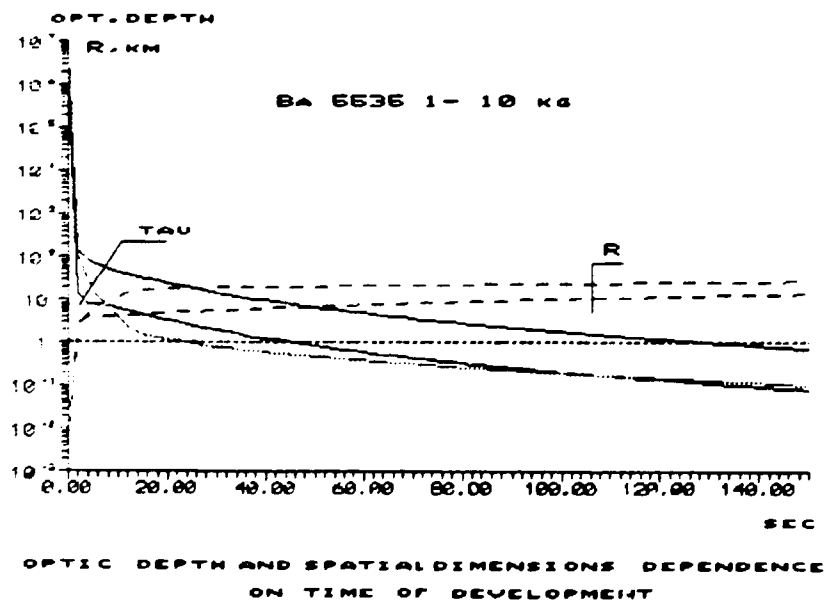
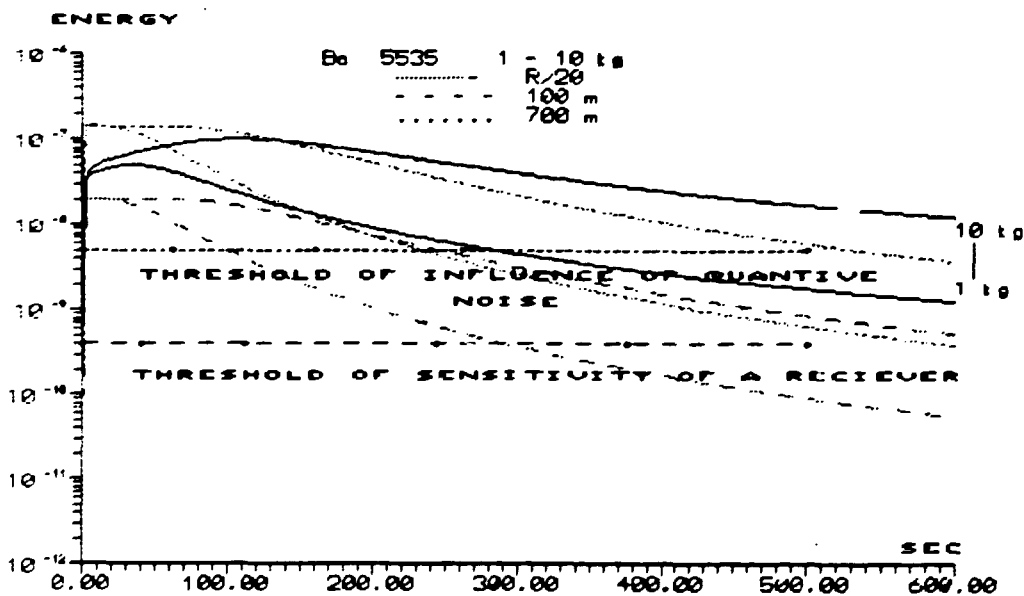


Fig. 1

TYPE OF OBJECT	STAGES OF OBJECT DEVELOPMENT	TIME AFTER INJECT. S	OPTICAL RADIUS	DIMENSIONS, KM	RATE OF SIZE VARIATIONS, KM/S:	Density of emission intensity near detector, erg/cm ² s	TOMOGRAPHIC CLASSIFICATION
CLOUDS OF ALKALI METALS	SCATTER	0-2	> 1	1-2	1-1.5	> 10 ⁻⁹	AVAILABLE SELF-BLOW
	RAPID DIFFUSION AND DRIFT	2-100	$T_x = 0.2-200$ $T_x \gg 1$ $T_x < 0.2$ $T_x \gg 1$ adding 0.001-1	2-10	30-100 M/S	> 10 ⁻⁸	TRANSMISSION
JETS	SLOW DIFFUSION AND DRIFT	> 100		30-50	5-100 M/S		TRANSMISSION
	SCATTER and CREATING	0-2 0-100	> 1	0.5 length up 70	1-1.5	> 10 ⁻⁸	AVAILABLE SELF-BLOW
AEROSOL CLOUDS	DIFFUSION AND DRIFT	> 2	0.001-0.1	0.5-30 length up 70	10-100 M/S drift up 1 M/S	> 10 ⁻⁸	TRANSMISSION
	SCATTER	0-10	>> 1	5-10	1-1.5	> 10 ⁻⁹	SELF-BLOW in WIDE RANGE
NEUTRAL INJECTIONS	DIFFUSION AND DRIFT	10-1000	>> 1	10-20	100-15 M/S	> 10 ⁻⁹	TRANSMISSION
	SCATTER	50-60	< 1	10-100	0.3-2 KM/S	> 40 R	EMISSION
	DIFFUSION	60-600	< 1	> 100	80-300 M/S	~ 50 R	SELF-BLOW in ATMOSPHERIC EMISSIONS

TABLE 1. ESTIMATES OF SOME CHARACTERISTICS OF AS FOR TOMOGRAPHIC CLASSIFICATION ANALYSIS OF AS.

Fig. 2



GLOW POWER DENSITY DEPENDENCE ON TIME OF DEVELOPMENT FOR DIFFERENT DIMENSIONS STRUCTURES.

Fig. 3

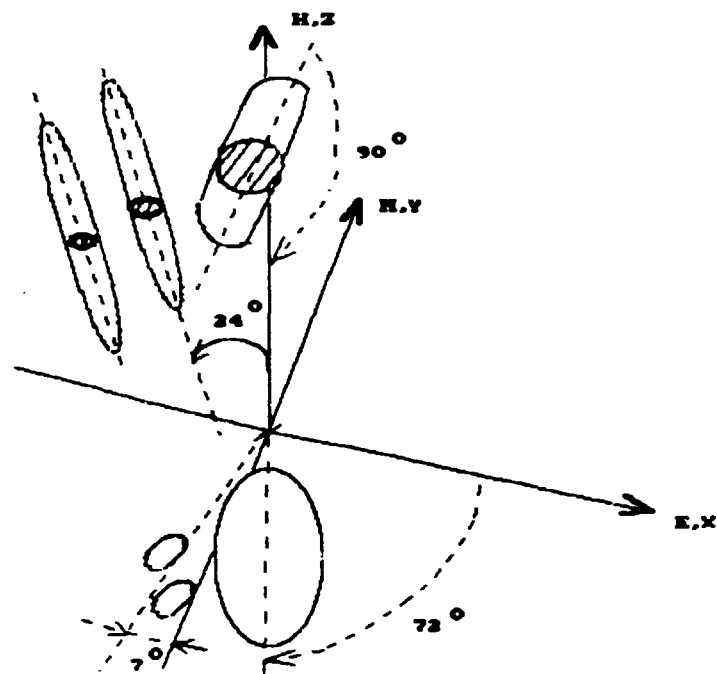


Fig4 Model AC, using in computer experiment.

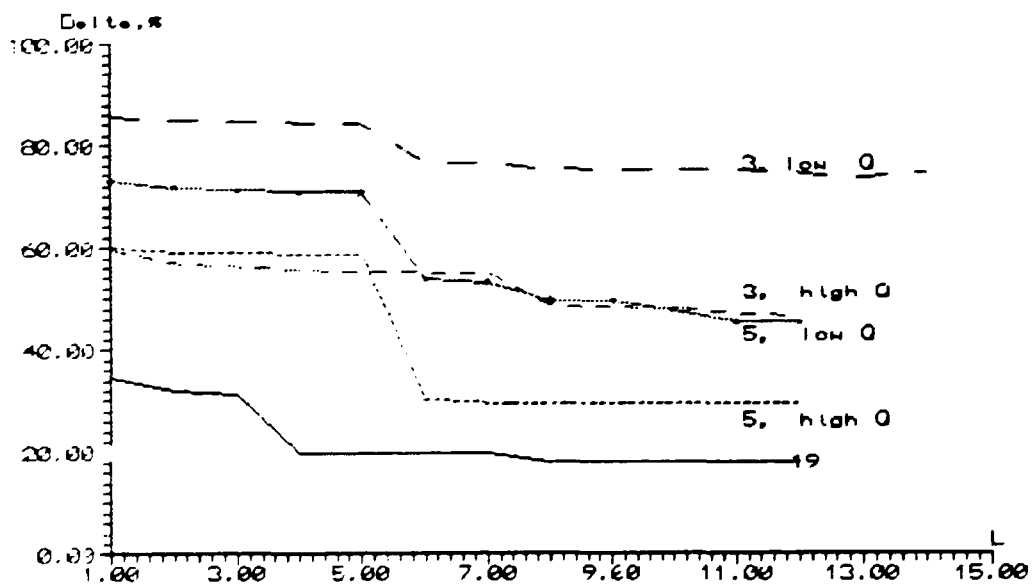
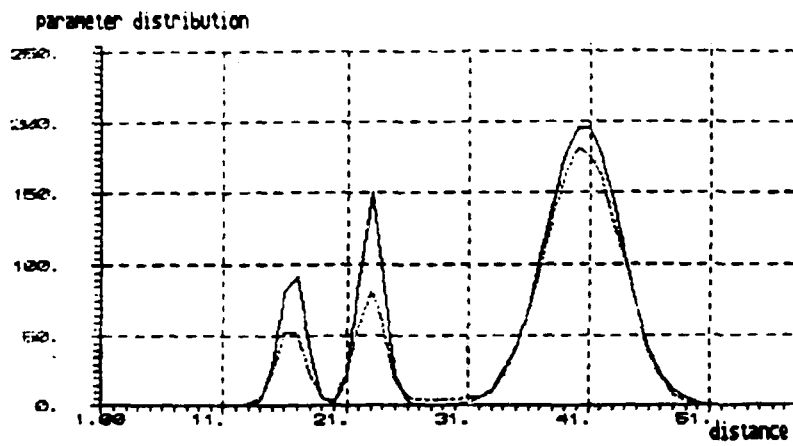
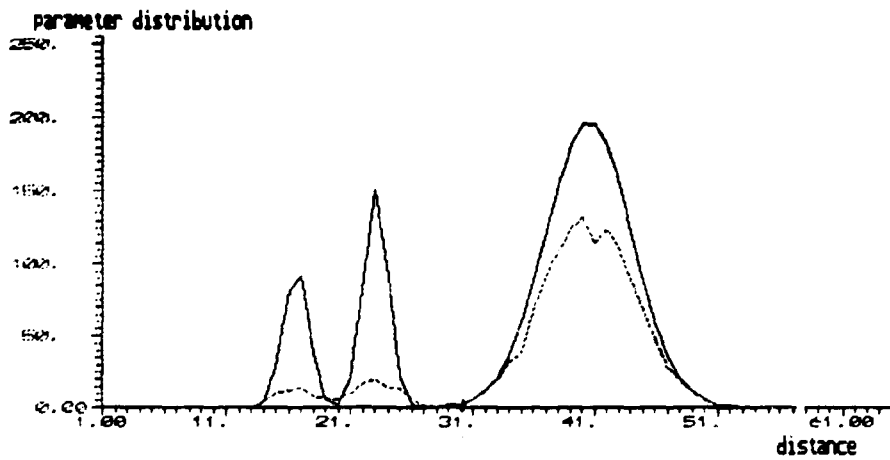


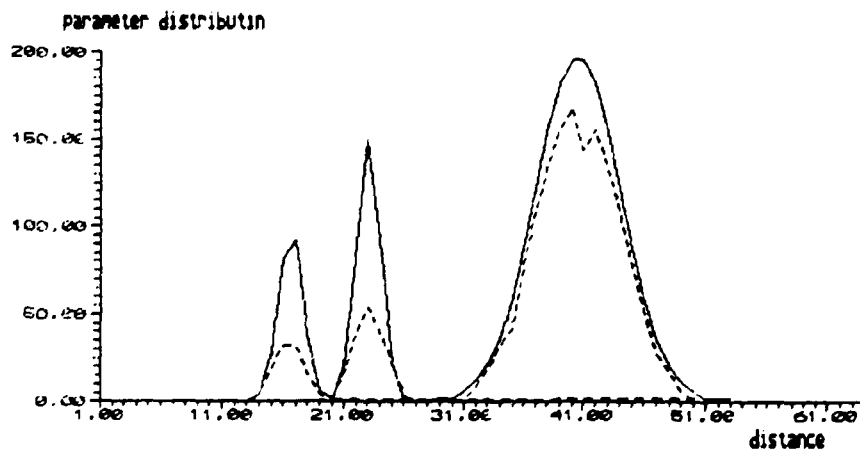
Fig. 5



Slice of model and reconstruction distributions for 19 projections.

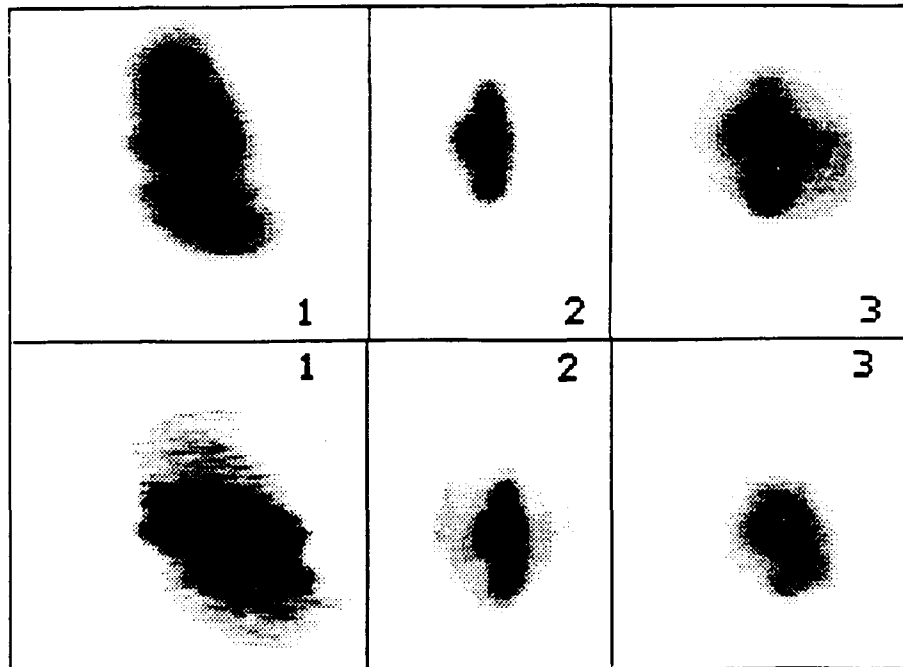


slice of model and reconstruction distributions for 3 projections.



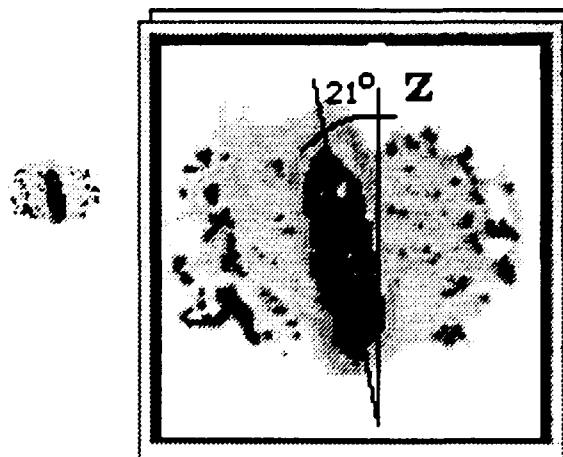
slice of model and reconstruction distributions for 5 projections.

Fig. 6



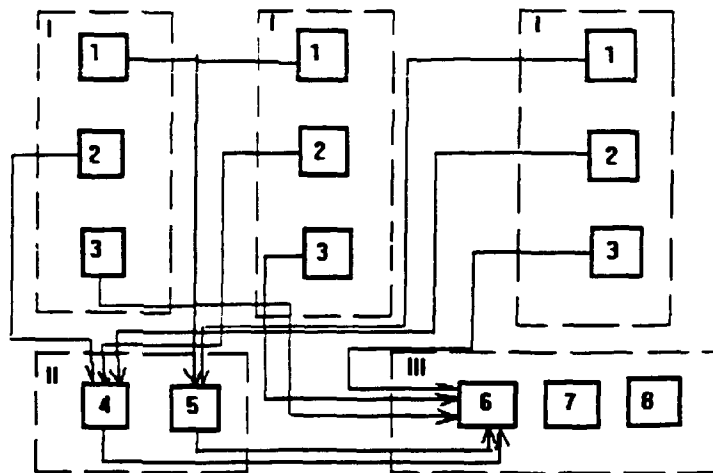
Experimental projects(top) and "pseudo projections" on reconstruction distribution(bottom).

Fig.7



Slice of object inner structure

Fig. 8



Block-scheme of optical tomograph.

- I - system of observation and registration : 1- optical block of image formation, 2- registration block, 3- memory block
 II - system of spatial orientation and time synchronizations: 4- block of time synchronization, 5- block of spatial orientation.
 III - processing system : 6- block preprocessing and sorting of projections data, 7- computer, 8 - block for forming apriory information

Fig. 9

Optical Devices Set

N	Apparature type	Measurement parameters	Parameters of apparatures		
			sensitivity	field of view,deg.	time constant
1	TV-cameras	Brightness, position,size	2-40kR	40-5	0.02s
2	Colour TV-camera	Colour, position, size	800kR	50-5	0.02s
3	Photo-camera	Brightness, position,size	40-60kR	40-5	300-100s
4	Photo-camera with image intensifier	Brightness, position,size	20-30kR	20-5	10s
5	Photometer	Intensity	20R	6-0.1	0.05s
6	Scan-Photometer	Intensity, size (one demension)	20kR	6-0.1	0.05s
7	Spectrograph + Photo	Spectr	100kR-100R	10-15	1-300s
8	Spectrograph + TV-camera	Spectr	500kR	10-15	0.02s
9	Spectrograph + IBM PC	Spectr	400kR-100R	10-15	0.05-300s

Fig. 10

A Note on the Computed Auroral Tomography by the MART Method †

T. Aso ¹⁾, K. Muguruma ¹⁾, T. Yabu ¹⁾, T. Hashimoto ¹⁾,
M. Abe ¹⁾, and M. Ejiri ²⁾

¹⁾ Department of Electrical Engineering, Kyoto University, Kyoto 606, Japan

²⁾ National Institute of Polar Research, Itabashi, Tokyo 173, Japan

- Contents -

- A numerical test for the MART (*Multiplicative Algebraic Reconstruction Technique*)
- A modified MART with correction based on aurora luminous characteristic
- A numerical test for multiple-station observation
- Modified MART analysis for Iceland stereo observation
- Summary

Formulation for MART

- **MULTIPLICATIVE ALGEBRAIC RECONSTRUCTION TECHNIQUE** - †

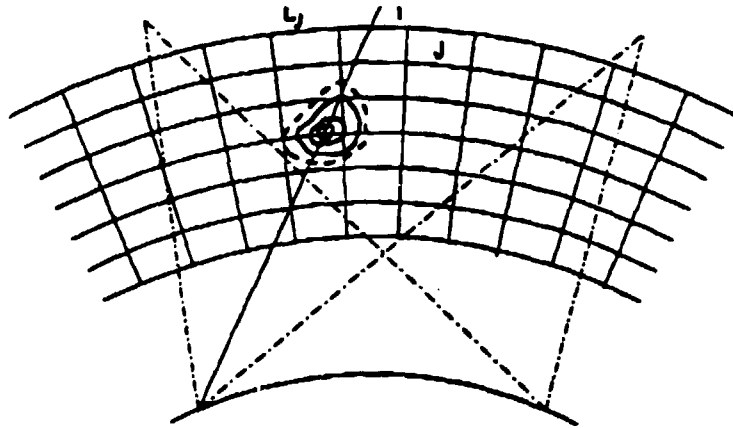


Image illuminance for i -th path

$$p_i \propto \int_{i\text{-th path}} L(r, \theta, \phi) dr \text{ [photons/m}^2\text{sec]}$$

$$= \sum_{j=1}^M s_{i,j} L_j$$

L_j [photons/m³sec] : Photo emission rate at j -th cell
 $s_{i,j}$: length of i -th path traversing j -th cell

Multiplicative Algebraic Reconstruction

$$L_j^{k+1} = L_j^k \left(\frac{p_i}{\langle a_i \cdot L^k \rangle} \right)^{\lambda_k s_{i,j}}$$

$i = k(\text{mod } N) + 1$, k : iteration number
 a_i : i -th row of $\{s_{i,j}\}$, i : path index
 N : Numbers of paths, M : Numbers of cells
 $\langle \cdot \rangle$: inner product
 $0 \leq \lambda_k s_{i,j} \leq 1$, divide by max of a_i
 λ_k : Relaxation parameter

Means to multiplicatively augment/reduce current j -th cell value with the weight of $s_{i,j}$ when calculated projection is smaller/greater than observed gray level p_i . This leads to maximize the entropy

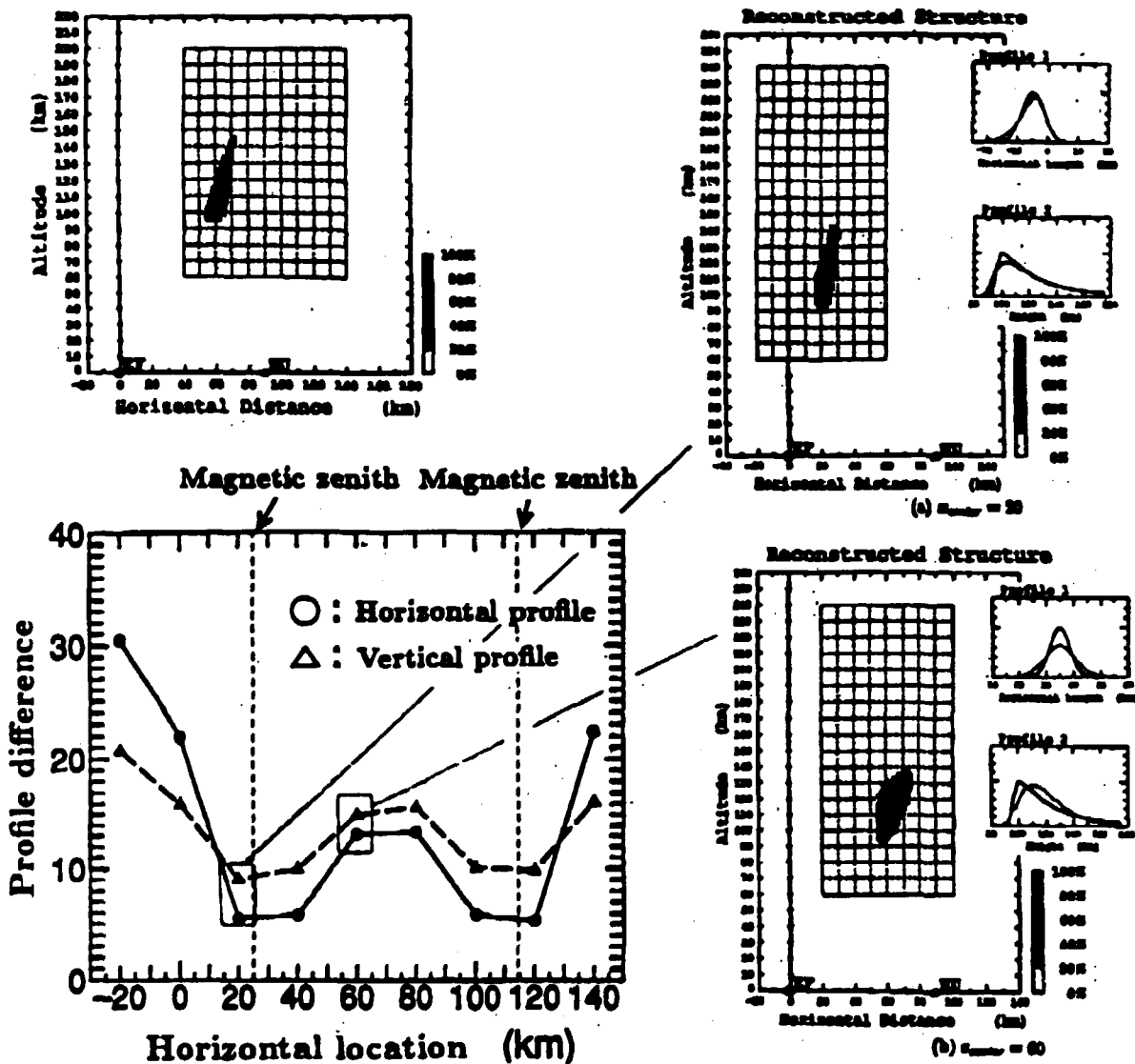
$$H = \frac{-1}{\ln(M^2)} \frac{1}{\|L\|_1} L^T \ln\left(\frac{L}{\|L\|_1}\right)$$

with the following constraints (cf Gordon et al., 1970).

$$p_i = \sum_{j=1}^M s_{i,j} L_j \quad i = 1, 2, \dots, N$$

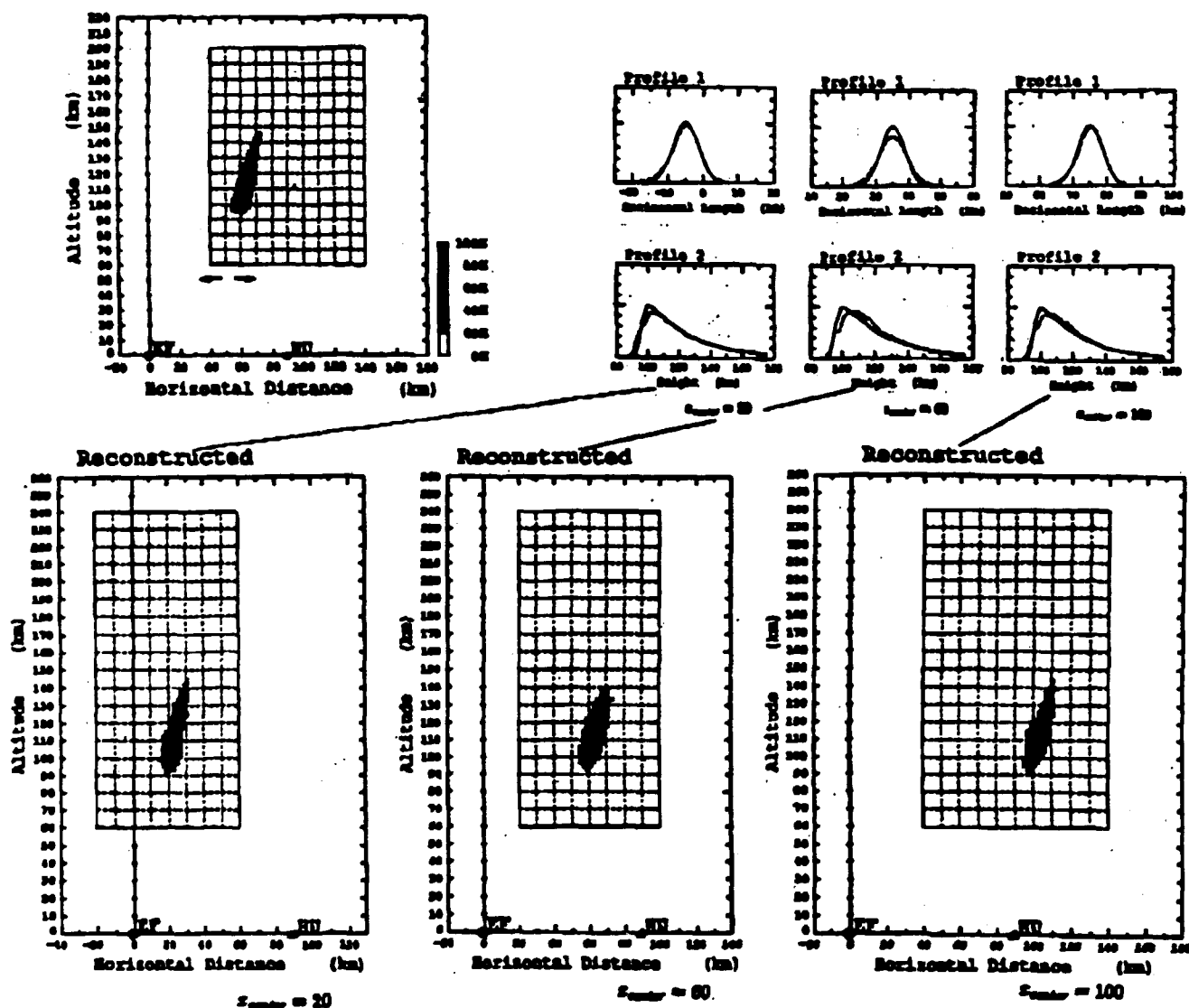
$$L_j \geq 0$$

Dependence on the auroral locations in the MART Analysis †



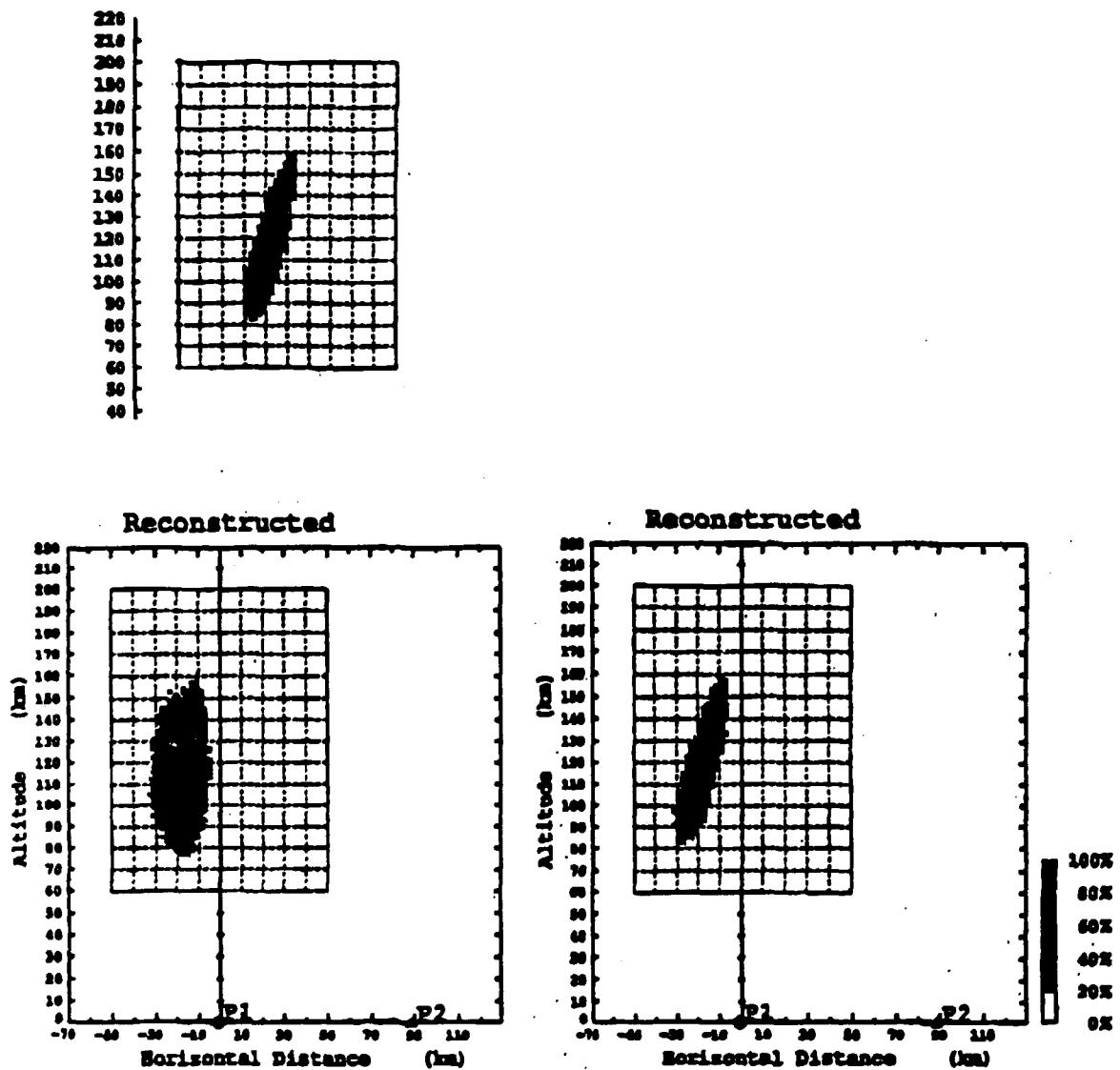
Numerical simulation for the reconstruction of auroral luminosity structure by the *2-dimensional* MART has been carried out. Dependence of reconstruction on the locations of aurora relative to observing points is shown. Top figure is the model, and horizontal location is varied. Two specimens of reconstruction are indicated. Degree of reconstruction defined as the difference in the vertical and horizontal profiles of luminosity structure is plotted versus aurora horizontal locations. As is intuitively understood, good result is obtained when aurora is seen in the local magnetic zenith direction of either of the observing point. In this case, fairly thin structure of aurora curtain is unambiguously recognizable.

Correction Scheme in the MART - modified MART Analysis †



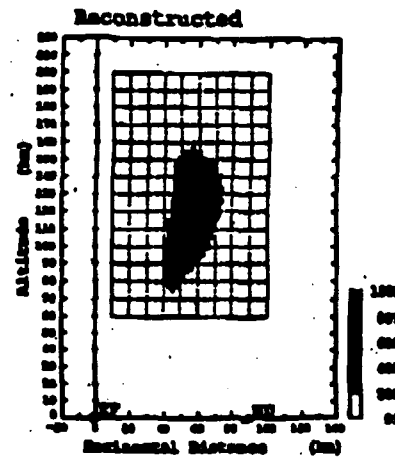
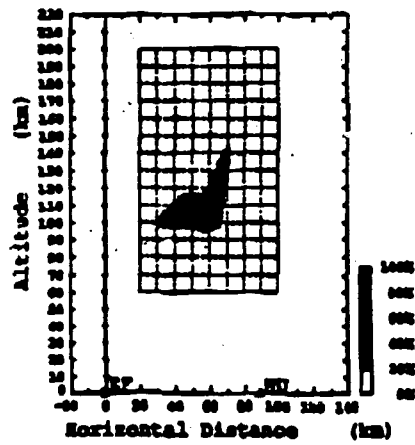
To compensate for the scarcity of information, constraint is interwoven such that the aurora is aligned parallel to the geomagnetic lines of force. More explicitly, cell values along each geomagnetic line is redistributed based on some plausible functional form corresponding to vertical distribution of aurora luminosity, and then the MART analysis is resumed. This is basically identical with our nonlinear fitting scheme of prescribed functional form. The results show some improvement, the reconstruction being consistent even when aurora is not located in the magnetic zenith direction.

Multiple Corrections in the modified MART Analysis †

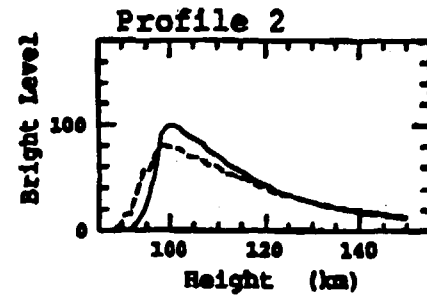
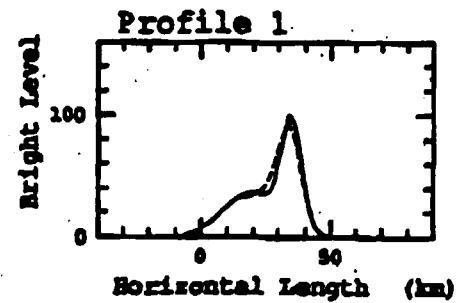
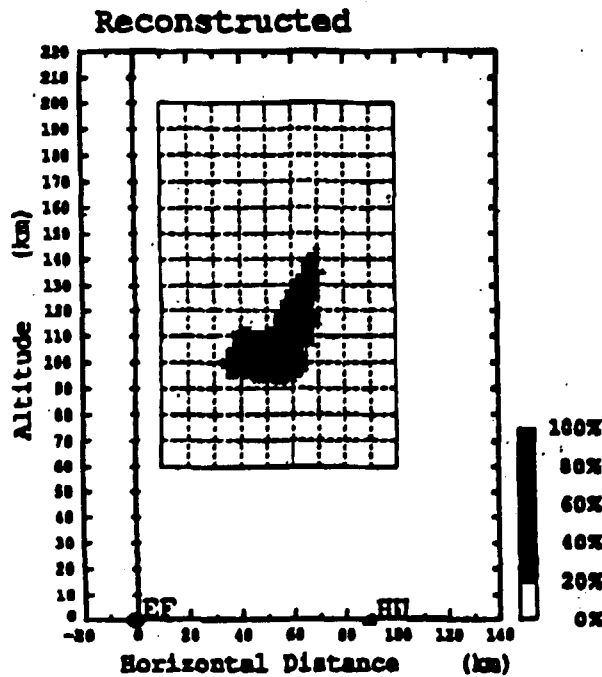


Multiple repetitions of MART and correction scheme improve the reconstruction even when aurora is laterally seen almost in the same direction from both sites. Top figure shows an aurora model. A bottom-left result relies only on one correction for MART. While, bottom right figure is obtained by repeated MART and correction scheme. The reconstruction compares well with the model even in the unfavorable aurora location.

Two-layered model for the modified MART Analysis †

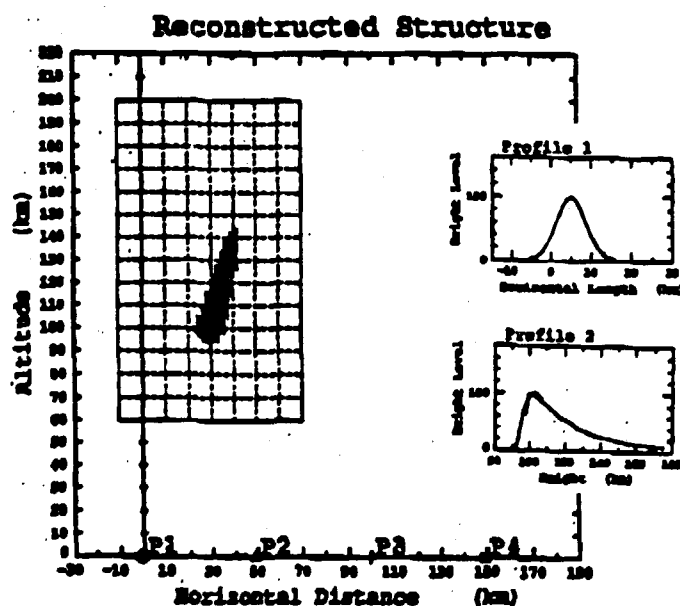
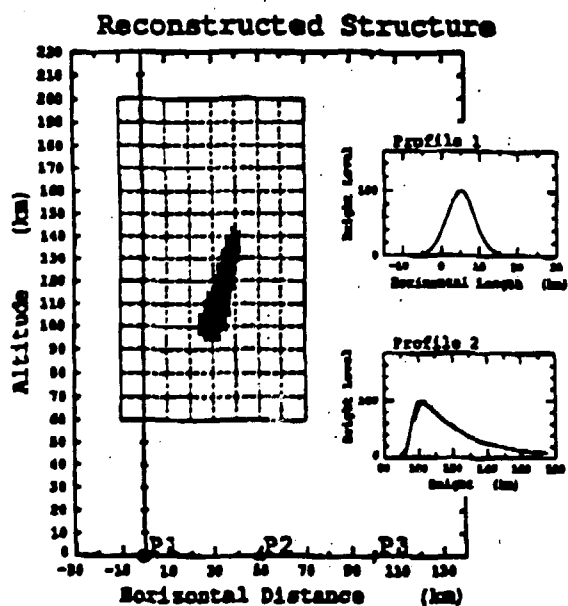
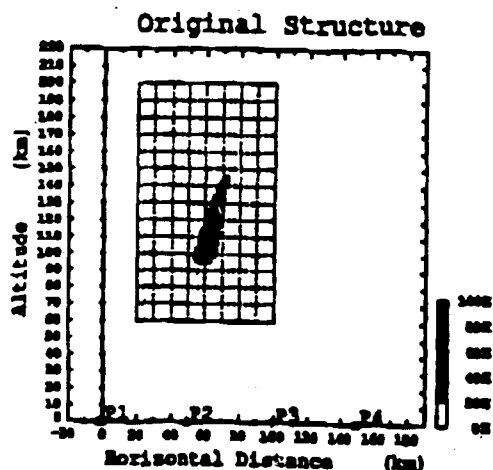


MART



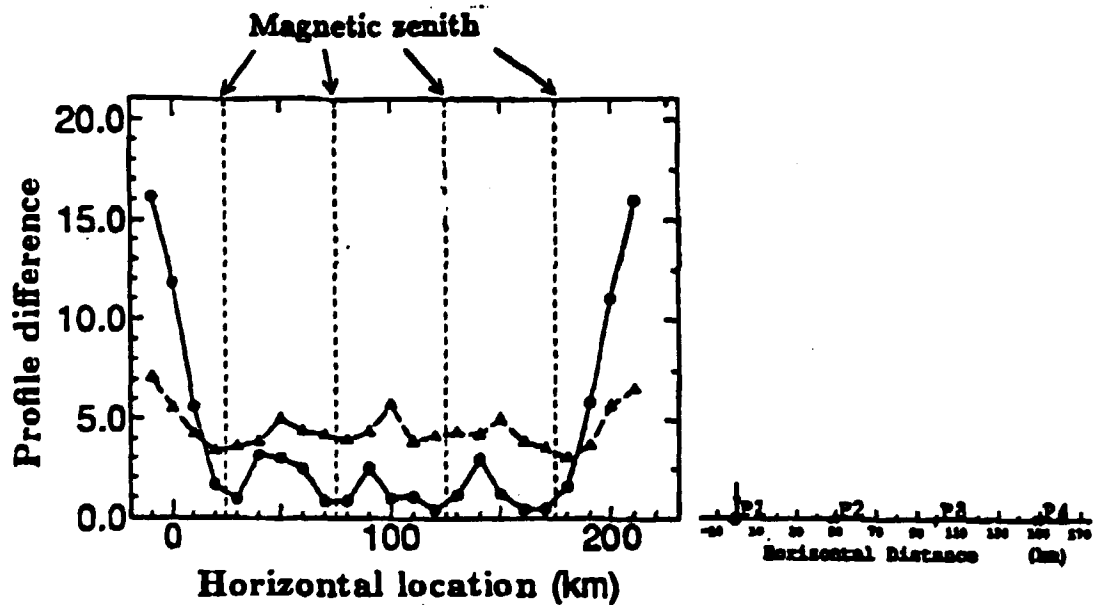
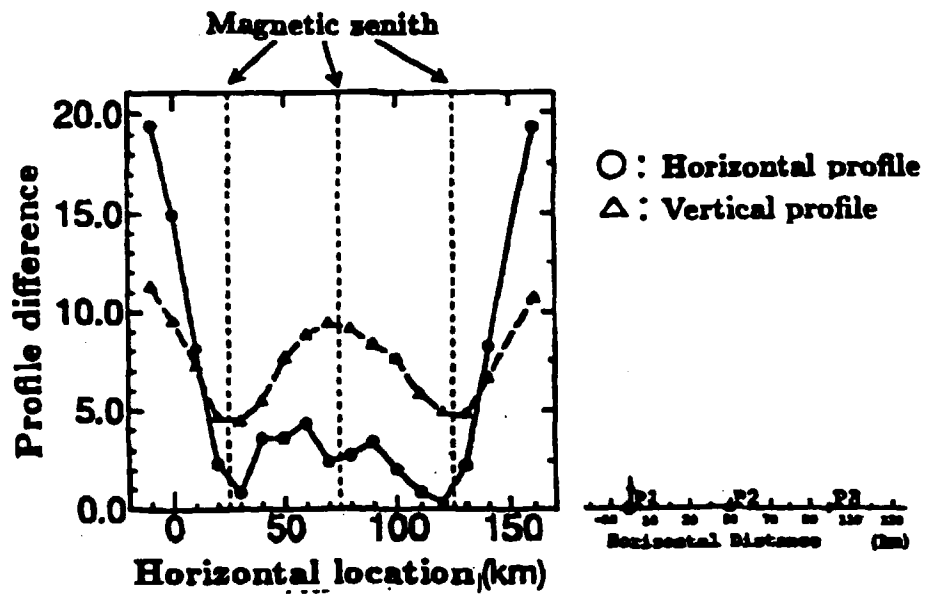
Two-layered aurora luminosity model is assumed as in the top-left figure. Simple MART analysis in the top-right figure only gives poor result due to lack of information. Modified MART reconstruction retrieves two-layer structures fairly well as shown in the bottom figure, with horizontal and vertical profiles of aurora structure (model : solid line, reconstruction : broken line).

MART Analysis for the Multiple-station observation †



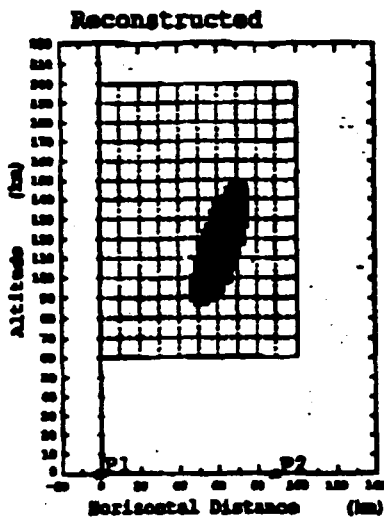
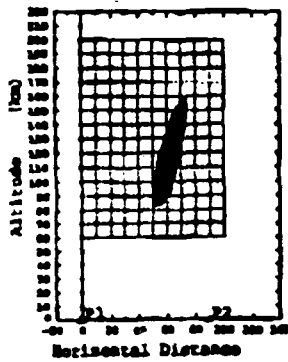
"Stereo" observations by *multiple* stations can convey more information for the reconstruction. Here, numerical test for the future cooperative experiment with ALIS is indicated, and aurora model with stations $P_1 \sim P_4$, 50 km apart, is in the top figure. The specimen results of MART analysis for three and four stations are indicated in the bottom. The reconstruction is fairly good in these cases.

MART Analysis for the Multiple-station observation †

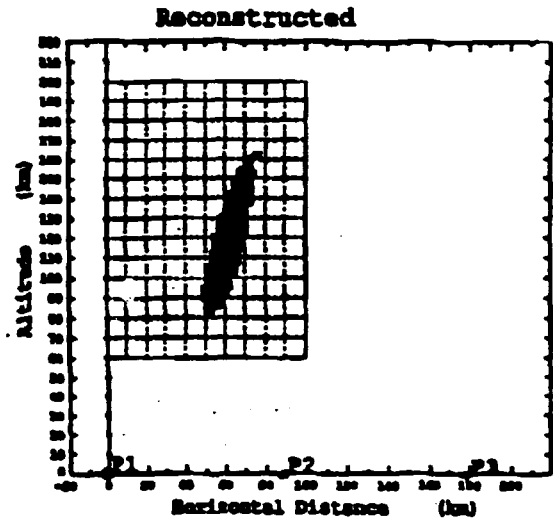


Degree of reconstruction for the MART analysis of "stereo" observations by multiple stations is indicated versus horizontal locations of aurora illuminating region. Reconstruction is, by and large, good compared to two-station case even when aurora is not very close to magnetic zenith of either of stations.

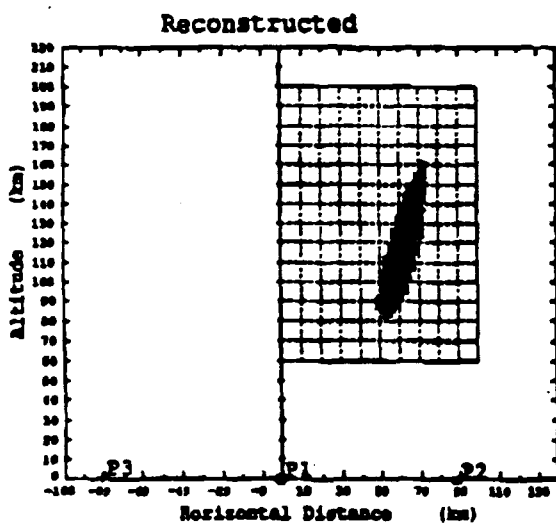
MART Analysis for the Multiple-station observation †



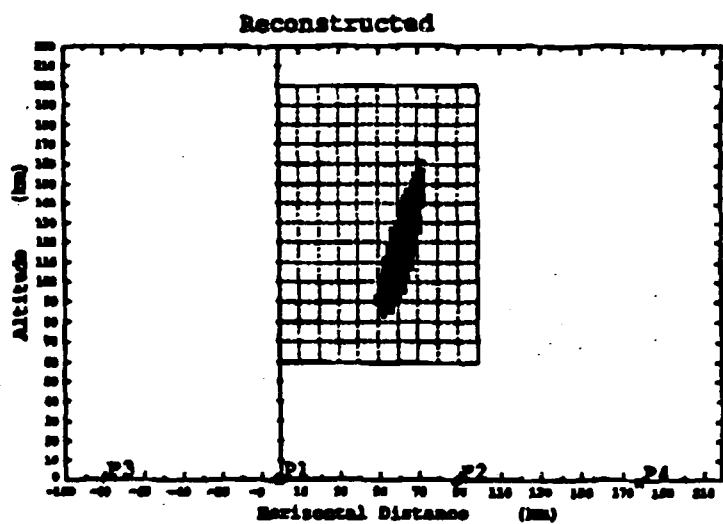
(a)



(b)



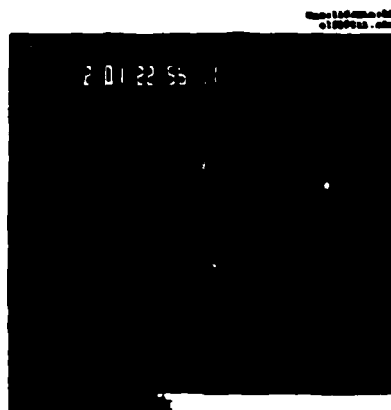
(c)



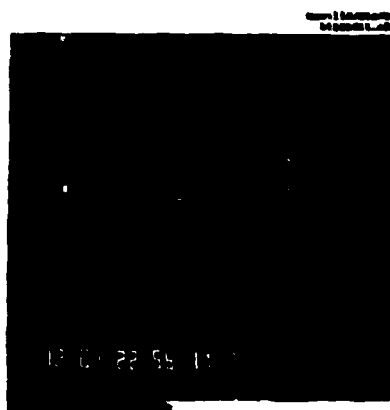
(d)

Numerical test for various observing locations is indicated. An aurora model is in the top-left figure. The specimen results of MART analysis with no correction for two[(a)], three[(b) and (c)] and four[(d)] stations (P_1, P_2, \dots) are indicated. The reconstruction for three or four station seems to be improved.

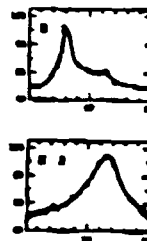
Modified MART Analysis of Stable Arc in Iceland †



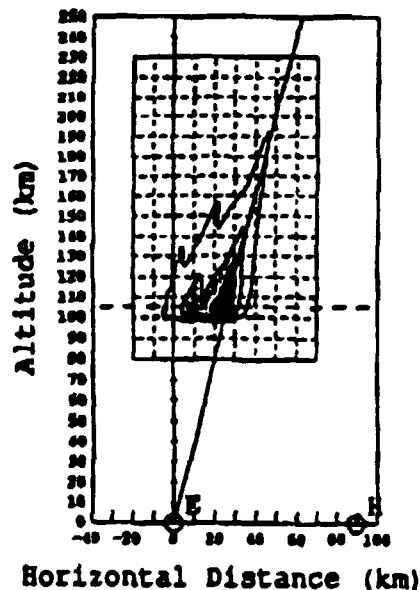
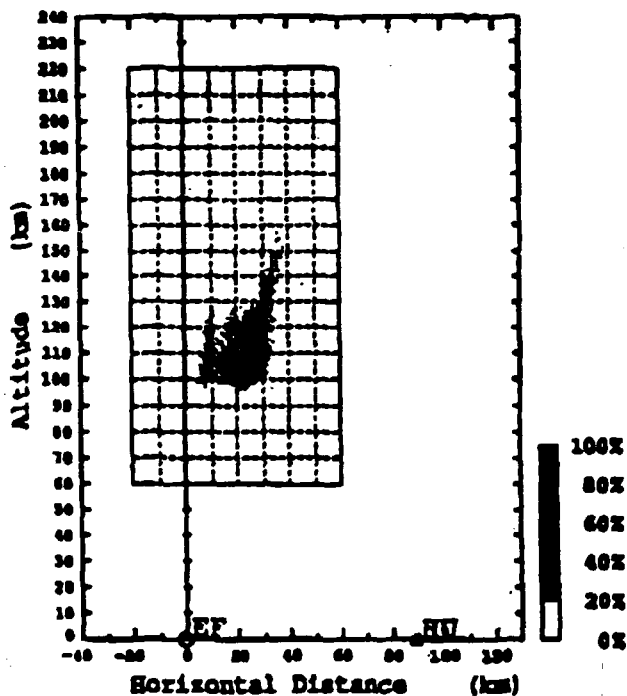
(a) Left Image



(b) Right Image



Reconstructed



This is the 2-dimensional modified MART analysis of the stereo image pair taken at 22:56 December 1, 1991 in Iceland. The analysis is in the *vertical epipolar plane*, of which the gray level profile is shown in the inset. In the analysis, 40 x 80 cells and 100 paths for each image are used, and gray level background was subtracted. Reconstructed structure is fairly compatible with the one based on the non-linear minimization scheme of assumed luminosity function model (bottom right).

Summary
for
***A Note on the Computed Auroral Tomography
by the MART Method***[†]

- A cell model analysis by MART (*Multiplicative Algebraic Reconstruction Technique*) has been numerically tested. For binocular stereo analysis, good reconstruction is only possible when aurora is simply layered and location is such that essential information is available.
- Correction resting on aurora characteristics that it is aligned with geomagnetic line of force and assumes plausible altitude distribution is added in the course of MART analysis. This modified MART method gives improvement for the analysis of binocular stereo observation.
- Multiple-station observation is informative for unambiguous reconstruction by the simple MART analysis. Coordinated stereo observation with ALIS and other colleagues are fairly promising.
- A few of Iceland stereo observation has been analysed based on the modified MART.

Informational analysis of auroral tomograph.

V.V.Alpatov, V.V.Pickalov, A.V.Lihachov

Institute of Applied Geophysics, Moscow, Russia
Institute of Theoretical and Applied Mechanics, Novosibirsk, Russia.

1. Abstract

The problem of optimal observation points localization is discussed. The quantitative estimation of inequality of projections obtained from different directions on reconstruction error is presented. The examples of using this estimation to artificial structures and auroral investigations are shown.

2. Introduction

The experience of working on problem the possibility to apply optical tomography methods to investigate natural and artificial optical irregularities in the near space allows to make a conclusion that the stage of informational analysis is one of the most important and practically useful when designing tomographic systems, intended for such kind of objects. It envisages a whole range of investigations. All of them are important in their own way, but in our view, there is a field of that failed so far to attract proper interest, for example, in medicine or nondestructive control, and this is the influence of projection informativity on reconstruction quality and the rate of obtaining acceptable results. But for such objects as natural and artificial irregularities in the near space, when the number of observation stations is scarce, and the cost of every new station is rather high, this issue may become one of priority ones. In fact, the problem lies in the possibility to optimize the location of observation stations. In this paper we shall try to illustrate importance of these investigations by the results obtained when modeling artificial structures and aurora to design ALIS

3. Criterion of informativity

It has been known long ago that projections obtained from different directions with respect to the object are unequal from the viewpoint of their contribution to the reconstruction process [Hamaker et.al., 1978, Luenberger, 1969]. The problem is that quantitatively evaluate this inequality. Of practical importance to our mind, are the results obtained by Dr. Kazantsev, who has suggested a quantitative estimate named "informativity" [Kazantsev, 1992]. A few words about this estimate.

If f is a true parameter distribution in the object, $f=R(G(\alpha))$ - distribution from reconstruction with help of operator R and $G(\alpha)$ - operator, describing data acquisition system, α - parameter of system rotation with respect to the object center, then the following requirement was considered:

$$(1) \quad d(f, f^\circ) = \min_{\alpha} d(f, R(G(\alpha))),$$

where d - is a chosen measure of image closeness. This equation leads to necessity of expression (2) minimization:

$$(2) \quad \|f_\alpha - Rf_\alpha\|^2 = \|f^2\|^2 - (\Gamma^{-1} p_\alpha, p_\alpha),$$

where p_α - projection of f in α - direction, Γ^{-1} - inverse Gram-matrix of system G .

This may be achieved by maximizing the second member in (2), but as the system G is generally non-orthogonal, it is difficult to obtain the informativity criterion in such a form. Therefore, Dr. Kazantsev supposed a simple case when system G is orthogonal, which leads to a possibility to obtain a simple analytical expression for quantitative informativity criterion.

In case of selected measure of closeness d for the 3- dimensional object, it will take the form:

$$(3) \quad Q(f, \alpha) = 1/2 \int \int (1-x^2-y^2)^{-1/2} p_\alpha^2(x, y) dx dy,$$

where p_α - projection of function f in α - direction.

Thus, at certain assumptions, we have a possibility to quantify the importance of projections obtained from different directions α . But one should prove that the criterion actually allows to choose projections which improve the results of reconstruction - to decrease the measure of closeness d or rise the rate of its decrease in the iteration process.

Drs. Kazantsev, Glazkov and Pickalov carried out modeling on certain regular objects which showed the reconstruction from a set of most informative projections to yield a 20-30% lower error, as compared to a less informative set of projections. The following value was used as a measure of closeness or reconstruction error:

$$(4) \quad d = \frac{\sum_{i=1}^N (f_i - f_i^*)^2}{\sum_{i=1}^N f_i^2}$$

where f_i and f_i^* - values of model and reconstruction in every point of definition region, N - numbers of discrete points in definition region.

4. Test of criterion to artificial structures.

We have also tested the above criterion on more complicated objects simulating the stratified stage of artificial ionospheric structure development using the sets of small number of projections. Our modeling also demonstrated the practical usefulness of criterion Q . Fig.1 shows the behavior of reconstruction error depending on the number of iteration for various amounts of projections and different high and low total informativity of projection sets. It follows from fig.1 that the difference in the accuracy of reconstruction is rather considerable, the more so, the less number of projections are used in the set. Thus, for instance, for 3 projections the difference can make up 40%.

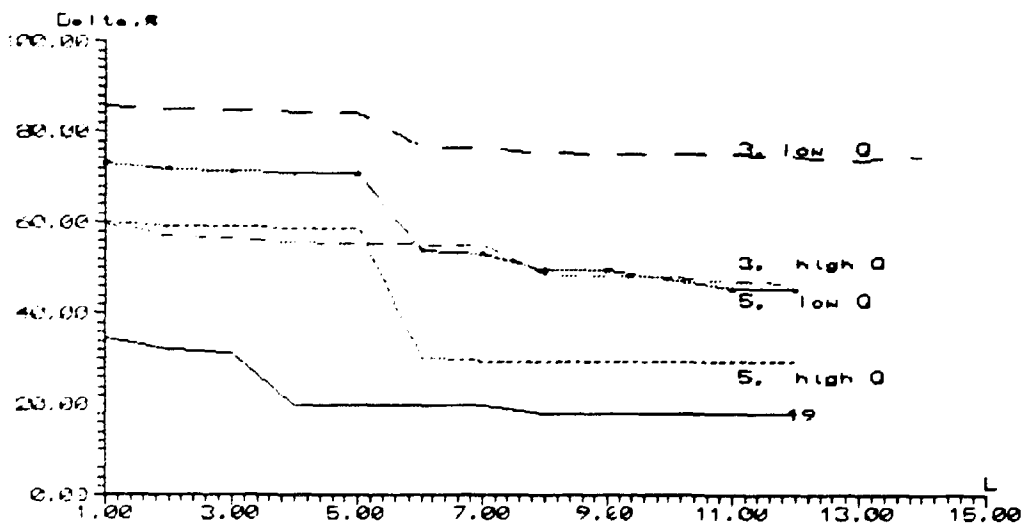
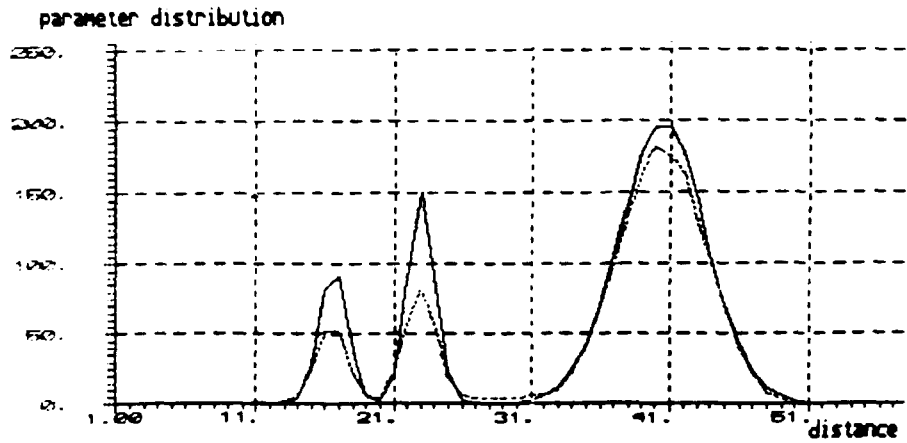


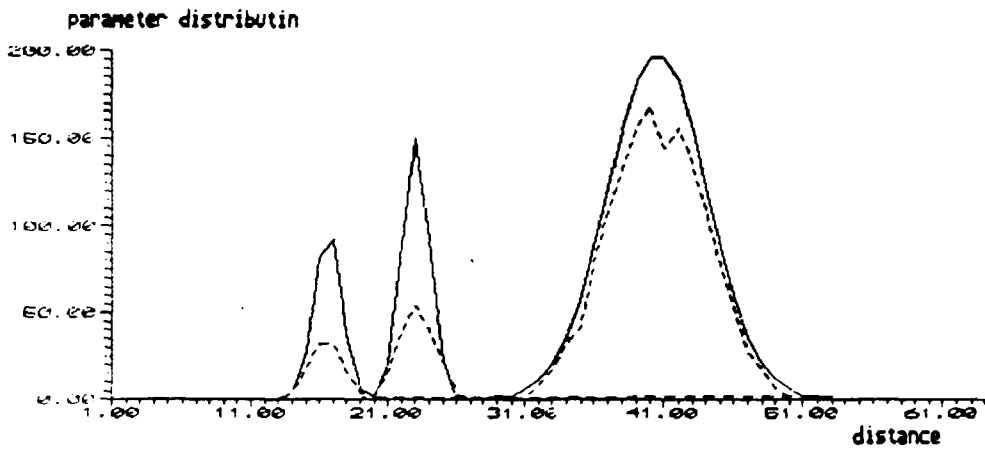
Fig 1

One should also estimate the importance of the measure of closeness, or error d in terms of its ability to reflect the similarity of the exact model and reconstructed solution. Fig.2 presents central cross-section of model and its reconstruction for the case of 19,5 and 3 projections, 3- and 5 -

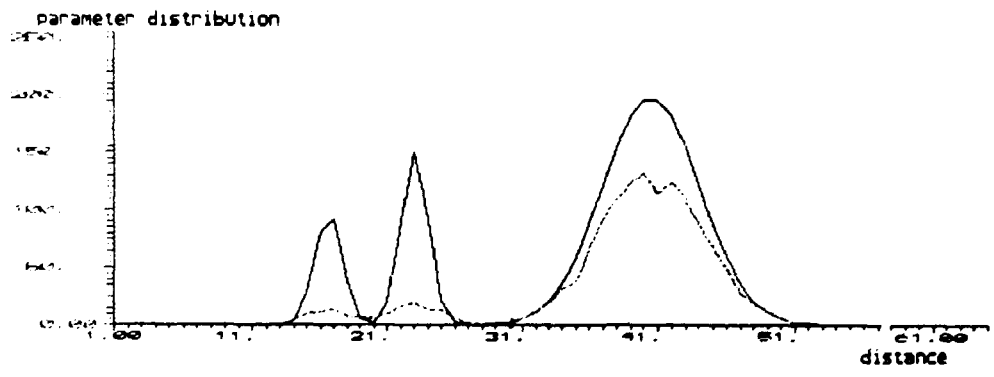
projection versions being based on the results obtained using a projection set of average informativity. I.e., errors were approximately equal to 20,50 and 70%.



Slice of model and reconstruction distributions for 19 projections.



slice of model and reconstruction distributions for 5 projections.



slice of model and reconstruction distributions for 3 projections.

Fig.2

It is seen from fig.2 how the error correlates with accuracy of the structure reconstruction. Even when the error is 75% at 3 aspects, the structure is reconstructed rather adequately, though the structure amplitude is attenuated and considerable artifacts appeared.

Thus, informativity criterion Q proved its operation capacity on regular models.

5. Test of criterion to auroral model.

The next stage involved modeling of a natural auroral irregularity. We have selected a model consisting of two arcs, each one being described by function f from Dr. Gustavsson's paper [Gustavsson, 1992]:

$$(5) \quad f = Kz^2 e^{-az - b(y - c \sin dx)^2}, z > 70 \text{ km}$$

where K - is a absolute value of stohastical process, a, b, c, d - any parameters.

We have realized the model in the form of two arcs on a grid of $64 \times 64 \times 64$ voxels with the same parameters a, b, c, d as in Gustavsson's paper.

Then we assumingly calculated conditions for derivation of parallel informativity projections for various projection directions with respect to the object mass center in the range of polar angles of $0-180$ and azimuth angles - $0-360$. For the sake of convenience we made use of relative informativities and the so called inhomogeneity index :

$$(6) \quad \gamma = Q_{\max}/Q_{\min}, \quad Q_{\gamma} = Q_i/Q_{\min},$$

where Q_i - informativity value for i -th projection, Q_{\max} and Q_{\min} - values of maximum and minimum of informativity

Fig.3 presents the distribution of relative informarivity for the accepted model of aurora on the Earth surface in the rectangular system of coordinates. Informativity decrease denoting the region of aurora projection on the earth surface.

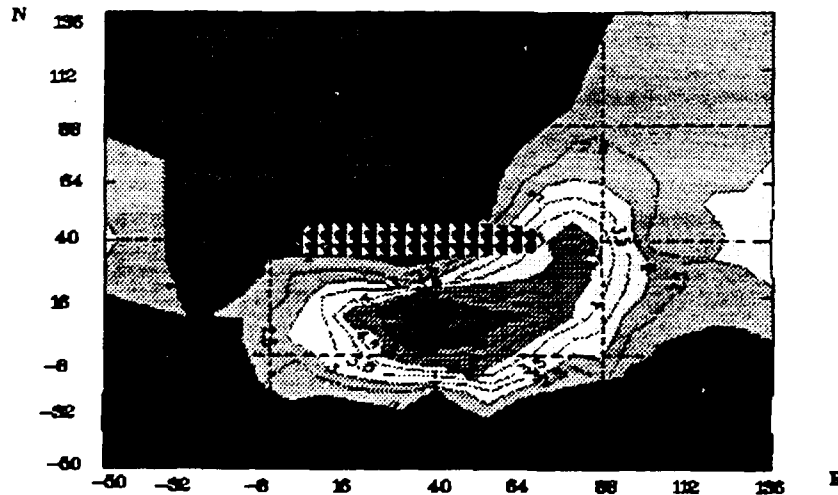


Fig. 3 Distribution of informative criterium.

Then we calculated informativities for 14 observation sites which are supposed to be in the ALIS system. Fig.4 and 5 show informativity distributions plotted on the locations of these sites for two different aurora positions. One can see which sites in which case are in the zone of high and low informativity.

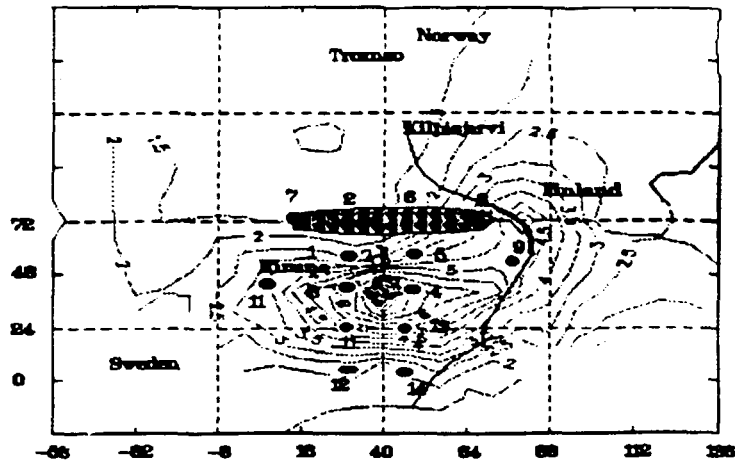


Fig.4

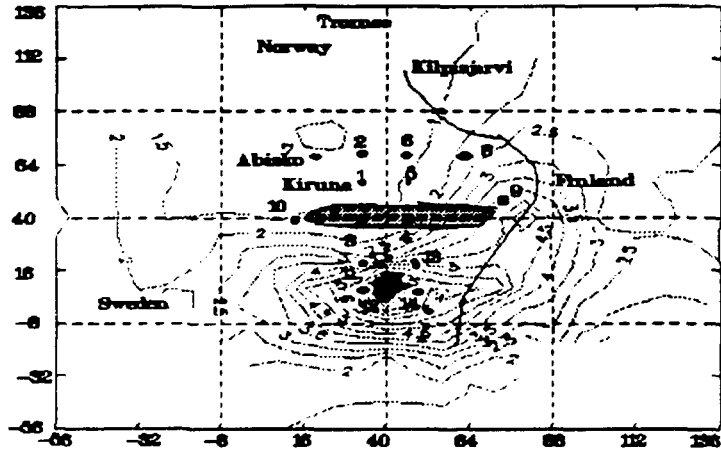


Fig.5

The next step was to compare registration errors at the most and least informative observation sites.

Modeling was carried out in the following way. At first we reconstructed all 14 projections, then 7 most informative and 7 least informative ones. In the first set the reconstruction was carried out according to projection numbering from Steen's paper [Steen, 1990], in the second - in the order of decreasing informativity, in the third one - in the order of increasing informativity. 3 iterations were made for each case. Fig.6 presents reconstruction error as a function of the projection number and iteration number.

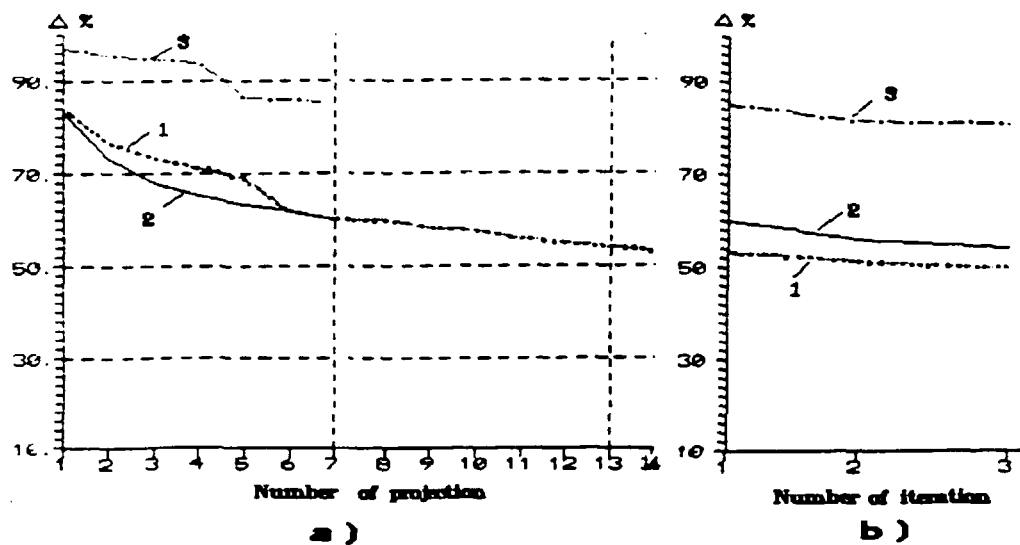


Fig. 8
Dependence of reconstruction error upon:
a) number of projection for first iteration
b) number of iteration. 1 - for 14 projections
2 - for 7 "informative", 3 - for 7 "uninformative"

It is seen that the error in the 2nd set decreases more rapidly as compared to the 1st one until an informative projection appears in the first set. It is seen from 9b that after 3 iterations the reconstruction error for the 2nd set is but 5% worse, as compared to the 1st set. A set of 7 non-informative projection produced a 80% error after 3 iterations. How did it really affect the structure reconstruction?

Fig. 7 presents vertical slices of the model region for the accurate and reconstructed solution of all the 3 sets, fig. 8 - same for perpendicular cross-sections. One can see that even after 3 iterations the model structure displays a good reconstruction both for 14 projections and the set of 7 informative ones. Whereas 7 non-informative projections produce an unsatisfactory reconstruction. Fig. 9 shows projection obtained from the model and from the reconstruction using all 3 sets, and confirms the abovesaid.

6. Possibility of optimization to cone beam projections.

The next stage should include the testing of criterion for cone beam projections typical of auroras. Several estimates using ART algorithm has been recently obtained for regular models.

Fig. 10 shows the scheme of cone beam modeling which produced a notable result. Theoretical concepts suggest that the reconstruction error should monotonously increase as the observation points stray away from the object. In our modeling the error has a minimum (see fig. 11) which varies depending on the model object. The minimum occurs at $S=5-15$, where S is the relative distance between the objects and the receivers. This can be measure of closeness d (see above) can be represented as:

$$(7) \quad d \approx \left(\frac{1}{\Sigma_1} + \frac{1}{\beta \Sigma_2} \right),$$

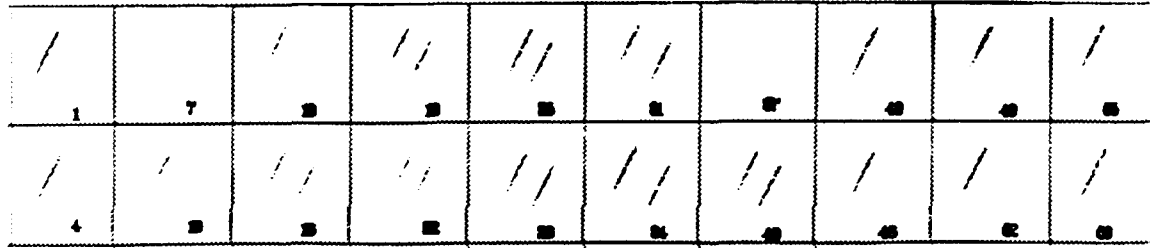
where Σ_1 - sum of intersection lengths of rays with object, Σ_2 - sum of intersection lengths of rays with shaped region
 β - coefficient, characterized relative importance of Σ_2 .

The dashed area in fig. 12 may be called a "stabilization" region, since the additions occurring in the region in the course of iteration will null or negative, which leads to artifact suppression. Hence, the above minimum.

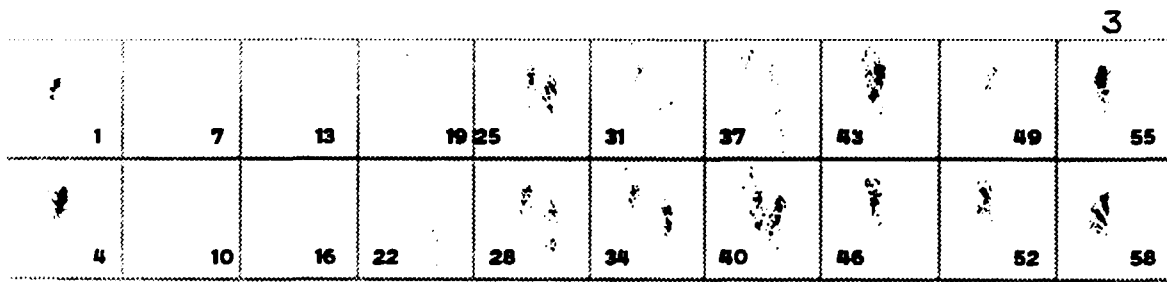
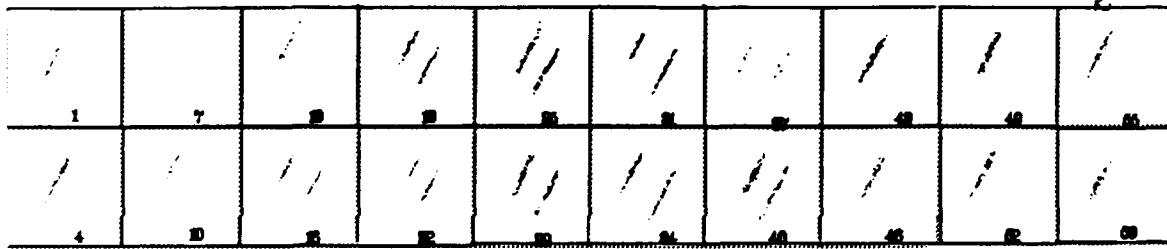
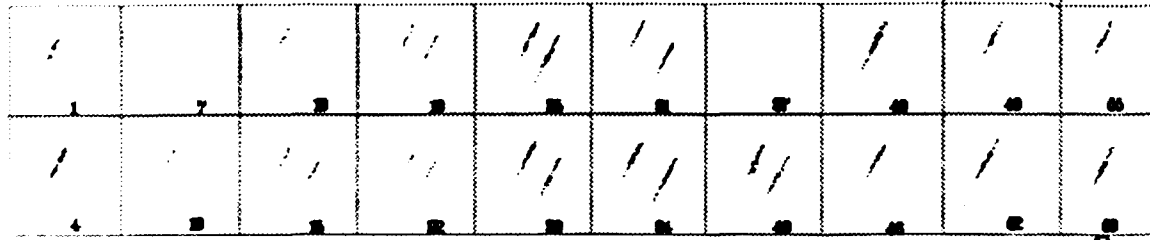
7. Conclusions.

Thus, the modeling has shown the informativity criterion Q to be applicable for various models and can be used for a priori informativity estimation of the suggested observation sites. Besides, the modeling has shown possible existence of an optimum distance between the observation sites and the object for the case of cone projection.

Model



Reconstructions 1

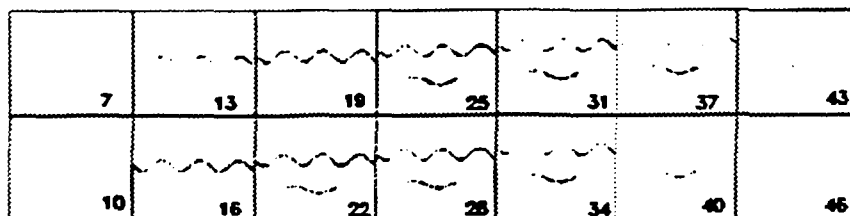


Comparison model and reconstructions
slice by slice in a vertical plane.

- 1) on 14 projections
- 2) on 7 "informative" projections
- 3) on 7 "uninformative" projections

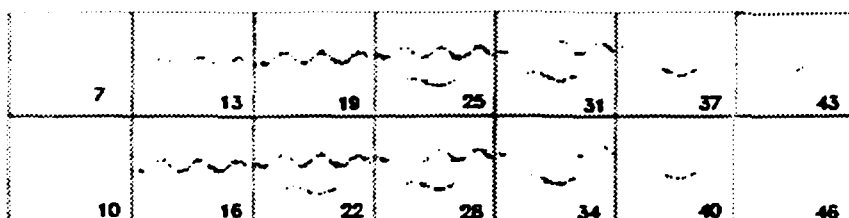
Fig.7

Model

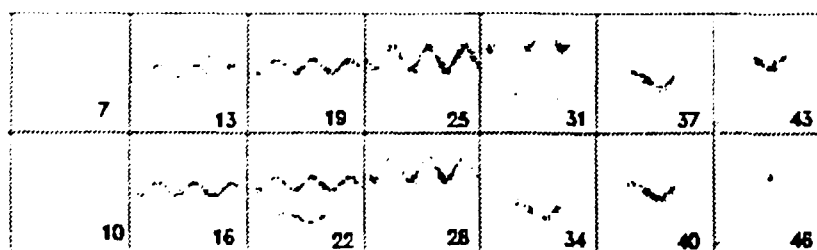


Reconstructions

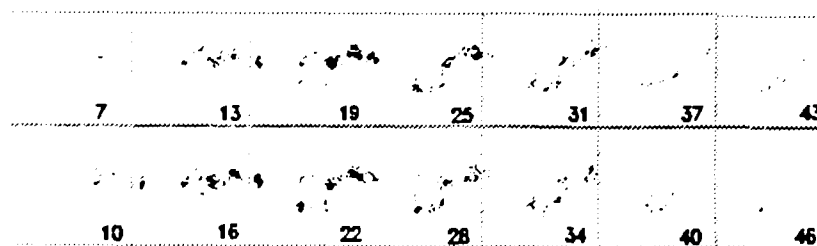
1



2



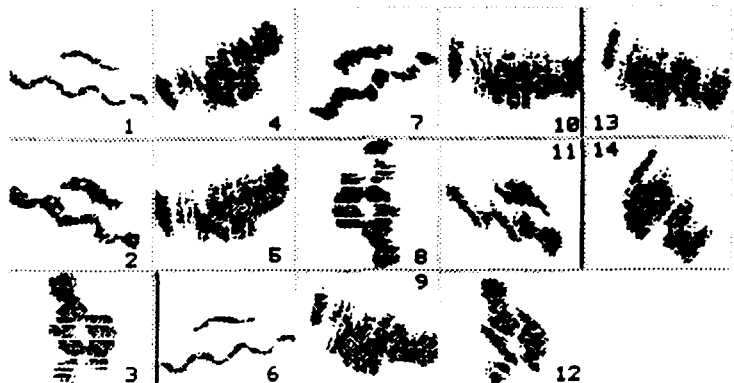
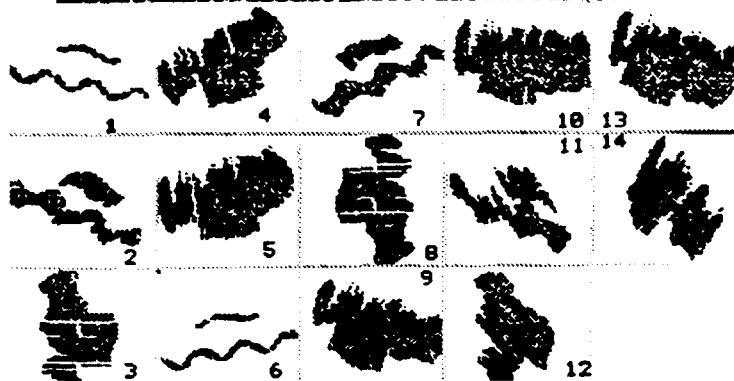
3



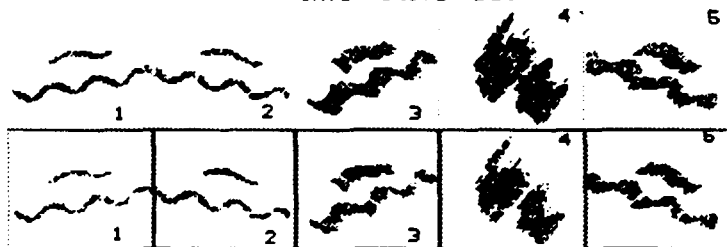
Comparison model and reconstructions slice by slice
 in a horizontal plane: 1) 14 projections of ALIS
 2) 7 "informative" projections 3) 7 "uninformative" projections.

Fig.8

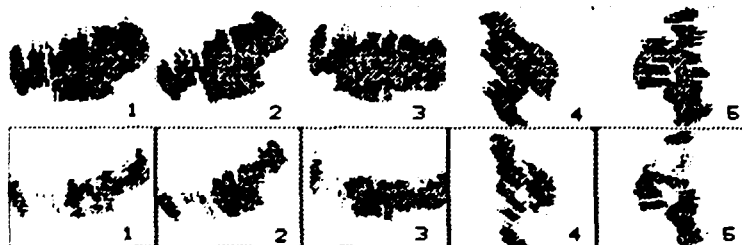
TOPAS - MICRO



"informative" set



"uninformative" set



Comparison projections made on model(top) and on reconstructions(bottom) for all 14 ALIS projections and for "informative" and "uninformative" sets.

Fig. 9

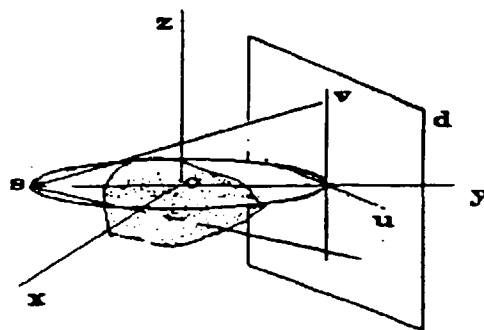


Fig 10 Scheme of cone beam modeling.

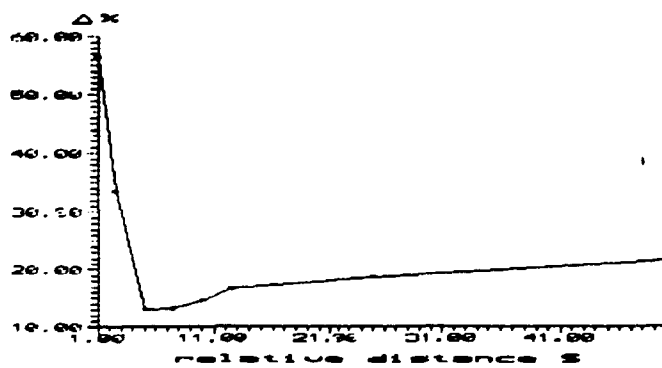


Fig.11

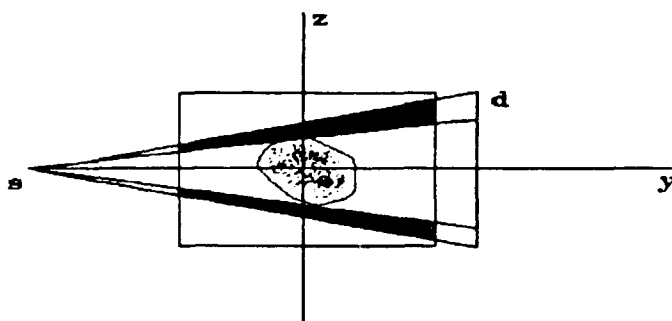


Fig 12 Scheme for explaining of minimum on curve.

This can also help to:

- a) optimize the observation scheme, which would improve the quality of reconstruction;
- b) optimize the reconstruction procedure so that it use the projections in the order of the decreasing informativity. Satisfactory results can be achieved more rapidly, which may be importance, for instance, when using the obtained solution in another reconstruction algorithm that requires a good initial approximation. To our mind, the results of the study may be used when constructing the ALIS .

8. Acknowledgments.

The authors gratefully acknowledge the help of Yu.A. Romanovsky and S.A. Chernous in discussion of problem and presentation necessary materials.

9. References.

- B.Gustavsson, "A study of feasible tomographic inversion techniques for ALIS", *IRF Technical Report 039, April 1992,ISSN 0284-1738*.
- C.Hamaker, D.C. Solmon, "The angles between the null spaces of X-rays", *J.Math.Anal.Appl.*,62,1978,pp.1-23.
- I.G. Kazantsev, "Information Content of Projections in Few-Views Tomography", *SPIE Vol.1843 Analitical Methods for Optical Tomography, 1992, pp.62-64*.
- D.C. Luenberger, "Optimization by Vector Space Methods", *Wiley,1969*.
- A.Steen , "A Scientific and Technical Description of ALIS", *Proc. NSSR Annual Meeting, Bolresjo, Norway,12-14 November,1990,pp.153-164*.

Imaging ionospheric electron density with tomographic techniques

Gijs Fehmers

T.U. Eindhoven, Department of Applied Physics
PO Box 513, NL-5600 MB Eindhoven, the Netherlands

Abstract

An important physical quantity of the ionosphere is the free electron density. Together with the magnetic field, this quantity determines the radio propagation in the ionosphere. The ionospheric plasma introduces a phase shift on the radiation going through it, eg. from stars or satellites. This phase shift can be measured if there is some reference phase. In the high frequency limit, the phase shift is found to be a measure of the line integral of the free electron density along the phase path. This line integral (the column density of electrons along the line of sight), is sometimes referred to as (slant) TEC, Total Electron Content. The line integrals can be converted to local electron density in the ionosphere using tomographic reconstruction methods.

Over the last few years people have done quite a lot of model calculations on this subject and some experiments have been executed as well. The experimental set-up is the following. A navigation satellite transmits two coherent carrier waves. The phase shift is measured using one of the carrier waves as a reference. The satellite is followed by a chain of receivers under the satellite's path on the earth. The satellite orbit and the receiver positions define a plane. The Total Electron Content along many lines in the plane is deduced from the measured phase shifts. These TEC data are used as input for the tomographic reconstruction of the electron density in the plane.

The rest of this contribution to the proceedings will be limited to the listing of some useful references:

Andreeva, E.S., Galinov, A.V., Kunitsyn, V.E., Mel'nichenko, Yu.A., Tereshchenko, E.D., Filimonov, M.A., and Chernyakov, S.M., 1990, "Radiotomographic reconstruction of ionization dip in the plasma near the earth", *JETP Letters*, **52**, 145.

Austen, J.R., Franke, S.J., and Liu, C.H., 1988, "Ionospheric imaging using computerized tomography", *Radio Science*, **23**, 299.

Fremouw, E.J., and Secan, J.A., 1992, "Application of stochastic inverse theory to ionospheric tomography", *Radio Science*, **27**, 721.

Kunitsyn, V.E., and Tereshchenko, E.D., 1992, "Radio tomography of the ionosphere", *IEEE Antennas and Propagation Magazine*, **34**, 22. Also appeared in *The Radioscientist*, **4**, 12.

Pryse, S.E., Kersley, L., Rice, D.L., Russel, C.D., and Walker, I.K., 1993, "Tomographic imaging of the ionospheric mid-latitude trough", *Annales Geophysicae*, **11**, 144.

Raymund, T.D., Austen, J.R., Franke, S.J., Liu, C.H., Klobuchar, J.A., and Stalker, J., 1990, "Application of computerized tomography to the investigation of ionospheric structures", *Radio Science*, **25**, 771.

Raymund, T.D., Pryse, S.E., Kersley, L., and Heaton, J.A.T., 1993 "Tomographic reconstruction of ionospheric electron density with EISCAT verification", submitted to *Radio Science*.

Yeh, K.C., and Raymund, T.D., 1991, "Limitations of ionospheric imaging by tomography", *Radio Science*, **26**, 1361.

Spectrotomography - a new method of studying the internal structure of the polychromatic objects

G.G. Levin, F.V. Bulygin, V.V. Alpatov

State Research Institute for Optophysical Measurements,
Institute of Applied Geophysics, Moscow, Russia

ABSTRACT

The paper describes a new approach to studying the spectral-spatial characteristics of the objects, proposed by the authors, and the results of its experimental testing. This approach is based on application of tomographic principles to the spectral investigations of the objects. The results obtained show the great advantages of this method for the spectral analysis of spatially extended objects.

1. INTRODUCTION

The valuable information about the structure and properties of various physical objects may be obtained by studying the spectrum of optical radiation formed by the object under study. The modern spectrometers have a high spectral resolution within the entire optical range. Anyhow, they help to produce the spectrograms of dotted or unidimensional objects only. But when studying the spatially extended objects using the spectral methods, it is necessary to obtain the information about the spatial distribution of object radiation spectral components. Such an information for two-dimensional objects is described by the expression $I(x, y, \lambda)$, which values correspond to the brightness of the point with coordinates x and y on the wavelength λ . Such a function, being a spectrogram of the two-dimensional object, is convenient to be represented in the form of the set of monochromatic images:

$$I_i = I(x, y, \lambda_i = \text{const})$$

One of the most simple methods of solving the given problem is to put the additional spectral filter to the recording optical channel. However, the interference filters make it impossible to reach both the high spectral resolution and the wide angular aperture needed for high spatial resolution. Besides, the necessity of its changing in optical channel considerably reduces the fast-response of such devices. The most substantial disadvantage of this method is the discrete character of the information on the object spectrum.

The use of the acousto-optical light filter gives the possibility to move quickly and continuously the transmission band of the device within the wide spectral interval. Anyhow, for such devices it is impossible to get simultaneously both the high spectral resolution and the wide angular aperture. One of the best results gained at the present time is the transmission band $\delta\lambda = 10\text{nm}$ at aperture value $\Delta\psi = 12^\circ$.

Described in paper² device had the Fabry-Perot interferometer used as a spectral filter. The set of monochromatic images was ob-

Described in paper² device had the Fabry-Perot interferometer used as a spectral filter. The set of monochromatic images was obtained at the interferometer output. Spatial separation of the images was effected with the help of the spectroscope provided with a wide inlet slit. The spectral interval of the device was determined by the working range of the interferometer reflecting coatings and amounted to 40nm. The device spectral resolution may reach 0.01 to 0.005nm, but the angular aperture was 13 only. The discrete information about the object spectrum may be also referred to the disadvantages of the device.

The other version for solving the problem of obtaining the spectrograms for two-dimensional objects is the spatial scanning of the object by means of a slit spectroscope. In this case a 2-D image is recorded, which represents the spectrum of the single image line of the object under study. If the high spatial resolution is needed, then it is necessary to get the considerable amount of spectrograms of such linear images. Such devices, called video-spectrometers, are widely used for the spectrozonal mapping of the Earth surface from space. In paper³ are described two of such devices, called AVIS and AVIRIS.

The polychromatic 2-D image can be presented as a three-dimensional spectral object $f(x, y, \lambda)$. Then, the device with a smooth or discrete readjustment of the transmission band actually records the image $f(x, y, \lambda = \text{const})$, i.e. the cross-section of the three-dimensional object. The scanning spectroscope gives the image $f(x, y = \text{const}, \lambda)$. We suggested a new method of obtaining the spectrograms of two-dimensional objects, which consists in recording the two-dimensional projections of three-dimensional spectral spatial objects, containing the integral information on all the cross-sections of the three-dimensional object simultaneously, instead of recording the individual cross-sections $\lambda = \text{const}$ or $y = \text{const}$. Further we show, that for the 3-D spectral object the set of the tomographic projections is possible to be obtained.

2. SPECTROTOMOGRAPHIC PROJECTION

Consider that the object is described by the function $f(x, y, \lambda)$ which corresponds to the intensities of 2-D image at various wavelengths λ (see Fig.1). Then we make the projection of this object on the surface (x, y) . It is evident that this projection at the angle $\theta = 0$ would be the photographic image of the object on the recorder sensibilized uniformly within the wide spectral range.

Projections for the angle $\theta \neq 0$ may be obtained when projecting to the dispersive element the two-dimensional image of the object but not the unidimensional slit as it is usually made in the spectroscopes. Thus, some images at the various wavelengths displaced and imposed on each other are obtained in the spectrum recording plane.

In paper⁵ the authors have proved that such projections possess all the properties of ordinary tomographic projections.

Using the spectral devices with various dispersions, it is

possible to obtain the set of projections with different probing angles. Then, using these data and the algorithms for 3-D image computed tomography, we can reconstruct the internal structure of the spatial-spectral object. The device for projection data acquisition may be the traditional optical spectrogram recording channel without the inlet slit, having the different dispersive elements subsequently introduced into it.

The other method for obtaining the spectrotomographic projections consists in varying the spatial probing angle φ with spatial-spectral probing angle θ remained constant. In this case, the totality of the probing beams for various angles φ in (X, Y, λ) -space is represented by the conical rotation surface, relative to λ -axis, with its top, located in the centre of the object under study, having the angle θ between the generatrix and the λ -axis.

The projection data acquisition device is similar to that described above except that, instead of changing the dispersive elements, the latter is rotated around the optical axis of the system. The spatial and spectral resolution of the reconstructed spectrotomograms are determined by the quantity, information content and the resolution of projection data, as well as by the type of the algorithm used. In the ideal case, we can expect that the spectrotomograms will combine the spectral resolution comparable with the resolution of the slit spectroscopes with the spatial resolution of the modern image input devices.

Another advantage of the spectrotomography is the possibility of employment of local tomographic algorithms.

The principle of the reverse Radon transform in the odd-dimensional space, which can be called the local transform, is presented in []. This transform allows to use for the reconstruction of the physical value in the determined point the set of the small parts of the projections, but not the full projections. The usage of this type of transform allows to create the algorithm of tomographic reconstruction without the procedure of the direct and reverse Fourier transform or unwieldy system of the algebraic equations.

The peculiarity of this transform is as follows. It uses the unidimensional projections, obtained as Radon integrals of the 3-D object through plane. In the most of the tomographic schemes the obtaining of such projections is impossible. The situation changes, when one of the directions of 3-D space is not spatial, but spectral. The device for obtaining unidimensional projection from 3-D polychromatic object can be easily realised in spectrotomography.

3. EXPERIMENTAL OBTAINING OF PROJECTIONS

The authors implemented the experiments for obtaining the projections and restoring the spatial-spectral objects using the both suggested probing techniques. In the first case, the spectral probing angle θ was varied and in the second one - the spatial azimuth angle φ .

3.1. Projections obtained in optical system with rotated dispersing element

The transparency with identical circular holes was used as an

object. The transparency was uniformly illuminated by two spectral lines of the mercury lamp $\lambda_1=546\text{nm}$ and $\lambda_2=577\text{nm}$, close in brightness. The projection recording optical channel was a confocal system similar to that described above. It is technically convenient to rotate the object image relative to the system optical axis, but not the dispersive element. The image was rotated using the mirror analog of the Dove prism. The prism was used as the dispersive element. The projection was read with TV camera and directed to the computer via FG 302 input device having 256×256 pixels. The probing spectral angle was defined similar to the previous experiment and amounted to 20° . We obtained 16 projections with rotation angle steps of $\Delta\varphi = 10^\circ$. The dimensions of the object spectral interval were taken to be equal to 130nm with boundaries at 500nm and 630nm . Spatial interval dimensions were selected so that the object image maximal size amounted to 0.7 of the spatial interval value. The centres of both intervals were chosen to coincide with the spectral and spatial 'centres of gravity' for the object.

3.2 Results of two-dimensional spectrograms reconstruction

The spectrograms were restored according to algebraic iteration algorithm on the grid $64 \times 64 \times 64$. The results of restoring are given in Fig. 4(a,b). The topograms of the restored object sections by planes (x,y) and (y,λ) (Fig. 4a) show, that the object spectrum consists of two spectral lines $\lambda_1 = 547\text{nm}$ and $\lambda_2 = 576\text{nm}$. The wavelength error relative to the spectral interval value is no worse than 7%.

The spatial characteristics of the object were determined from the topograms crossed by the planes (x,y) at a level, correspondent to λ_1 and λ_2 (Fig. 4b). These topograms are essentially the object images at the wavelengths λ_1 and λ_2 .

The circle diameter was determined at 0.5 level. The circle diameter ratio, the distances between the centres versus to cross-section sizes and the coordinates of the circle centres, lying within the reconstruction error of 10%, coincide with the actual object characteristics. After reconstruction, the object amplitude distribution in cross-sections (x,y) took the Gauss character and the spectral peaks widened. This can be explained from the properties of the tomographic reconstruction algorithm transfer function. Nevertheless, the true reconstruction of the studied object characteristics from the obtained topograms has become possible.

The authors have carried out the experiments on the obtaining the unidimensional projections and reconstructing the internal spatial and spectral structure of the model of the plasma jets and of the fluorescent crystal of carbon (diamond).

The results of the reconstruction are presented on the figures.

4. CONCLUSIONS

Two different types of optical data acquisition systems for spectrotomography were proposed and tested experimentally. The method of projections preprocessing, which allows to use tradi-

tional spatial tomographic reconstructive algorithms, was worked out.

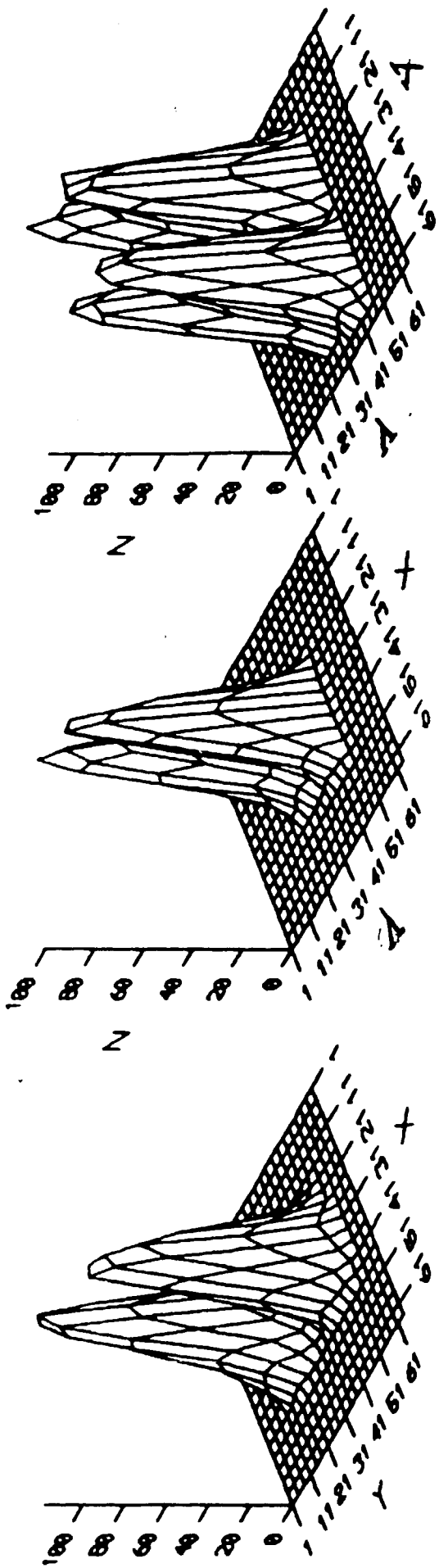
The local tomographic algorithms and software according to it was worked out and applied to reconstruction of the internal spectral-spatial structure of plasma jets and fluorescent crystal. This experiment has shown that speed of processing is much higher than when using traditional tomographic software.

The accuracy of reconstruction, achieved in the experiments, coincides with the accuracies, obtained in the model experiments with the same algorithms of spatial tomography, and provides the true reconstruction of spatial and spectral characteristics for the object of study.

The results obtained show the potentialities of the proposed method and the possibility of its wide application to different branches of science and technology.

5. REFERENCES

1. I.V.Belikov, G.Ya.Buimistryuk, V.B.Voloshinov et al., *Letters to the Journal of Technical Physics*, vol.10, no.20, p.1225, 1988 (in russian).
2. C.Korendyre, *Appl.Optics*, vol.27, no.20, pp.4187-4192, 1988.
- 3.A.Goetz, J.Wellman, W.Barnes, *Proc. of IEEE*, vol.73, N 6, 1985, p.7-29.
4. G.G.Levin, G.N.Vishnyakov, *Opt.Commun.* vol.56, N 4, 1985 p.231-234.
5. F.V.Bulygin, G.N.Vishnyakov *Proc of SPIE Analytical methods for optical tomography*, vol.1843 p.315-322, 1991.



Reconstruction of the model of the artificial barium cloud:
 Spatial section - xy , Spectral section - x_1 and y_1 .

Topograms of the sections.

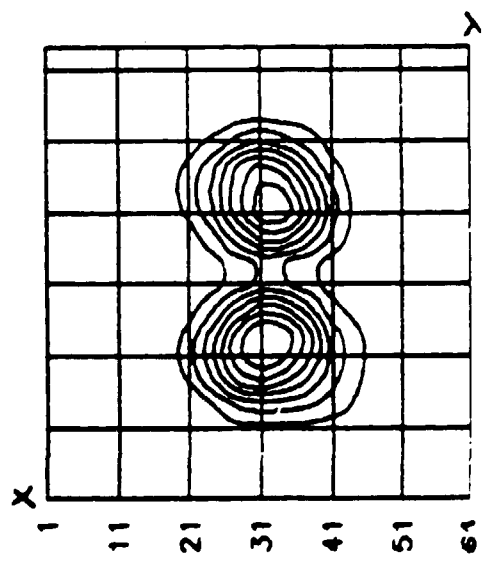
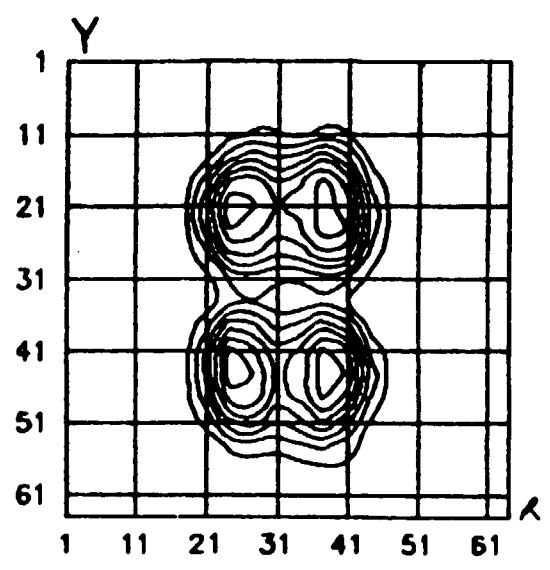
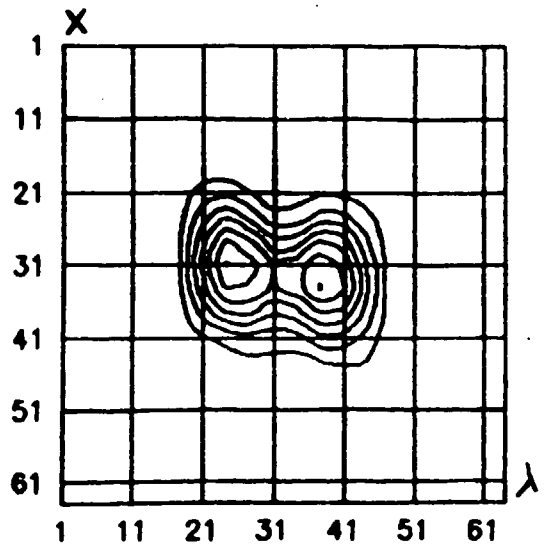




Image of the spectral - spatial section.

Fig.2

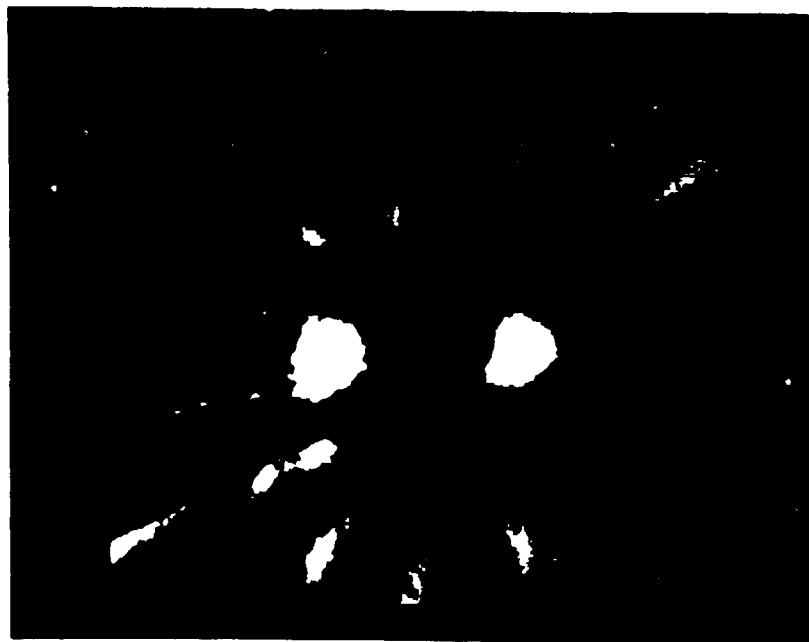


Image of the spatial section.

Reconstructed spectrum of plasma jets

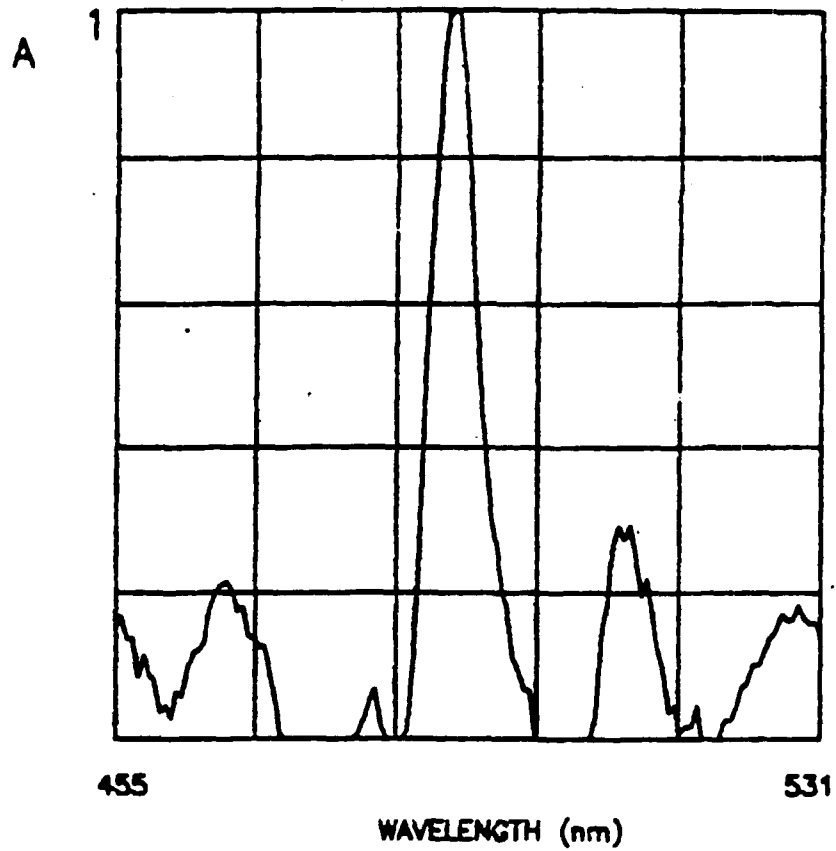


Fig.4

Isometry of the spectral-spatial section.

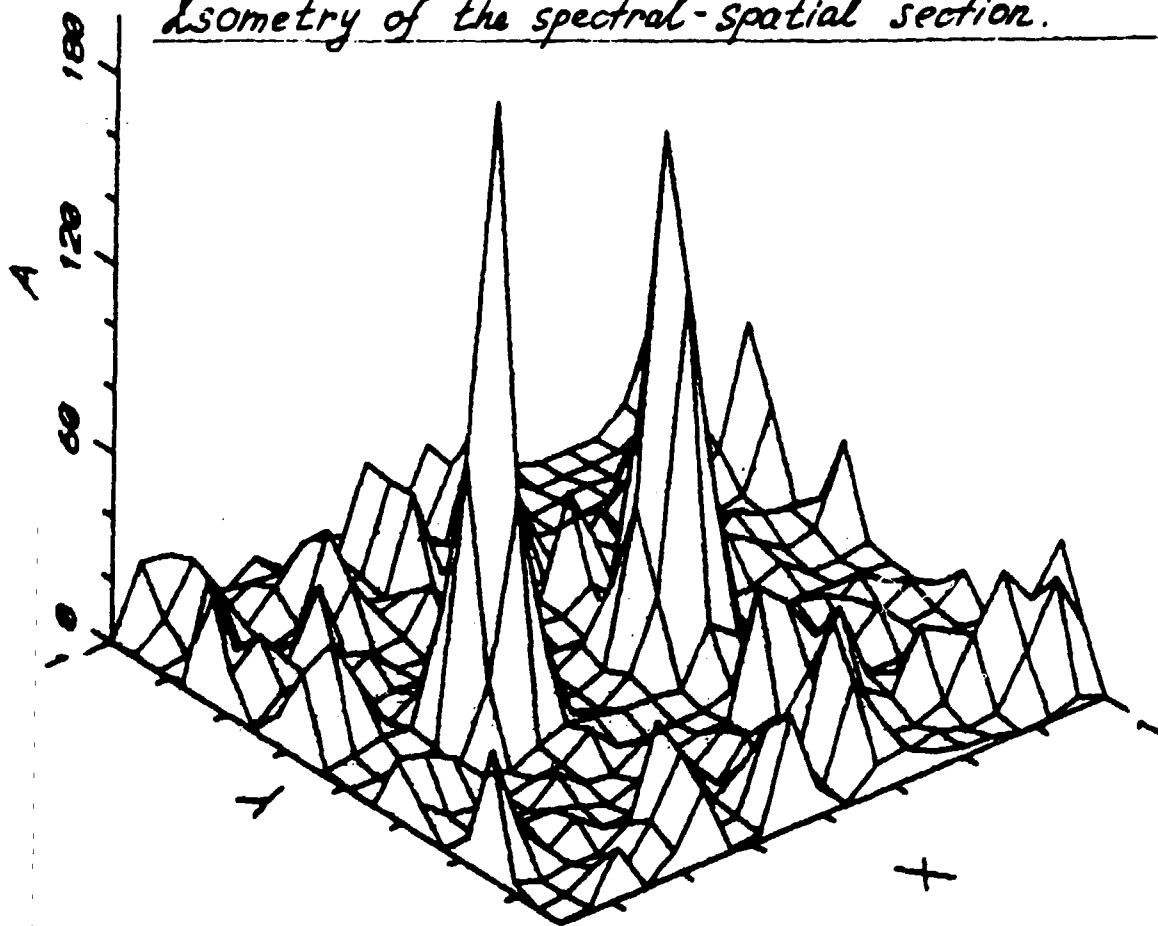
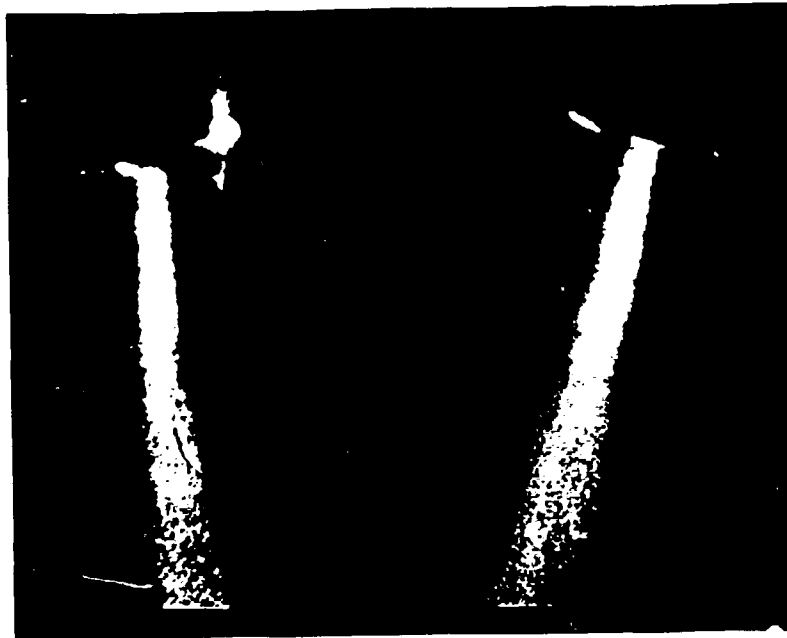


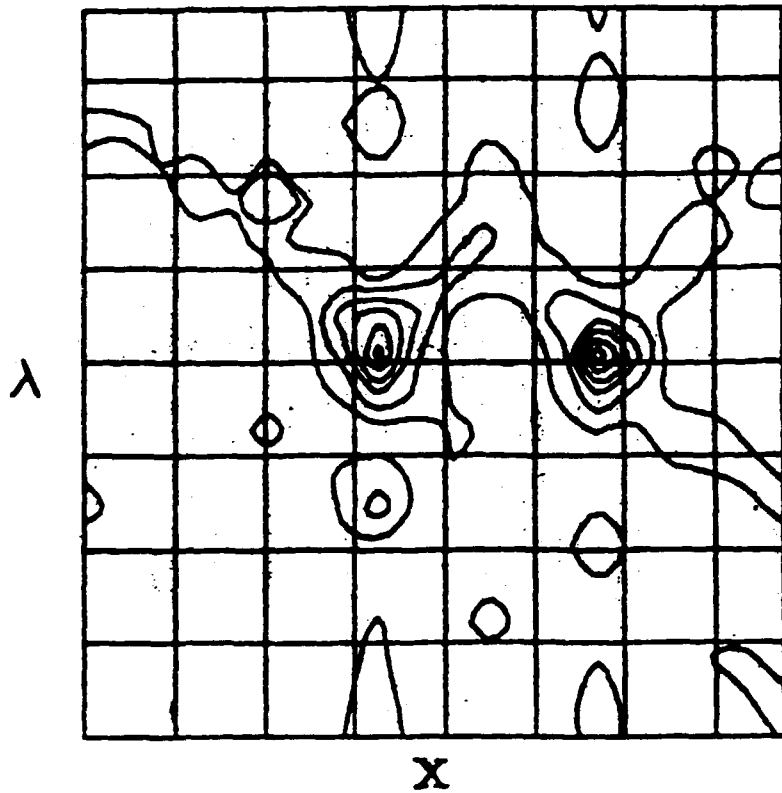
Fig.3



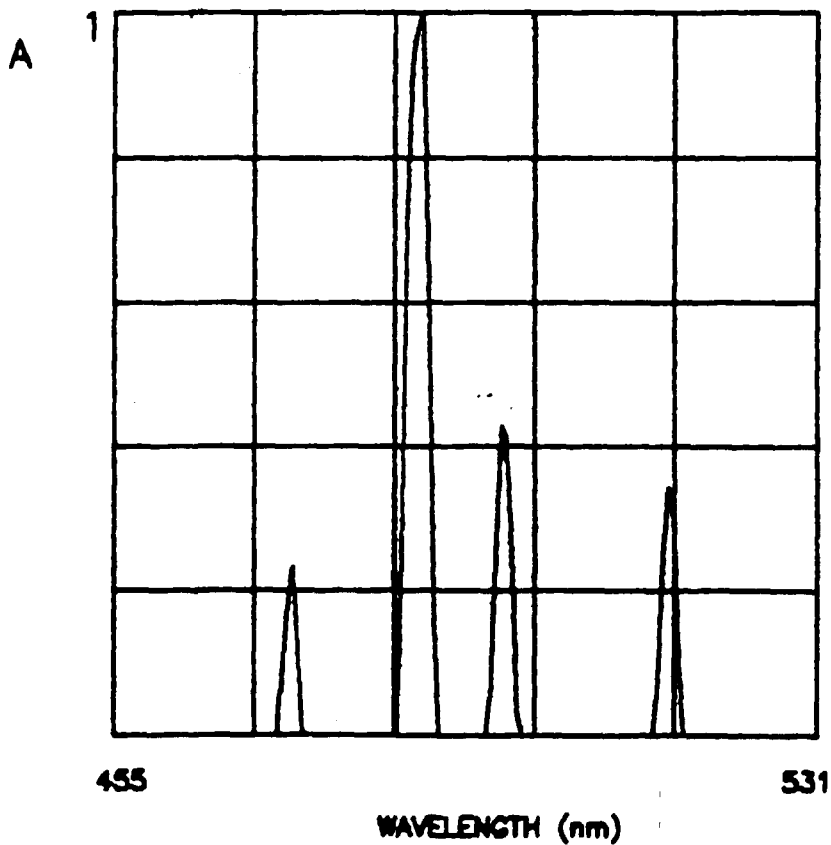
Projection of the plasma jets.

Fig. 5

Topogram of the spectral-spatial section



Real spectrum of the plasma jets



Test of auroral tomography methods for the ALIS project

V.S.Davydov, V.V. Pivovarov

State Optical Institute, 199034, St.Petersburg, RUSSIA

Abstract

Different techniques of evaluation of reliability of auroral tomography methods have been considered. Iterative algorithm of tomographic reconstruction of approximate 3-D aurora image based on single 2-D TV image and height brightness profiles obtained by geophysical rockets has been developed. Based on this algorithm, 3-D aurora model (50x128x128 with spatial resolution 1.5 km) designed for different tomographic techniques testing has been developed. Preliminary results of evaluations of noise, ALIS TV camera field of view size and spatial resolution influences on accuracy and convergence of ART method are presented.

Introduction

The problem of reconstruction 3-D aurora picture on basis of 2-D ALIS images can be solved by using tomographic inversion methods [1 - 7]. The accuracy of these methods depends on many factors, that's why it is necessary to develop the evaluation procedure of reconstruction quality for ALIS TV-cameras. Probably, a final conclusion on quality of reconstruction can be made only after simultaneous observation of aurora by ALIS system and geophysical rockets. This experiment allows to compare reconstructed aurora brightness altitude distribution with direct rocket measurements. The development of approximate 3-D computer models for the main auroral morphological forms and corresponding TV-images provides another way of tomographic inversion methods testing. A set of 3-D aurora models is also necessary for numerical experiments intended for determination of optimal TV-cameras field of view, spatial resolution of reconstruction, noise influence evaluation, e.t.c.

3-D model of aurora.

The 2-D projection of auroral brightness, obtained by i-TV camera is:

$$P_{i,\Delta\lambda} = \int_{\Delta\lambda} \int_V \frac{k(\lambda) \cdot B(\vec{r}, \lambda) \cdot \exp(-c(\lambda) \cdot |\vec{r} - \vec{r}_i|)}{|\vec{r} - \vec{r}_i|^2} dv d\lambda \quad (1)$$

where $B(r, \lambda)$ - the auroral intensity at wavelength λ at a point with coordinates r ; $c(\lambda)$ - atmospheric attenuation, $k(\lambda)$ - relative spectral sensitivity of TV camera, r_i - coordinates of i-camera.

Our laboratory conducted 5-rocket experiments at the Heiss island, exploring aurora at 70-170 km altitudes. Two spectroradiometers were installed on each rocket [9]. Both spectroradiometers had 30° field of view. One was directed along the axis of the rocket, another at 55° angle to the axis which made possible to scan in the upper hemisphere using the rotation of the rocket. Measurements were made at 391.4, 427.8, 530.0, 557.7 nm and 300-600 nm. Examples of height profiles of auroral emissions 557.7 and 391.4 nm, obtained in these experiments are presented in fig 1 [8].

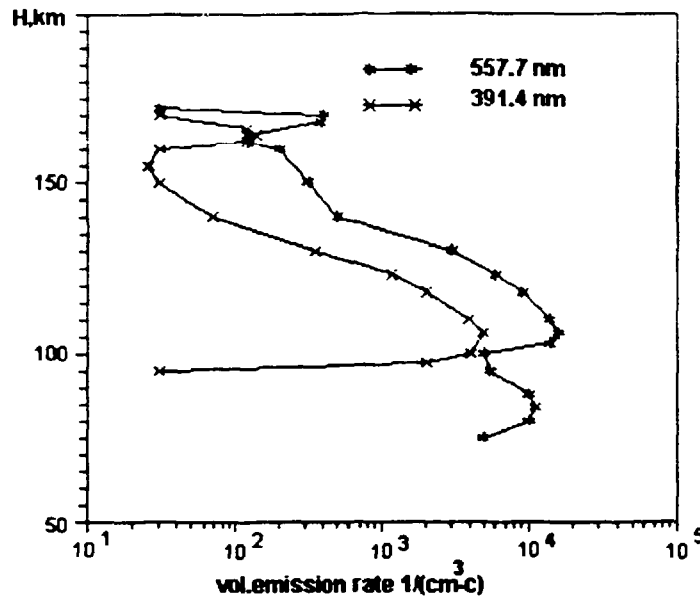


Fig. 1 Height profiles of volume emission rate .

From equation (1) and fig.1 one can realize that the difference of auroral spectra at different altitudes should be considered in the reconstruction method which uses wide spectral and images. That's why the test model should consist of two parts:

- model for one of the main auroral emissions (557.7 nm for example);
- model for a wide spectral band, concerning the difference of altitude distribution of main auroral emissions.

Our laboratory in cooperation with Polar Geophysical Institute have also made statistical investigations of auroral disturbances using ground based TV-cameras [10].

An analysis of auroral brightness height profiles have shown that their form in the absence of rays is approximately stable and only their amplitude changes. This fact allows to develop a method of tomographic reconstruction of approximate 3-D aurora image using single 2-D TV image and height brightness profiles obtained by geophysical rockets. The simple iterative methods similar to Gordon's ART [1] method have been developed.

If $B(h,x,y)$ is 3-D array of brightness then the TV image pixel intensity is:

$$P_{\varphi,\theta} = \sum_{(h_1,x_1,y_1)} \frac{B(h_1,x_1,y_1) \cdot \exp(-c(\lambda) \cdot |\bar{r} - \bar{r}_{h_1,x_1,y_1}|)}{|\bar{r} - \bar{r}_{h_1,x_1,y_1}|^2}, \quad (2)$$

where (h_1, x_1, y_1) are all points that lies within the solid angle which is projected on the pixel (φ, θ) . Brightness in the m-th iteration step is given by:

$$B^{m+1}(h_2, x_2, y_2) = \max [B^m(h_2, x_2, y_2) + \xi \cdot (P_{\varphi,\theta} - P_{\varphi,\theta}^m) \cdot B(h_2 = h_0, x_2, y_2) \cdot B_R(h_2) / N_{\varphi,\theta}, 0], \quad (3)$$

where (h_2, x_2, y_2) are all points on the ray parallel to magnetic field line, $B_R(h_2)$ - averaged relative rocket height profiles, $N_{\varphi,\theta}$ - is the number of points in the solid angle (φ, θ) , ξ - empirical constant. The numerical experiments have shown the good convergence of this method

after 20-30 iterations. The 3-D auroral model (50x128x128 pixels, 8 bit/pixel, with spatial resolution 1.5 km) based on TV image (256x256 pixels, 60x60 field of view) have been developed by means of this method.

Test of Algebraic Reconstruction Technic (ART).

Three iterative tomographic inversion methods were tested using a simple 3-D model. They are ART, Maximum Likelihood Reconstruction method and Multiplicative method. Numerical experiments have shown that ART method possesses the maximal accuracy. Probably Maximum Likelihood method can also be used in ALIS system after some improvements.

Evaluations of noise and spatial resolution influences on the reconstruction accuracy for ART method were obtained. The mean square error of reconstruction for such points in the 3-D region which lie within the TV cameras field of view was used as index of reconstruction quality. The uniformly distributed random component with maximal amplitude 2%, 5% and 10% was added to all TV images in order to evaluate the noise influence on reconstruction quality. The results of evaluation are shown in fig. 2. If maximal noise amplitude is >10% then ART method diverges after 8-10 iterations (see fig. 2). The influence of a spatial resolution on reconstruction accuracy was evaluated for TV cameras with 60° field of view. The ratio of the spatial resolution of a region under reconstruction to the spatial resolution corresponding to one TV image pixel (altitude 170 km, zenith angle 30°) was 0.6, 1.0, 1.5, 2.0.

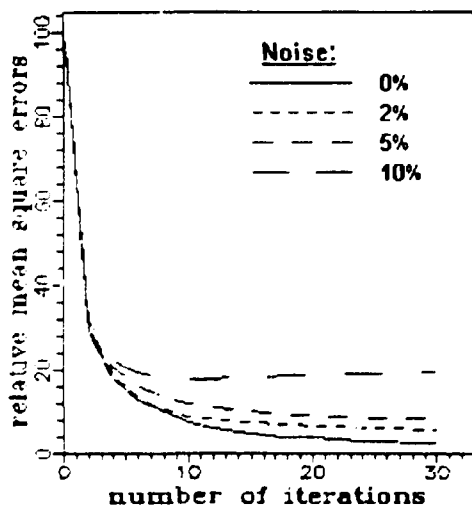


Fig. 2 Estimations of noise influence.

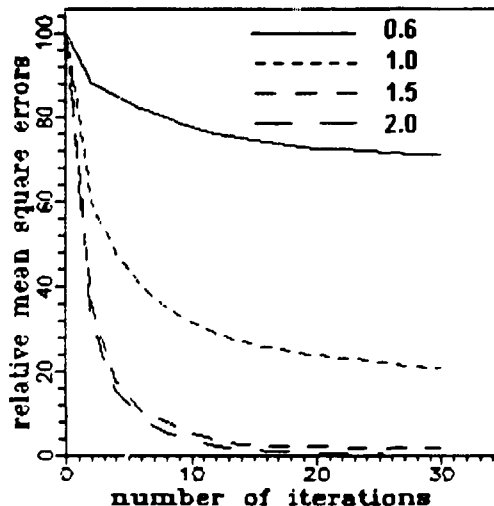


Fig. 3 Estimations of field of view influence.

The results of evaluation are shown in fig. 3. Experiments have demonstrated that the reconstruction accuracy is practically independent of TV cameras field of view (within 60°-90° range) if the rate of one pixel spatial resolution to spatial resolution of a region under reconstruction is constant.

The accuracy evaluations presented in this paper are preliminary and demand more detailed investigations.

REFERENCES

- 1 Gordon R and Herman G. "Algebraic reconstruction techniques (ART) for three-dimensional electron microscopy and x-ray photography", J. Theor. Biol., vol. 29, 1970.
- 2 Veclerov E and Llacer J. "Statistically based image reconstruction for emission tomography", Int J Im. Syst. and Tecn., vol. 1, 1989.

3. Shepp L. and Vardi Y. "Maximum likelihood reconstruction for emission tomography", IEEE Trans. Med. Im., vol MI-1, No. 2, oct. 1982.

4. Peyrin F.C. "The generalization back projection theorem for cone beam reconstruction", IEEE Trans. Nuc. Sci., vol NS-32, No 4, aug. 1985.

5. Вишняков Г.Н. "Восстановление томограмм трехмерных объектов по двумерным проекциям", Оптика и спектроскопия, т. 65, вып. 3, 1988.

6. Tom K.C. "Multispectral limited-angle image reconstruction", IEEE Trans. Sci., NS-30, No 1, 1983.

7. Gustavsson B. "A study of feasible tomographic inversion techniques for ALIS", IRF Technical Report, april 1992.

8. Давыдов В.С., Орлова М.В., Хохлов В.Н. "Соотношение интенсивностей эмиссий [O] и N₂⁺ в полярных сияниях в светлое время суток." В кн.: Полярные сияния, М. ВИНТИ, ' 32, 1985.

9. Давыдов В.С., Блинков Ю.Ш., Микиров А.Е. и др. "Спектрорадиометры СР-184, СР-185 для измерения яркости верхней атмосферы Земли." Труды ИПГ, вып. 36, 1979.

10. Пивоваров В.В., Черноус С.А. "Цифровая обработка измерений пространственных неоднородностей яркости полярных сияний телевизионной аппаратурой." В кн.: Методы и средства вычислительного эксперимента, Апатиты, изд. КНЦ АН СССР, 1991.

Possibilities of calibration of auroral tomography methods by direct rocket measurements

V.S. Davydov ¹⁾, V.V. Pivovarov ¹⁾, S.A. Chernouss²⁾

¹⁾ State Optical Institute, 199034, St. Petersburg, RUSSIA

²⁾ Polar Geophysical Institute, 184200, Apatity, RUSSIA

Abstract

In this paper we demonstrate how the Auroral tomography method may be calibrated by rocket photometers measurements. The rocket payload for measurements of altitude distribution of auroral emissions is under consideration. Technical parameters of the existing Russian rocket filter photometers are discussed. Proposals for the experiment of simultaneous measurements of the aurora by ground-based camera of ALIS and by rocket photometers are advertised.

Introduction

The problem of recovering three-dimensional spatial distributions of auroral emission from ground-based auroral brightness measurements is an essential task of the ALIS project [1]. It can be solved by the tomography inversion procedure, described in [2-5]. The accuracy of the tomography inversion method depends on many factors and that should be tested both by numerical evaluation procedure and by direct measurements of brightness in the aurora. The single possibility to measure an altitude distribution of auroral intensity are measurements by geophysical rocket optical payload. From the other side this altitude profile could be reconstructed on the base of 2-D data of ALIS cameras. Thus a final conclusion on the quality of reconstructed of 3-D aurora by 2-D images of ALIS camera network could be done on the base of comparison of simultaneous rocket and ground-based observations.

The rocket photometry measurements are widely used to study aurora and airglow. State Optical Institute in cooperation with Polar Geophysical Institute and Hydrometeorological Service of Russia carried out more than 70 launches of geophysical rockets in different points of the Globe. The main payload optical instruments used in this launches were spectroradiometers (filter photometers "TWA" and "JAWA").

In this report we propose to organize ALIS-Rocket campaign with using of the Russian payloads. The main scientific objective of the ALIS-Rocket experiment is to obtain height profiles of the aurora simultaneously by direct "TWA" and "JAWA" rocket photometers measurements and by the reconstruction tomography methods from ALIS pictures. The experiment permits us to choose the most sophisticated tomographic inversion procedures from different methods of auroral tomography.

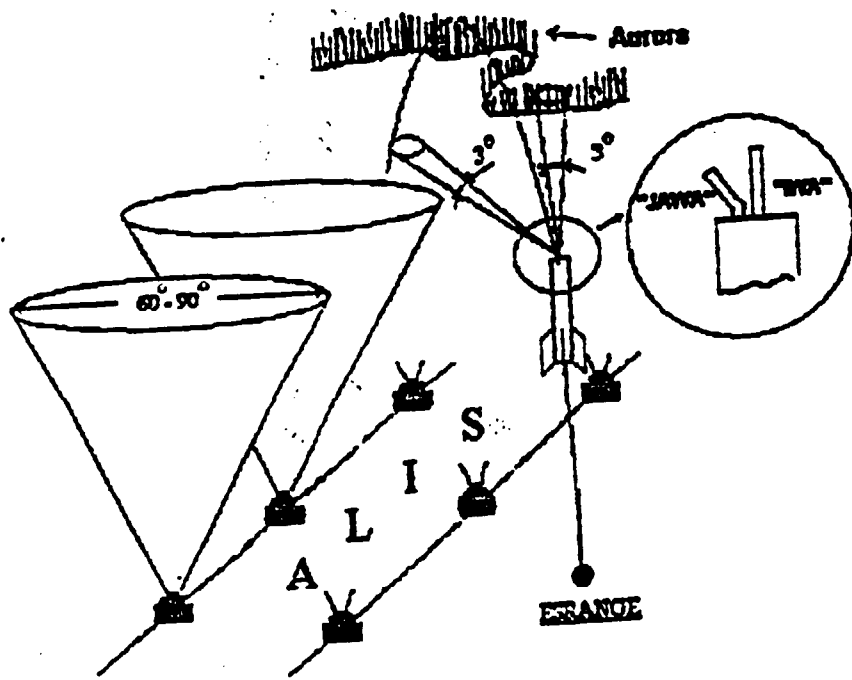


Fig. 1 Scheme of the ALIS-Rocket experiment

Scheme of the proposed experiment is given in Fig. 1. Height profiles could be obtained from both vertically-directed and side-directed rocket photometers. The accuracy of the measurements of the altitude profiles could be in the order of 1-2 km. Of course the stable auroral arc is the best object for this kind of experiments because both spatial and time variation at the aurora can influence on the accuracy of measurements.

Instrumentation

Filter photometers "IVA" and "JAWA" were intended for upper Earth atmospheric radiation research from the geophysical rockets. View of photometer "JAWA" (1,2) and solar protection sensor (3,4) is shown in fig. 2. Photometer "IVA" was directed along the axis of the rocket. Measurements are available at 391.4, 427.8, 530.0, 557.7 nm with $\Delta\lambda=4$ nm and 300-600 nm. Other arbitrary filters in the range 300-600 nm also available. Photometer "JAWA" was directed at 55° angle to the axis of the rocket which made possible to scan in the upper hemisphere using the spinning of the rocket. Measurements are available at 369, 457, 530, 576 nm with $\Delta\lambda=20$ nm and 300-600 nm. Both photometers have 3° field of view and similar optical architecture. The optical scheme of photometer "JAWA" is shown in fig. 3. The scheme consists of light baffles (1-3), objective (10), opaque screen (11), inner baffle (4,5), stop aperture (12), lenses (13,16), mirror (14), interference filter wheel (6), condenser (8,9), chopper (20), photomultiplier tube (21), reference light source system (15,17-19).

Cinematical scheme of photometers (see fig. 4) consists of reducer (1), radioluminescence light source (6), variable density ring-shaped neutral filter (7), the beginning of measurement cycle sensor (8), wheel (9) with mirrors (2) and filters (3), mirror of radioluminescent source (10), solar protection sensor mechanism (11), lamp for photomultiplier tube training (14).

A typical sequence of operations of the photometers is shown in fig. 5. Signals are simultaneously registered from three outputs I, II, III with gain factors which differ approximately by a factor of 4 from each other. Each cycle of measurements consists of nine equal intervals. Six times per cycle signal passing through different neutral or interference filters and three times per cycle linearly increasing calibration signal is registered. Calibration signal in the cycle of measurements allows to control the instability of photomultiplier tube and electronic path of instrument. The control is based on the comparison of measured signal with the known calibration signal, passing through identical stages of transformation, amplification and processing.

Technical characteristics of photometers

	"IVA"	"JAWA"
Threshold sensitivity	$3 \cdot 10^{-11}$ w/cm ² /sr	$1 \cdot 10^{-10}$ w/cm ² /sr
Field of view		3°
Response time	100 ms	5 ms
Power supply voltage		27V
Power consumption		80W
Weight		17.5 kg

The photometers have been tested at special vibrostands for rocket payload and several ones are conserved in State Optical Institute in the special container with nitrogen atmosphere.

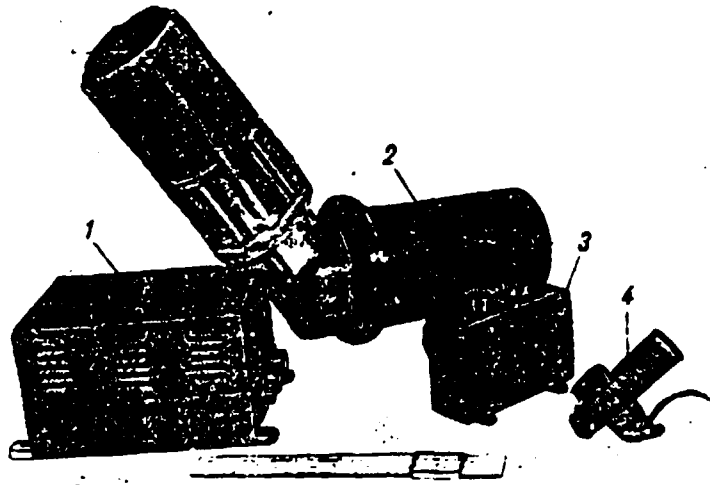


Fig. 2 Photometer "JAWA".

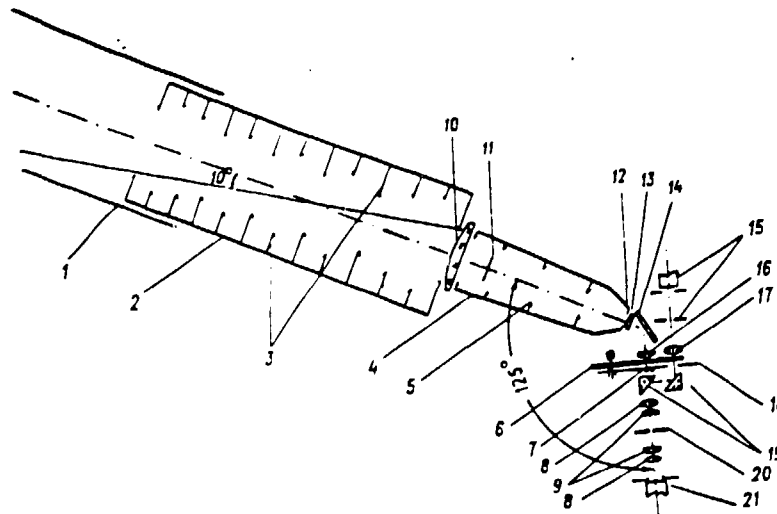


fig. 3 Optical scheme of photometer "JAWA".

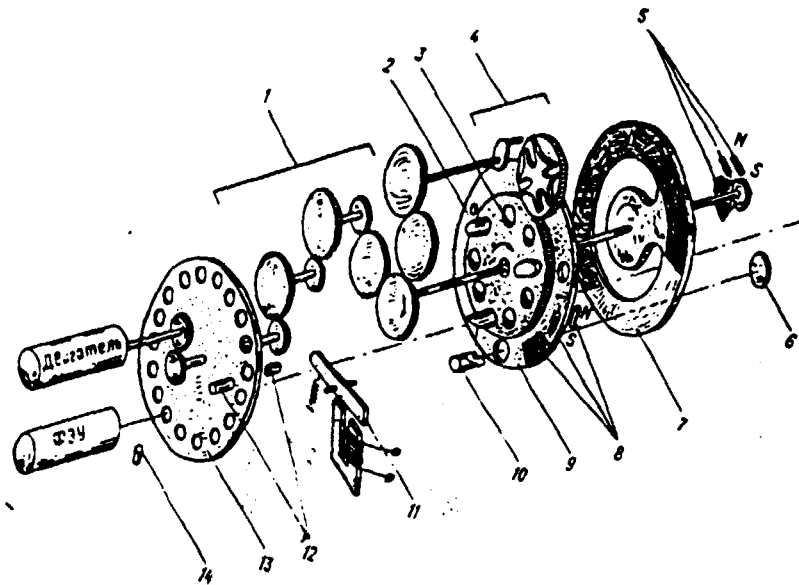


Fig. 4 Cinematical scheme of photometer "JAWA".

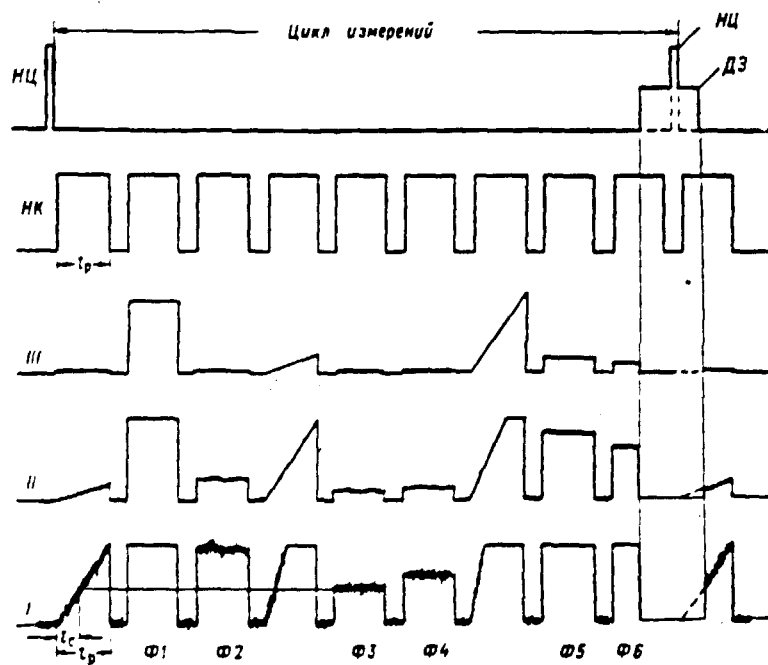


Fig. 5 A typical sequence of operations of the photometers.

Discussion and conclusion

There are scientific objections and technical possibilities of the providing the project ALIS-Rocket. First of all the aim of the experiment is the direct calibration of tomographic reconstruction of 3-D aurora from ALIS 2-D pictures. We suppose that this experiment will give better quality of the scientific results received in the future scientific studies connected with ALIS project. It is valuable and cheap to use already prepared and tested optical instrument payload. The launches could be provided by ESRANGE for example by Nike-Orion or other motors. It is obvious that the problem of adaptation of telemetry and mechanics should be solved. To promote the development of those works it is reasonable to gather well experienced participants from State Optical Institute (St. Petersburg) . Polar Geophysical Institute (Apatity) and Polar Range to prepare together with IRF (Kiruna) and ESRANGE scientists and engineers well-based project ALIS-Rocket for 1994-1995 . We hope to search financial support for that in ESA and the Russian Government Science department and in some special funds for Eastern Europe.

REFERENCES

1. Brandstrom U. and Steen A. "Report on the ALIS-project", Proc. of the 19th Annual European Meeting on Atmospheric Studies by Optical Methods, Kiruna, Sweden, August 10-14, 1992.
2. Gordon R. and Herman G. " Algebraic reconstruction techniques (ART) for three-dimensional electron microscopy and x-ray photography", J. Theor. Biol., vol. 29, 1970.
3. Veclerov E. and Llacer J. "Statistically based image reconstruction for emission tomography", Int.J.Im. Syst. and Tec., vol. 1, 1989.
4. Shepp L. and Vardi Y. " Maximum likelihood reconstruction for emission tomography", IEEE Trans. Med. Im., vol MI-1, No. 2, oct. 1982.
5. Peyrin F.C. "The generalization back projection theorem for cone beam reconstruction". IEEE Trans. Nuc. Sci., vol NS-32, No 4, aug. 1985.

Feasibility study of ionospheric tomography with radio telescopes

Gijs Fehmers

April 28, 1993

Abstract

With radio telescopes astronomers monitor cosmic radio sources. The observations are affected by the troposphere and ionosphere. A few times a day they do calibration measurements of point sources with known position and intensity to correct for this. These data contain information on the ionospheric electron content (column density).

Over the last few years there has been a great deal of interest in ionospheric tomography using beacon satellites. Data on electron column density from these satellites is used in tomographic inversion to image the electron density. It has been suggested to use data from spaced radio telescopes for ionospheric tomography as well. This paper deals with the question whether this is possible.

It is found that only a very basic form of diffraction tomography offers possibilities. For the Westerbork Synthesis Radio Telescope, it would permit location of a scatterer up to a maximum altitude of ~ 32 km, with a horizontal resolution of 144 m and a vertical resolution of ~ 6 km. Please note that this is well below the ionosphere.

1 The idea

The radio interferometer is the most important tool in radio astronomy. It consists of an array of radio telescopes placed along a line, or sometimes in a more complex geometry. For most purposes the interferometer can be considered as the combination of interferometer pairs. Every interferometer pair measures time delay and amplitude of the incoming radiation.

The amplitude is a measure of the brightness of the source. The time delay τ , is the delay in the signal over the two telescopes. Now, from figure 1,

$$\tau = \frac{D_{12} \cos \beta}{c}, \quad (1)$$

where c is the speed of light. From D_{12} , τ , and (1) the astronomer calculates β , which is a fix on the position of the source in the sky. Determining τ for baselines with different

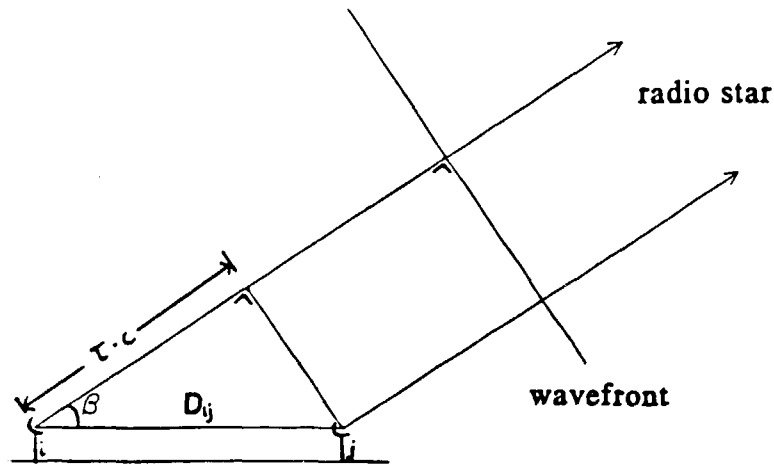


Figure 1: A radio interferometer measures the time delay τ in the radiation from a cosmic point source.

orientation and length, allows calculation of the position of the source in the sky. The larger the baseline D , the higher the resolution.

It is clear that the radiation at the two antennas must be correlated, for there is no time delay between two uncorrelated signals. If the radiation at the antennas is uncorrelated, the measured amplitude is zero and the time delay is undefined. (In fact the instrument is based on electronic correlators.)

Here we will limit ourselves to the response of the instrument to monochromatic cosmic point sources; this makes things easy, while it is sufficient for our purposes. Please keep in mind that the wavefront is plane. As the source is monochromatic, the amplitude of the electro magnetic field at the antenna is harmonic. In that case the time delay can be substituted by a phase difference $\Delta\psi_{ij}$,

$$\Delta\psi_{ij} = \psi_i - \psi_j = 2\pi f\tau, \quad (2)$$

where ψ_i is the phase at telescope i , and f is the frequency. Now (1) becomes,

$$\Delta\psi_{ij} = 2\pi \frac{D_{ij} \cos \beta}{\lambda} \pmod{2\pi} \quad (3)$$

Due to ionospheric refraction, a phase shift ϕ_i^{ion} is introduced in the radiation on its way to telescope i . The phase difference measured at interferometer pair ij then becomes

$$\Delta\psi_{ij}^* = \psi_i + \phi_i^{\text{ion}} - (\psi_j + \phi_j^{\text{ion}}) = \Delta\psi_{ij} + \phi_i^{\text{ion}} - \phi_j^{\text{ion}} = \Delta\psi_{ij} + \Delta\phi_{ij}^{\text{ion}} \quad (4)$$

In its turn, this shift $\Delta\phi_{ij}^{\text{ion}}$, through (3), causes an error in β and in the determined position. To correct for this effect, and to calibrate the brightness, astronomers carry

out calibration measurements of point sources with known position and brightness. The calibration gives $\Delta\phi_{ij}^{ion}$. Next we will derive an expression for ϕ^{ion} and we shall see what the calibration measurements say about the ionosphere.

Most observations in radio astronomy are carried out at frequencies $f > 100$ MHz. The electron gyrofrequency f_{ce} in the ionosphere is given by

$$f_{ce} = \frac{eB}{2\pi m_e} \approx 1.4 \text{ MHz}, \quad (5)$$

with $B \approx 0.5 \times 10^{-4} T = \frac{1}{2}$ gauss. As $f \gg f_{ce}$, the high frequency limit in ionospheric radio propagation is reached. In that case the Appleton Hartree formula for the index of refraction is well approximated by

$$n^2 = 1 - \frac{f_p^2}{f^2}, \quad (6)$$

where f is the frequency of the radiation and f_p is the electron plasma frequency:

$$f_p^2 = \frac{e^2 N_e}{4\pi^2 m_e \epsilon_0}. \quad (7)$$

N_e is the electron density. In the ionosphere, $N_e \lesssim 2 \times 10^{12} \text{ m}^{-3}$, thus $f_p \lesssim 13$ MHz. As $f^2 \gg f_p^2$, we are allowed to approximate n from (6) by the first order Taylor expansion:

$$n \approx 1 - \frac{f_p^2}{2f^2}. \quad (8)$$

Now, $\phi^{ion} = 2\pi\Delta L^{ion}/\lambda$ where ΔL^{ion} is the change in optical path length due to ionospheric refraction. It can be expressed as:

$$\Delta L^{ion} = \int_{source}^{telescope} n ds - \int_s^t ds_0 = \int_s^t (n-1) ds_0 + \left[\int_s^t n ds - \int_s^t n ds_0 \right] \quad (9)$$

where ds is a path element along the (curved) ray path and ds_0 is a path element along a straight line between source and telescope. It can be shown that the term in brackets on the right hand side of (9), which represents a correction for the bending of the ray, is proportional to $(n-1)^2$, if n is close to unity. As $n \approx 1$, this term goes to zero. We will neglect the term and thus use the straight line approximation (Weenink 1987, van Veldhoven 1990). Now, from (7), (8) and (9):

$$\phi^{ion} = \frac{2\pi}{\lambda} \Delta L^{ion} = \frac{2\pi}{\lambda} \int_s^t (n-1) ds_0 = \frac{-e^2}{4\pi m_e \epsilon_0 f c} \int_s^t N_e ds_0 \quad (10)$$

We refer to the integral $\int N_e ds_0$ as *TEC*, which stands for Total Electron Content. This definition of *TEC* is called *slant TEC* by some workers in the field, indicating that it is

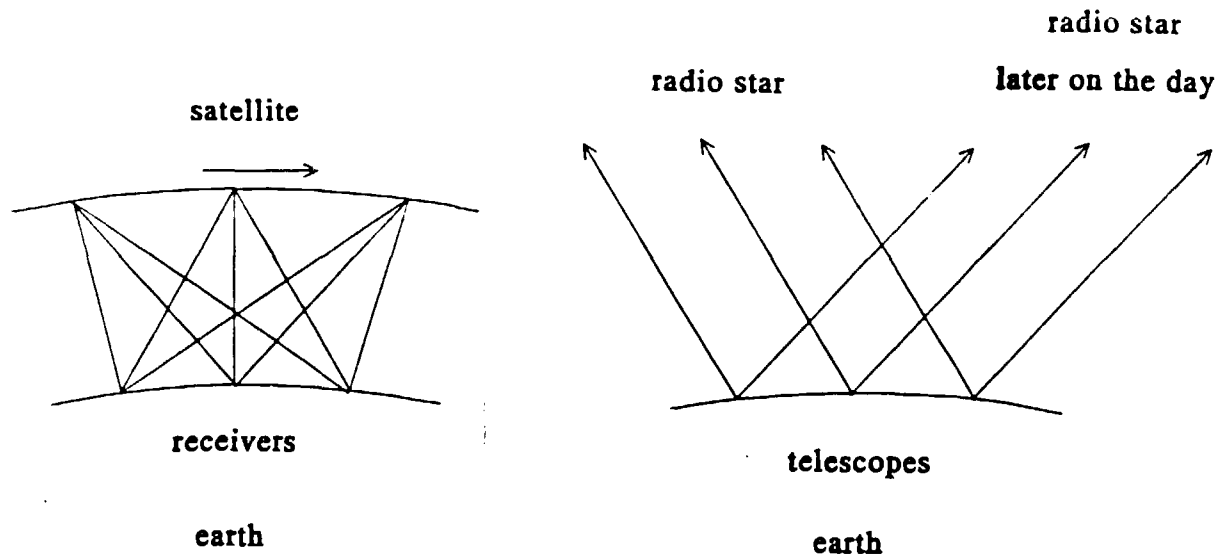


Figure 2: A: The geometry of satellite ray tomography. B: The geometry of the proposed radio telescope tomography. The lines of sight are drawn. Along these lines the electron density is integrated to obtain the Total Electron Content (*TEC*).

not the *TEC* value for a line of sight through the zenith (*vertical TEC*). *TEC* is a column density. At moderate latitudes it is of the order of $TEC \approx 10^{17}$ el m^{-2} , which gives, at $f = 150$ MHz, $\Delta L^{ion} = -178$ m.

While calibrating, the observer measures $\Delta\phi_{ij}^{ion}$, which gives ΔTEC_{ij} . The observer thus samples the gradient of *TEC* over the baseline: $\frac{dTEC}{dB}$. These measurements are carried out a few times a day and the data are stored. This forms a good data base for ionospheric research. The Westerbork Synthesis Radio Telescope data base has been used for this purpose by Spoelstra (eg Spoelstra 1992) and van Veldhoven (1990). An example of its use in tropospheric research is found in Hamaker (1978).

Austen *et al.* (1986) have suggested to use *TEC* data obtained by beacon satellite measurements for ionospheric tomography. Since then, many researchers have worked on this. The idea is that an orbiting satellite is tracked by ~ 5 receivers placed along the projection of the orbit on the ground. Orbit and receivers lie in a plane. The receivers produce *TEC* data along many intersecting lines in this plane. These *TEC* data are used for tomographic inversion to obtain a map of the electron density in the plane. See figure 2A.

This form of ionospheric tomography is very promising, we name some preliminary experiments: Andreeva *et al.* 1990, Pryse *et al.* 1992, 1993, Raymund *et al.* 1993.

In addition, many model calculations for these experiments have been made. See for example: Austen *et al.* 1986, 1988, 1990, Raymund *et al.* 1990, 1992, Yeh *et al.* 1991, Afraimovich *et al.* 1992, Terekhov 1992, Fremouw *et al.* 1992.

Spoelstra (1991) and Kunitsyn *et al.* (1992) have suggested to use *TEC* data from radio telescope calibrations for ionospheric tomography. The orbiting satellite is replaced by a cosmic source moving in the sky by the rotation of the earth. The satellite receivers are replaced by spaced radio telescopes. See figure 2B. Whether the idea of ionospheric tomography with radio telescopes is feasible, is the question of this paper.

2 The possibilities

We could think of three experimental set ups for ionospheric tomography with radio telescopes. Before we mention them it is necessary to explain some jargon. An array radio telescopes is the instrument we explained in section 1. The technique is called (local) interferometry. The use of data from different radio observatories over the world, allows the astronomer to increase the length of the baselines, and hence the resolution. This is called Very Long Baseline Interferometry (VLBI).

There are basically two kinds of tomography: ray tomography and diffraction tomography. The distinction depends on the propagation of the probing waves through the material that is being imaged. If the geometrical optics approximation is valid, the idea of a ray path is sound and the researcher is employing ray tomography (figure 2). If the geometrical optics approximation is not valid (diffraction on small scale irregularities, physical optics) he is doing diffraction tomography.

These are the three set ups:

1. Ray tomography with an array of radio telescopes (local interferometry).
2. Ray tomography with telescopes at large mutual distances (VLBI).
3. Diffraction tomography with an array of radio telescopes.

2.1 Ray tomography with an array

Let's consider the largest array in the world: the VLA (Very Large Array) in New Mexico, USA. The maximum separation between two telescopes is about 30 km. At an altitude of 300 km, the region of maximum electron density, the ray paths make a maximum angle of about $\frac{30}{300} = 0.1$ rad, or 6° . For complete angular coverage 180° is needed. Six degrees angular coverage is not limited angle tomography, it is unlimited fantasy tomography.

Well, let's put the telescopes further apart and try again.

2.2 Ray tomography with VLBI

If all ray paths lie in a plane we need only a few telescopes, just as we need only a few (3-5) receivers in satellite tomography: reconstruction of electron density in a plane, 2D tomography, is easier than reconstruction in a volume, 3D tomography. All lines of sight lie on a surface if telescopes at the same latitude b (ie. along an east-west line) track a cosmic source above the equator, declination $\delta = 0^\circ$. This is clear from figure 3, where the traces of cosmic sources through the ionosphere are indicated. In this case all ray paths

lie on a surface defined by lines of constant latitude at a certain altitude. An observer at latitude b sees this surface as an imaginary arc across the sky: the trajectory of a star above the equator.

For good angular coverage the telescopes have to be placed far apart. This condition was not met in section 2.1. This condition can be met with the European VLBI Network (EVN). Three observatories of EVN are at nearly the same latitude, $b \approx 53^\circ$ N. These telescopes are: Jodrell Bank (England, $53^\circ 6'$ N; $2^\circ 18'$ W), Westerbork (the Netherlands, $52^\circ 54'$ N; $6^\circ 36'$ E) and Toruń (Poland, $53^\circ 6'$ N; $18^\circ 36'$ E). See figure 3B. The separation between the observatories in Poland and England is about 21° . At this latitude and at an altitude of 300 km, the ray paths make a maximum angle of 133° , which is quite satisfactory. However, VLBI data do not allow tomography for the following two reasons.

It takes a source above the equator exactly 12 hours to go from horizon to horizon. This entire time span is necessary to carry out the measurements needed for the whole of the map. One cannot use a quarter of the time to make a quarter of the map with the same resolution. In these 12 hours the ionospheric electron density will vary enormously, making the image worthless.

Apart from this, there is a more fundamental problem. In the section 1, we have seen that one measures the differences in TEC along the various lines of sight. As a consequence there is an unknown offset in the absolute value of TEC . For tomography one needs the value of TEC , not its gradient. In satellite tomography there is also an unknown offset in TEC , but this offset is constant. In radio telescope tomography it changes constantly and in a random way. This difference is caused by the nature of the sources. The carrier wave transmitted by a satellite is coherent in time. In contrast, a cosmic source is not coherent in time. It emits just noise (Remark that this is opposed to the assumption from section 1 that the radiation be monochromatic. Pulsars are coherent in time, but they are very weak.) The consequence of this incoherence is that in radio telescope tomography we end up with too few independent data points to do tomography.

This problem can also be explained from a different point of view. One wants to measure the phase shift introduced by the ionosphere. In order to do this, one needs to know the unperturbed phase, which one doesn't. This could be overcome, if the unperturbed phase would change in a predictable manner. But it doesn't, because a cosmic source is incoherent in time.

2.3 Diffraction tomography with an array

In the case of diffraction, radiation is scattered in all directions and it is no longer possible to confine the radiation to a plane, as we have done above. Keeping the radiation in a plane allows the observer to place the antennas along a line on earth which is in the plane. If radiation is scattered out of this plane into all directions, antennas must also be placed off this line, on a surface of the earth. This requires more equipment, on a more extended area. As the geometry conditions for ray tomography with radio telescopes were not met, this option seems hopeless.

wavelength (cm)	6	21	49	92
frequency range (MHz)	4770-5020	1365-1425	607-610	320-330
Half Power Beam Width α ($^\circ$)	0.17	0.6	1.4	2.6
diffraction tomography parameters (telescopes pointed at zenith):				
maximum altitude H (km)	485	138	59	32
vertical resolution $h = H/5$ (km)	97	28	12	6
horizontal resolution d (m)	144	144	144	144

Table 1: *WSRT observing wavelengths and diffraction tomography parameters*

However, the finite beamsize of the telescopes may allow us to employ a trick, a rudimentary form of diffraction tomography. We consider the possibility that an irregularity inside the antenna beam scatters the radiation from a strong source, which is outside the beam. Radiation is then scattered into the beam. In this configuration we point the telescopes towards a radio silent spot in the sky. Any power on an antenna, means that there is a scatterer in the beam. The position of the scatterer can be deduced from the positions of the telescopes that do register some power and of the telescopes that do not. See figure 4.

We will now give a short description of the Westerbork Synthesis Radio Telescope (WSRT), and we will see how we could use it for the experiment. A more complete description is given by Baars *et al.* (1973). There are four observing wavelengths, see table 1. WSRT consists of 14 telescopes placed along an east-west line, 10 telescopes are fixed and 4 can be moved on rails, see figure 5. All antennas are steerable paraboloids of 25 m diameter. The fixed telescopes (numbered 0-9) are placed at 144 m intervals. Two movable telescopes, named A and B, are positioned close to the fixed telescopes, but we will fix them at 72 and 144 m from telescope 9. Two other movable telescopes (C and D) are over a kilometer away from telescope 9, in the rest of the paper we will disregard these. This leaves us with 12 fixed telescopes. For astronomical purposes, only the fixed-movable telescope pairs are used. The others are called redundant interferometers: if two baselines have the same length and orientation, the interferometers are equivalent, in the absence of an atmosphere. The redundant baselines are used for calibration. In total we have $\frac{1}{2} \times 12 \times 11 = 66$ interferometer pairs, and we use them all. Let's consider figure 4 again. We assume square antenna beam profiles of width α . There is no cosmic source in the beam, so only telescopes 4,5,6 and 7 receive (scattered) radiation. These telescopes are marked +, the telescopes without power in the beam are marked -. The radiation at the telescopes is correlated, on the condition that the scattering process is coherent. Thus only pairs 45,46,47,56,57 and 67 measure nonzero amplitude. All other interferometer pairs give zero amplitude: for example pair 2A (no radiation on either antenna) and pair 26 (uncorrelated). This information fixes the position of the scatterer to within the parallelogram indicated.

If we point the Westerbork telescopes at the zenith, the horizontal resolution would be $d = 144$ m, the distance between two adjacent antennas. The vertical resolution is $h = 288/\sin \alpha$ (metres), small. Localization of a scatterer is possible to a maximum

altitude of $H = 1440 / \sin \alpha = 5h$. See table 1 for the numbers. When the telescopes are pointed at lower elevation, the horizontal resolution deteriorates and the vertical resolution improves. However, the maximum altitude $H = 5h$ then decreases with h . It is clear from table 1 that the vertical resolution h is poor, namely one-fifth of the maximum localization height H . Scattering is most likely to occur at the longest wavelength, in that case $H = 32$ km and $h = 6$ km, this is the neutral atmosphere. Time resolution is the integration time of the instrument, in fact 10-60 seconds.

In principle it is possible to use a man-made emitter, instead of a cosmic source, of which the scattered radiation is received. We have then made a coherent scatter radar.

The set-up we have described needs further study. What kind of atmospheric scatterers are we thinking of: do they exist, are they strong enough, are they coherent? If so, what is the effect of a more realistic beamshape on the localization procedure? Most of all, are there any advantages over conventional radar?

3 Conclusion

From section 2.1 and 2.2 we conclude that ray tomography of the ionosphere with radiotelescopes is impossible. We think that the only way to use radiotelescopes for atmospheric tomography purposes, is to do the crude diffraction tomography experiment from section 2.3.

References

- Afraimovich, E.L., Pirog, O.M., and Terekhov, A.I., 1992, "Diagnostics of large-scale structures of the high-latitude ionosphere based on tomographic treatment of navigation-satellite signals and of data from ionospheric stations", *Journal of Atmospheric and Terrestrial Physics*, **54**, 1265.
- Andreeva, E.S., Galinov, A.V., Kunitsyn, V.E., Mel'nichenko, Yu.A., Tereshchenko, E.D., Filimonov, M.A., and Chernyakov, S.M., 1990. "Radiotomographic reconstruction of ionization dip in the plasma near the earth", *JETP Letters*, **52**, 145.
- Austen, J.R., Franke, S.J., Liu, C.H., and Yeh, K.C., 1986, "Application of computerized tomography techniques to ionospheric research", *International Beacon Satellite Symposium June 9-14 1986, Oulu Finland, Proceedings part 1*, 25-36.
- Austen, J.R., Franke, S.J., and Liu, C.H., 1988, "Ionospheric imaging using computerized tomography", *Radio Science*, **23**, 299.
- Austen, J.R., Raymund, T.D., Liu, C.H., Franke, S.J., Klobuchar, J.A., and Stalker, J., 1990. "Computerized ionospheric tomography", *Ionospheric Effects Symposium, June 1-3 1990*.

Baars, J.W.M., van der Brugge, J.F., Casse, J.L., Hamaker, J.P., Sondaar, L.H., Visser, J.J., and Wellington, K.J., 1973, "The synthesis radio telescope at Westerbork", *Proceedings IEEE*, **61**, 1258.

Fremouw, E.J., and Secan, J.A., 1992, "Application of stochastic inverse theory to ionospheric tomography", *Radio Science*, **27**, 721.

Hamaker, J.P., 1978, "Atmospheric delay fluctuations with scale sizes larger than one kilometer, observed with a radio interferometer array", *Radio Science*, **13**, 873.

Kunitsyn, V.E., and Tereshchenko, E.D., 1992, "Radio tomography of the ionosphere", *IEEE Antennas and Propagation Magazine*, **34**, 22. Also appeared in *The Radioscientist*, **4**, 12.

Pryse, S.E., and Kersley, L., 1992, "A preliminary experimental test of ionospheric tomography", *Journal of Atmospheric and Terrestrial Physics*, **54**, 1007.

Pryse, S.E., Kersley, L., Rice, D.L., Russel, C.D., and Walker, I.K., 1993, "Tomographic imaging of the ionospheric mid-latitude trough", *Annales Geophysicae*, **11**, 144.

Raymund, T.D., Austen, J.R., Franke, S.J., Liu, C.H., Klobuchar, J.A., and Stalker, J., 1990, "Application of computerized tomography to the investigation of ionospheric structures", *Radio Science*, **25**, 771.

Raymund, T.D., 1992, "A review of various techniques for computerized tomographic imaging of the ionosphere", *AGARD Conference Proceedings 502*, 14-1.

Raymund, T.D., Pryse, S.E., Kersley, L., and Heaton, J.A.T., 1993 "Tomographic reconstruction of ionospheric electron density with EISCAT verification", submitted to *Radio Science*.

Spoelstra, T.A.Th., 1991, "Ionosphere and troposphere seen through a radio interferometer", *AGARD Conference Proceedings 502*, 16-1.

Spoelstra, T.A.Th., 1992, "Combining TID observations: NNSS and radio interferometry data", *Journal of Atmospheric and Terrestrial Physics*, **54**, 1185.

Terekhov, A.I., 1992, "Reconstruction of travelling ionospheric disturbances parameters by a tomographic method", *Journal of Atmospheric and Terrestrial Physics*, **54**, 1295.

van Velthoven, P.F.J., 1990, "Medium scale irregularities in the ionospheric electron content". Ph.D. thesis T.U. Eindhoven.

Weenink, M.P.H., 1987, "A new method for the calculation of the phase path in the geometrical optics approximation", *Manuscripta Geodaetica*, **12**, 99.

Yeh, K.C., and Raymund, T.D., 1991, "Limitations of ionospheric imaging by tomography", *Radio Science*, **26**, 1361.

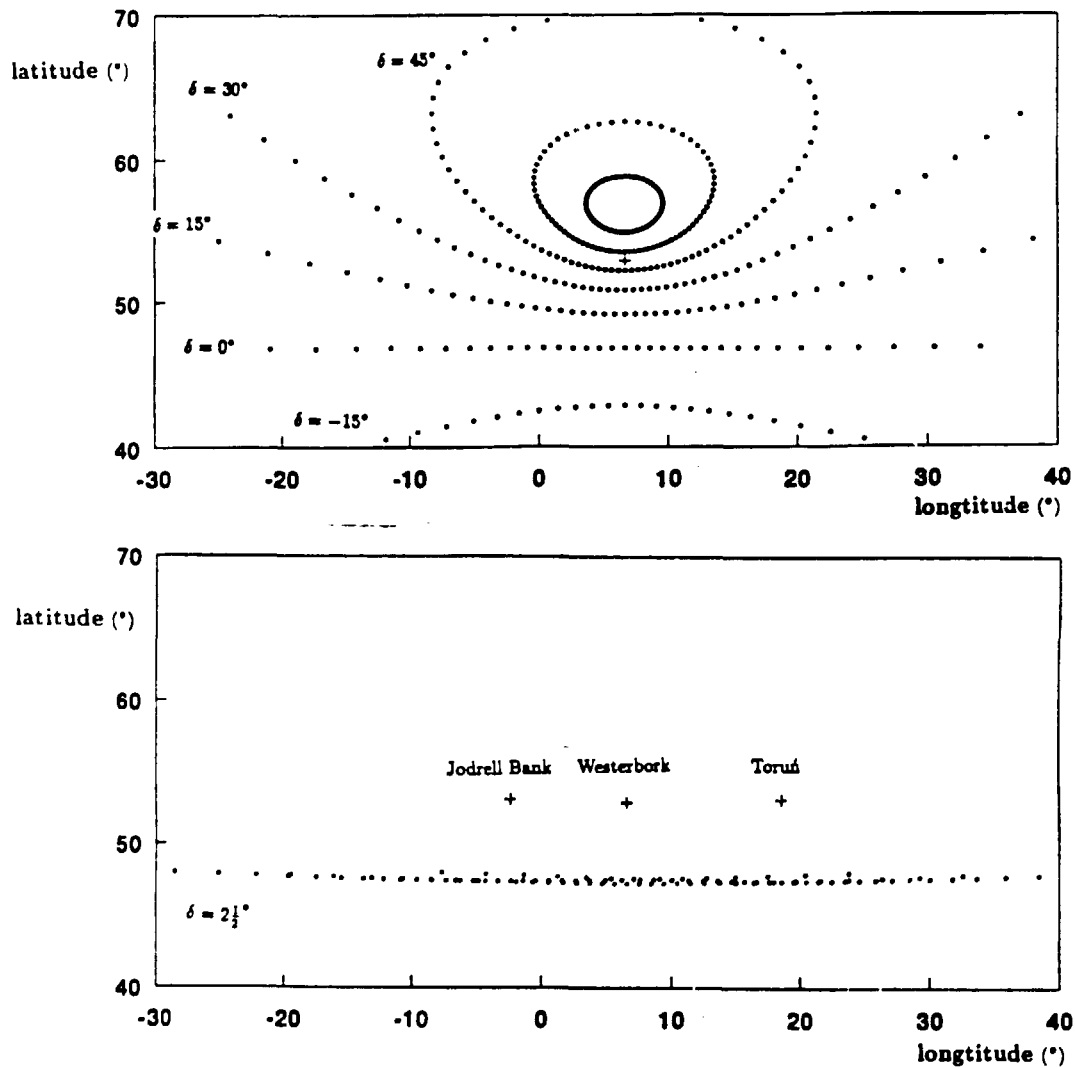


Figure 3: Traces of cosmic sources through the ionosphere at 600 km altitude. + observer, • position of line of sight at 20 min intervals. A: Sources of different declination seen from Westerbork, only sources above the equator have straight traces. B: A calibration source (3C273) just north of the equator seen from three observatories at nearly the same latitude. The traces define a line. Combining these for different altitudes, defines a surface. See text section 2.2.

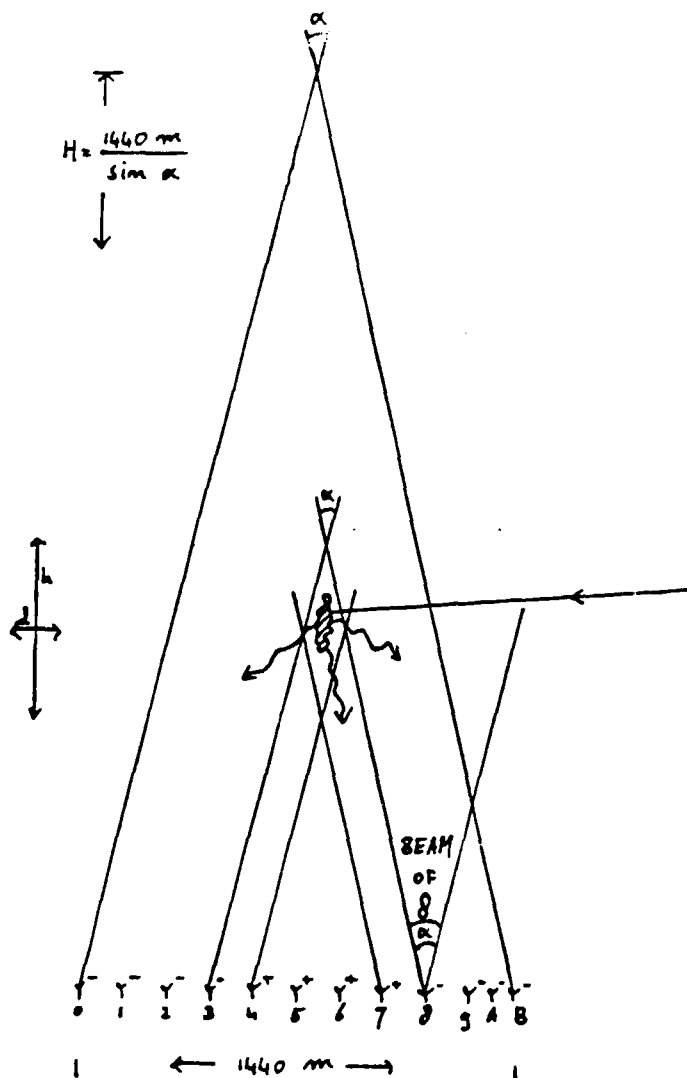


Figure 4: Geometry of crude diffraction tomography experiment with Westerbork Synthesis Radio Telescope. See text section 2.3.

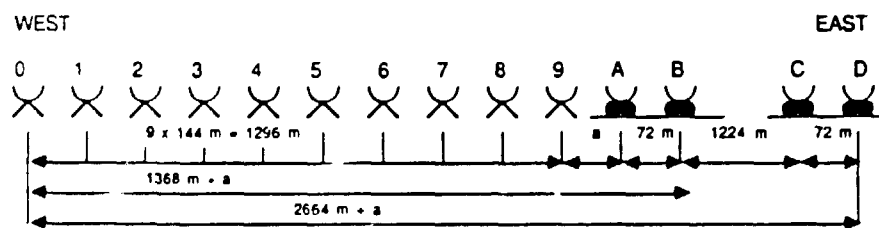


Figure 5: Schematic description of Westerbork Synthesis Radio Telescope. It consists of 10 fixed telescopes at 144 m intervals, and 4 movable telescopes. The separation a lies between 36 and 108 metres. See text section 2.3.

Prospects for 3-D Visualisation

Åke Steen

*Swedish Institute of Space Physics
Kiruna, Sweden*

Abstract

Practical problems are encountered when a three-dimensional time-dependent signal such as the aurora should be displayed and visualised in a way perceivable to human beings. Research on techniques for 3-D displays is ongoing and several directions can be identified, e.g. holographic display techniques, virtual reality.

Mainly based on a report from the Swedish Institute of Optical Research the 3-D visualisation technologies are discussed.

TOMOGRAPHY RECONSTRUCTION OF A 3 D- AURORAL
LUMINOSITY DISTRIBUTION

M.I.Pudovkin, V.N.Troyan, and G.A.Ryzhikov

Abstract

For the reconstruction of auroral luminosity a modified back-projection algorithm including the information sensitivity of tomographic experiment is suggested. The back projection algorithm is based upon tomographic functionals containing the photometric factors. This algorithm allows to obtain the reconstruction of auroral luminosity.

To test the algorithm proposed for solving the problem of calculating the 3D spatial distribution of auroral luminosity according to the data from a network of ground based all-sky cameras, there was constructed a series of simulated "all-sky films". For this purpose, some artificial auroral homogeneous and rayed arcs were modelled.

Then model all-sky images of the arc were calculated for a network of "cameras" by integrating the luminosity of the light sources along sight beams radiating from the camera sites under various zenith and azimuth angles with the angle resolution $\Delta \theta = \Delta \varphi = 5^\circ$.

Comparison of the original and reconstructed distributions of the "auroral" luminosity has shown their reasonable agreement.

TOMOGRAPHY RECONSTRUCTION OF 3D - AURORAL LUMINOSITY DISTRIBUTION

M.I.Pudovkin, V.N.Troyan, G.A.Ryshikov

Institute of Physics, University of St.Petersburg,
St.Petersburg, Petrodvorets 198904, Russia

1. Introduction

For the reconstruction of three dimensional auroral distribution we suggest to use a modification of back projection algorithm of tomographic inversion (Ryzhikov and Troyan, 1988, 1992). The algorithm takes into account the main features of the experimental data such as ALIS (Auroral Large Imaging System), that is a ground-based optical system (Steen, 1990). The suggested algorithm contains three main steps:

1. The reconstruction of the three dimensional auroral distribution by the modified RT-back projection tomographic algorithm (the first approximation of 3-D distribution of auroral emission).

2. Detection and parametrization of the luminosity are by using pattern recognition methods and spline approximation.

3. The reconstruction of the true luminosity distribution correcting the first step estimation.

Another setting of the problem consists of the reconstruction of the precipitating particle energy spectrum from the spectroscopic data. This problem does not need obtaining the luminosity distribution as an intermediate step of the inverse problem solution. In this case we have to use the physical

model of the interaction of precipitating particles with the Earth atmosphere. However, this approach is not considered in this paper.

2. Model of measurement

Let the experimental data be represented by the function $u \in R^n$, where index n corresponds to the number of digital data from all stations. The aim of tomographic methods is to reconstruct the unknown spatial auroral emission source distribution from sets of experimental observations u . The general equation of measured data is the linear operator equation containing the additive noise ε :

$$\begin{aligned} u_1 &= P_1 \psi + \varepsilon_1 \\ u_2 &= P_2 \psi + \varepsilon_2 \\ &\dots \\ u_n &= P_n \psi + \varepsilon_n \end{aligned} \quad (1)$$

where P is the projection operator, ψ is the unknown auroral emission distribution which we want to reconstruct:

$$P_i(\cdot) = \int_{V_{\vec{e}_i}} d\Omega dr A_{\vec{e}_i}(y, \theta) e^{-\lambda(\omega)|\vec{r}-\vec{r}'|} \frac{1}{|\vec{r}-\vec{r}'|^2}(\cdot)$$

$d\Omega$ is the solid angle spanned by a pixel and λ is the atmospherical attenuation. In our numerical experiments the attenuation is neglected. The function $A_{\vec{e}_i}$ corresponds to the aperture of the observation camera. We assume also that the noise ε is described by the normal distribution law with the known mathematical expectation being equal to zero and covariance matrix K_ε :

$$\varepsilon \sim N(0, K_\varepsilon)$$

So the tomography experiment is determined by the mapping of the functional space Ψ into the Euclidian measurement space R^N . Hence the ray tomography inverse problem dealing with the finite set of data is the essentially ill-posed one, even in the case when the noise ε tends to zero (Ryzhikov and Troyan, 1988).

3. Reconstruction algorithm

For the reconstruction of 3-D auroral distribution we use the modification of back projection algorithm

$$\psi^l = \frac{\langle u | u^l \rangle}{I_{(s)}^l + \gamma} = \frac{\sum_{i=1}^N u_i u_i^l}{I_{(s)}^l + \gamma}$$

where $\langle u | u^l \rangle = P | l \rangle$, l is a functional, f.e. it is the mean value of the unknown field ψ in the vicinity of the point $\hat{r}(\hat{x}, \hat{y}, \hat{z})$.

$$l_{\hat{r}} = \frac{1}{abc} H\left[\frac{a}{2} - |x - \hat{x}|\right] H\left[\frac{b}{2} - |y - \hat{y}|\right] H\left[\frac{c}{2} - |z - \hat{z}|\right]$$

where $H = \begin{cases} 1 & x \geq 0 \\ 0 & x < 0 \end{cases}$

Then

$$u_i^l = \int_{V_{\hat{r}_i}} dr d\Omega A_{\hat{r}_i}(\theta, \varphi) e^{-\lambda |\vec{r} - \hat{r}|} \frac{1}{|\vec{r} - \hat{r}|^2} l_{\hat{r}}(\vec{r})$$

is a parameter of regularization. We have suggested the notion of information sensitivity. In particular, we use the information sensitivity of the observation field u with respect to a linear functional $l_{\hat{r}}$ of the field of the emission distribution. The information sensitivity is the measure of the variability of the information contained in the experimental data with respect to desired linear functional. This

measure allows us to take into account the different contribution of the spatial variations to measured data.

Mathematically the information sensitivity is determined by the limit of the derivative with respect to α (the signal/noise ratio) with α tending to zero from the Shannon information $I_\alpha(l/u)$ (Ryzhikov and Troyan, 1992):

$$I_{(s)}^l = \lim_{\alpha \rightarrow 0} \frac{\partial}{\partial \alpha} I_\alpha(l/u)$$

where
$$I(l/u) = \frac{1}{2} \ln \frac{E_{apr}[l(\delta\psi)]^2}{E_{apost}[l(\delta\psi)]^2}$$

$$\delta\psi = \psi' - \psi_{true}$$

$$I_{(s)}^l = \frac{1}{2} \frac{\langle l | P^* P | l \rangle_{R^n}}{\langle l | l \rangle_{L^2}}$$

This algorithm has given excellent results in seismic diffraction tomography in which there is used a lot of input data for the reconstruction of the medium imaging.

3.1. Detection and parametrization of the luminosity arc.

The second step is ment to detect the aurora arc line. Assuming that the shape of arc line is independent of the height we may use the correlation between slices for the estimation of the arc line.

3.2. The reconstruction of true luminosity distribution.

The second step provides us the possibility of basis function choice to carry out parametrization of the inverse problem. The main equation in this case can be written as

$$u = P \sum_{j=1}^J \sum_{k=1}^K \beta_k \xi_k(s_z(x,y), d_s, \Delta z_j) + \varepsilon$$

where basis function

$$\xi_k = \cos\left(2\pi k \frac{d_s}{D_s}\right)$$

$j = 1, \dots, J$ is the number of slices and z is the coordinate

$$\hat{\beta} = \arg \inf E \|u - P\Psi\beta\|^2$$

$$\hat{\beta} = (\Psi^* P^* K_\varepsilon^{-1} P \Psi + K_\beta^{-1})^{-1} \Psi^* P^* K_\varepsilon^{-1} u$$

if the operators K_ε^{-1} , K_β^{-1} exist.

We may write the solution in the equivalent form:

$$\hat{\beta} = K_\beta \Psi^* P^* (P \Psi K_\beta \Psi^* P^* + K_\varepsilon)^{-1} u$$

Covariance matrix of the estimate is $\hat{K}_\beta = E(\beta - \hat{\beta})(\beta - \hat{\beta})^*$

$$\hat{K}_\beta = (\Psi^* P^* K_\varepsilon^{-1} P \Psi + K_\beta^{-1})^{-1}$$

4. The numerical experiments

The algorithm proposed was tested by solving the inverse problem for some model distributions of the auroral luminosity. For this purpose there were constructed some artificial "auroral" bands; then "all-sky" images of those bands were constructed for a net-work of all-sky cameras, and, finally, those images were used for reconstruction of the original luminosity distribution.

Let us consider these models in more detail, and analyze results of the solution of the inverse problem.

Model I.

The relative disposition of the model auroral arc and of the net-work of "all-sky" cameras corresponding to that in the ALIS project is shown in Fig.1. As is seen from the Figure, the model arc is spiral-shaped, and it is located mostly within the area of the "cameras", which provides favour-

able conditions for solving the inverse problem, and only the most western part of the arc is situated outside that region. The maximum of the luminosity is supposed at the altitude $h_0 = 105$ km; above this level the luminosity decreases as $\exp(-\frac{h-h_0}{50})$, and below this level as $\exp(-\frac{h_0-h}{5})$. Concerning the luminosity distribution in the horizontal plane, it is supposed to be weakly inhomogeneous as is shown in Figure 2a and 3a for altitudes 105 km and 120 km correspondingly.

Images of the model auroral arc under consideration were calculated by integrating the luminosity along sight beams radiating from the camera sites; angular resolution in our calculations equaled $\Delta \theta = \Delta \varphi = 5$ degrees.

Results of the solution of the inverse problem are presented in Fig. 2 b and 3 b, where the reconstructed distributions of the luminosity are shown for the same altitudes as in Fig. 2a and 3a.

Having compared Figure 2b and 2a, one can see that

a) Location of the auroral form under consideration as well as its outlines are reconstructed reasonable well. At the same time, the following characteristic misrepresentation may be noticed in Fig. 2b; segments of the auroral band situated outside the area of "camera" turn to be shifted towards the centre of that area with respect to their real position.

b) The maximum intensity of the auroral luminosity is obtained with accuracy of about 15 per cent. However, the distribution of the luminosity across the band noticeably differs from that supposed by the model. In particular, the intensity of the reconstructed luminosity decreases to the centre of the band curvature much slower than in the model;

this results in appearance of a vast area of false luminiscence within the region outlined by the band. On the other hand, the transversal gradient of the calculated luminosity in the vicinity of the outer edge of the band is close to the model one.

Turning to the data for the altitude $h = 120$ km, one can see the main features of the solution discussed above to be preserved; at the same time, the spatial displacement of the reconstructed band segments situated outside the camera regions seems to disappear in the last case.

Model II.

In this model the auroral band presented in the previous section is supposed to have the rayed structure. The "rays" are modelled by vertical cylinders; the height distribution of the luminosity in the rays is supposed to be the same as described above; besides, the luminosity of a "ray" decreases with the distance from the axis of the cylinder as $\exp(-r^2/10^2)$. The resulting luminosity distribution at the horizontal planes at altitudes $h = 105$ km and 120 km are shown in Figure 4 a and 5 a. Results of the solution of the inverse problem for the height $h = 105$ km is shown in Fig. 4b. As is seen from the Figure, the main features of the auroral band (the outlines of the latter, the maximum intensity) are reconstructed in the same manner as in Fig. 2 b, and with the same defects. Concerning the rayed structure of the band, it is distinguishable though with some difficulties caused by the appearance of numerous false maxima of the luminosity.

The reconstructed luminosity distribution at the altitude $h = 120$ km is shown in Fig. 5 b. And once again, one can see that the agreement of the original and reconstructed distri-

butions of the luminosity at the height $h = 120$ km is significantly better than at the height $h = 105$ km; false maxima of the luminosity have almost disappeared, and all the "rays" may be surely distinguished.

The last result may be explained by that the algorithm used in our calculations was originally destined for search of greatly localized sources. The diameter of the "rays" in the model under consideration was supposed to be unchangeable with height, so that the apparent size of the luminosity sources decreased with the height providing better conditions for the solution.

5. Conclusions

The first results of testing the algorithm discussed above have shown a sufficiently high spatial resolution of the solution and the principal possibility of application of that algorithm for the reconstruction of the auroral luminosity distribution using the data from a network of ground-based all-sky cameras.

At the same time, one can see from the data presented above that the solution obtained by means of the algorithm proposed is attended by a series of defects which have to be eliminated. Thus, this version of the algorithm may be considered as the first one, and it needs an essential improvement.

Acknowledgements: We are greatly thankful to Dr. Å. Steen for stimulation of this work.

References

- Ryshikov, G.A., and Troyan, V.N. (1988) The solution of inverse dynamic seismic problem for 3-dimensional inhomogeneous media. *Rev. de Geofisica*, 44, p.53-59.
- Ryzhikov, G.A., and Troyan, V.N. (1992) 3-D diffraction tomography. *Proc. of 2-nd Russian-Norv. seminar, 2-9 May, 1992. Bergen, p.185-199.*
- Steen, Å. (1990) A scientific and technical description of ALIS. *Proc. NSSR Annual Meet. Bolkesjø, Norway, 12-14 November, p.153-164.*

FIGURE CAPTIONS

Fig.1. A scheme of the disposition of the model "auroral band" and of the "all-sky cameras".

Fig.2. Isolines of the model "auroral band" at horizontal planes (Model I):

a - h = 105 km;

b - h = 120 km.

Fig.3. Isolines of calculated for model I "auroral luminosity":

a - h = 105 km;

b - h = 120 km.

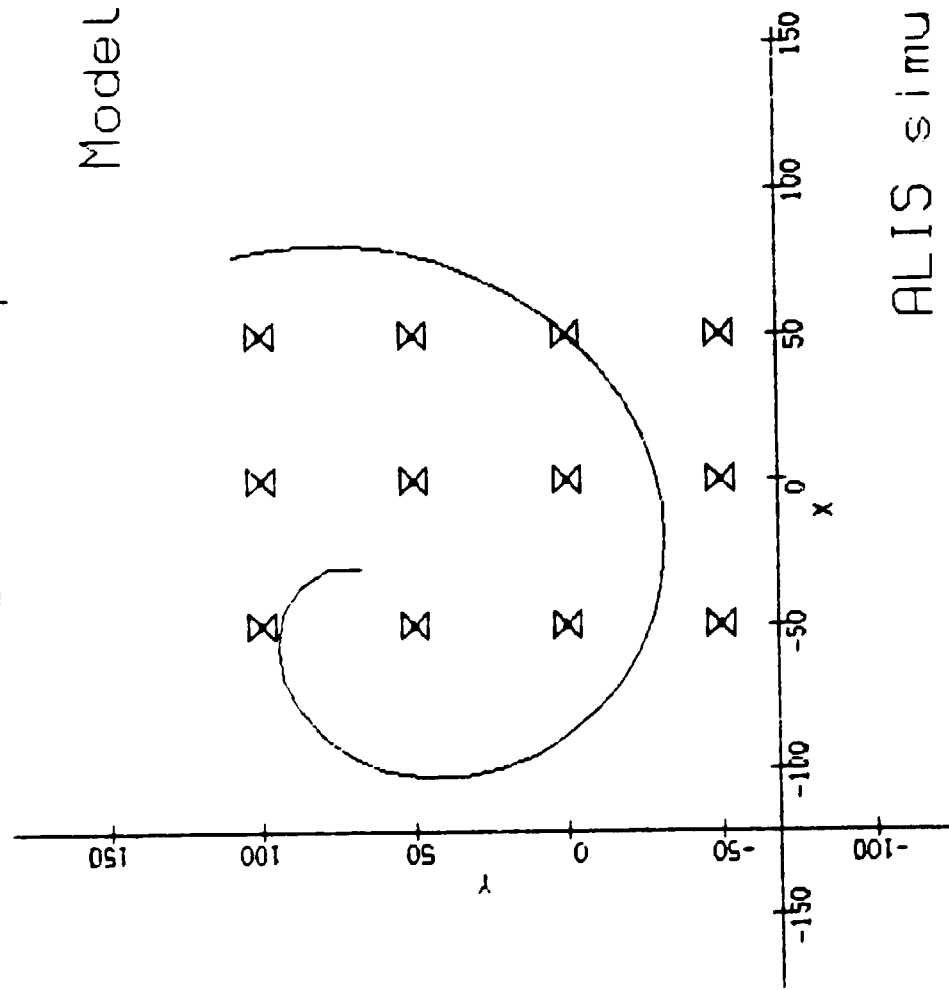
Fig.4. The same as in Fig. 2 for Model 2.

Fig.5. The same as in Fig. 3 for Model 2.

Geometry of ALIS experiment

Model 1 of auroral arc

$z = 105 \text{ km}$

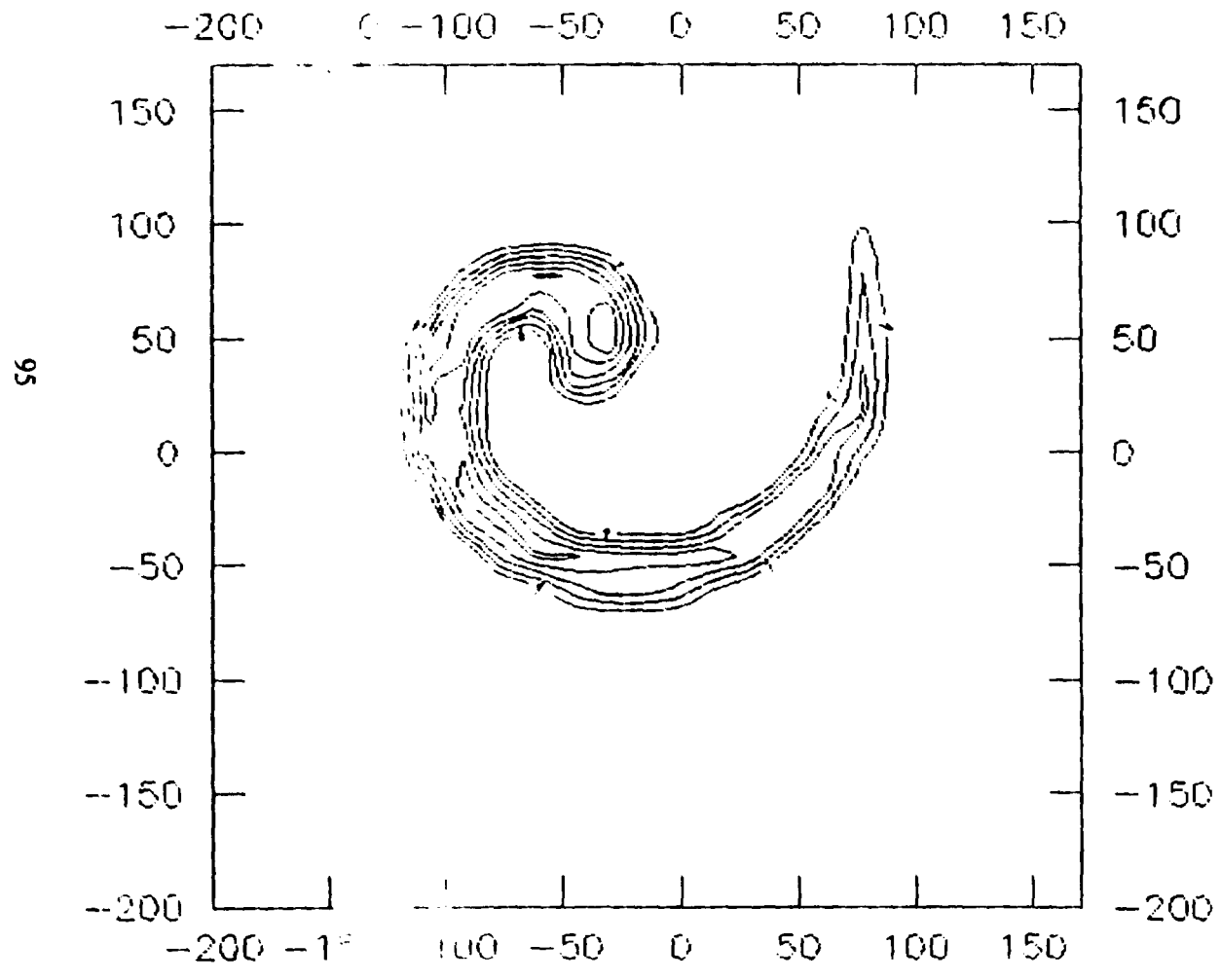


ALIS simulated

Fig. 1

auroral model

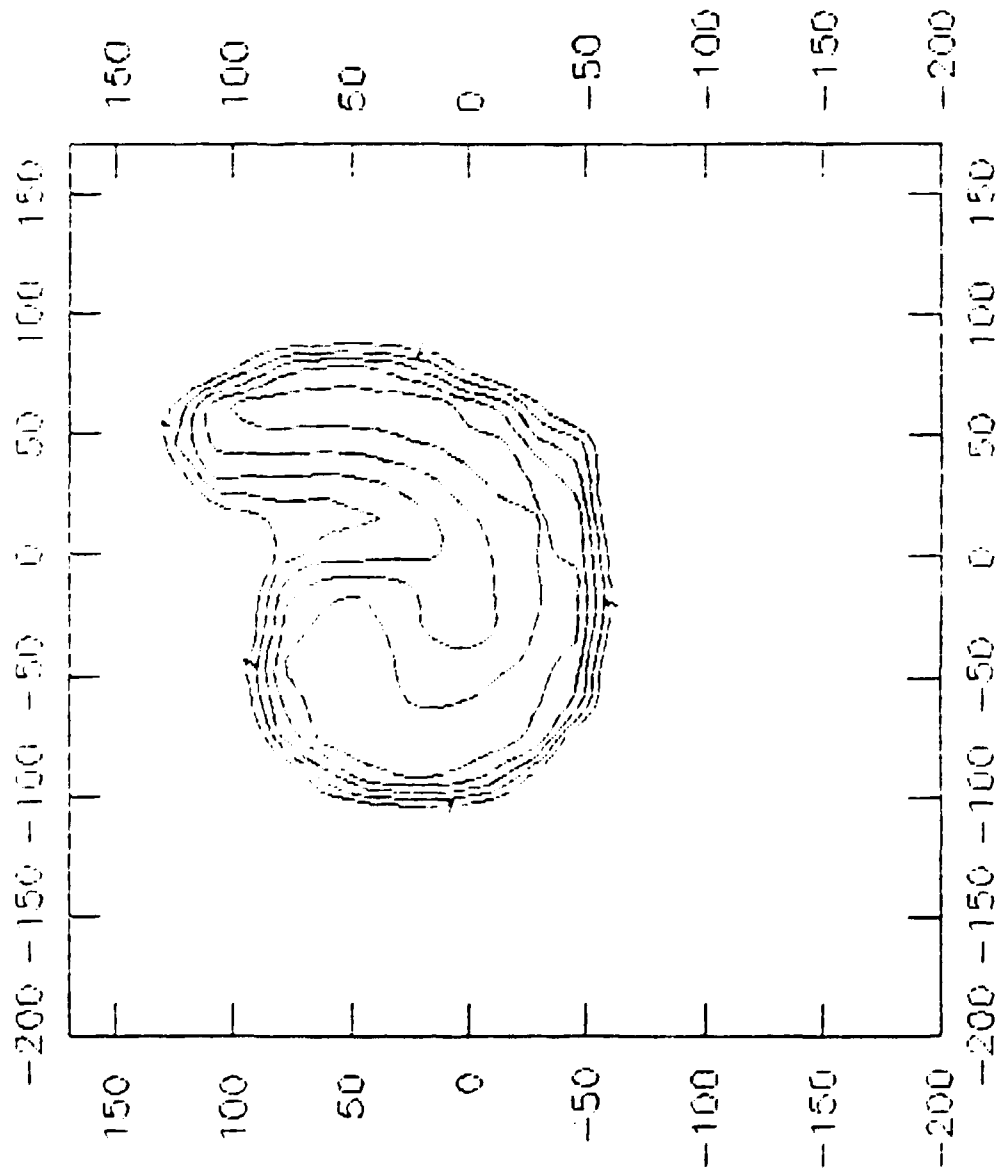
height 105 km



Minimum contour: 1
Maximum contour: 3.852
Contour interval: 0.5

Fig.2a

RT back-projection reconstruction
midcell |
height 105 km



Minimum contour: 1
Maximum contour: 3.47
Contour interval: 0.5

Fig. 2b

The auroral model 1

height 120 km

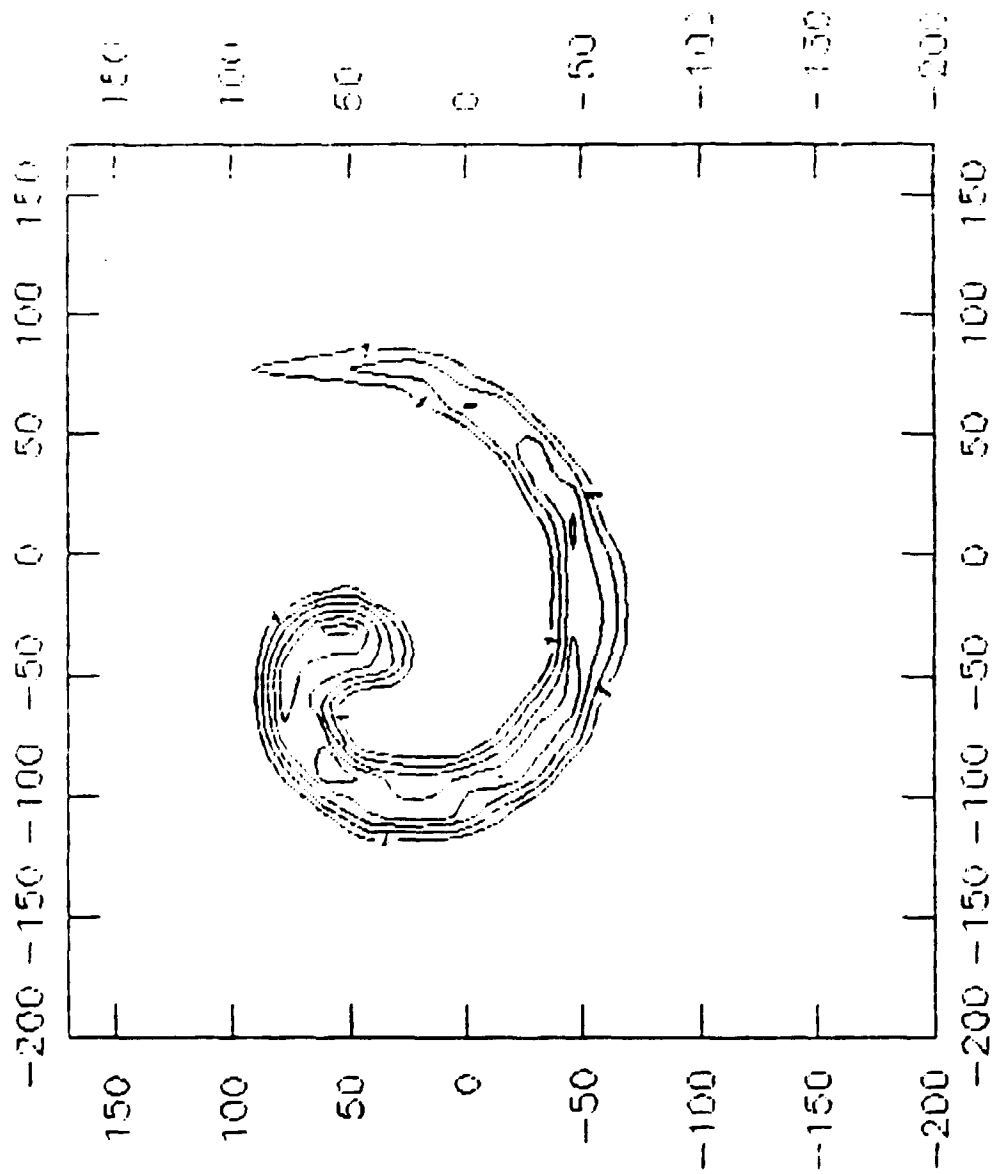


Fig.3a

RT back-projection reconstruction
model 1
height 120 km

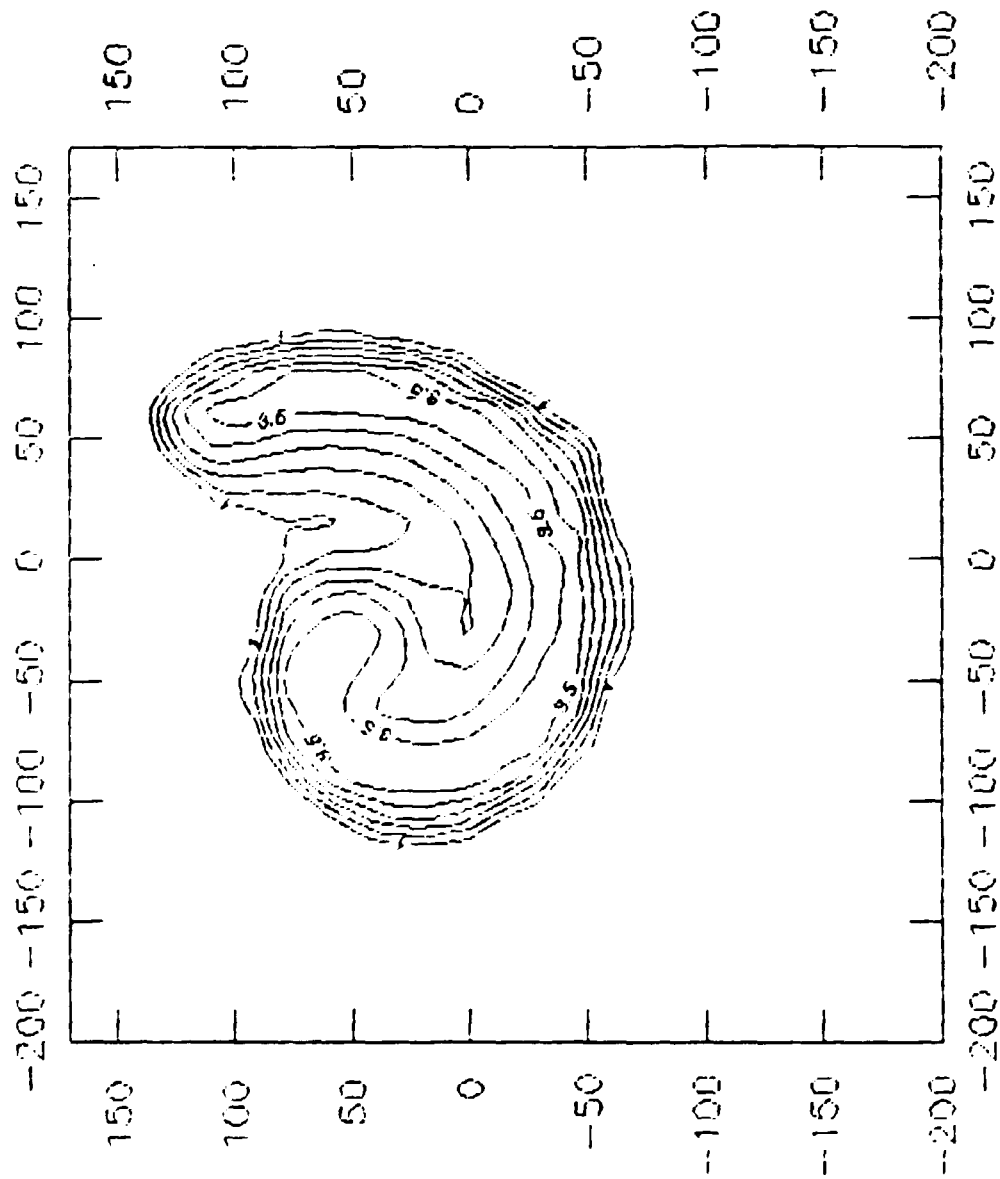


Fig. 3b

The coronal model 2

height 105 km

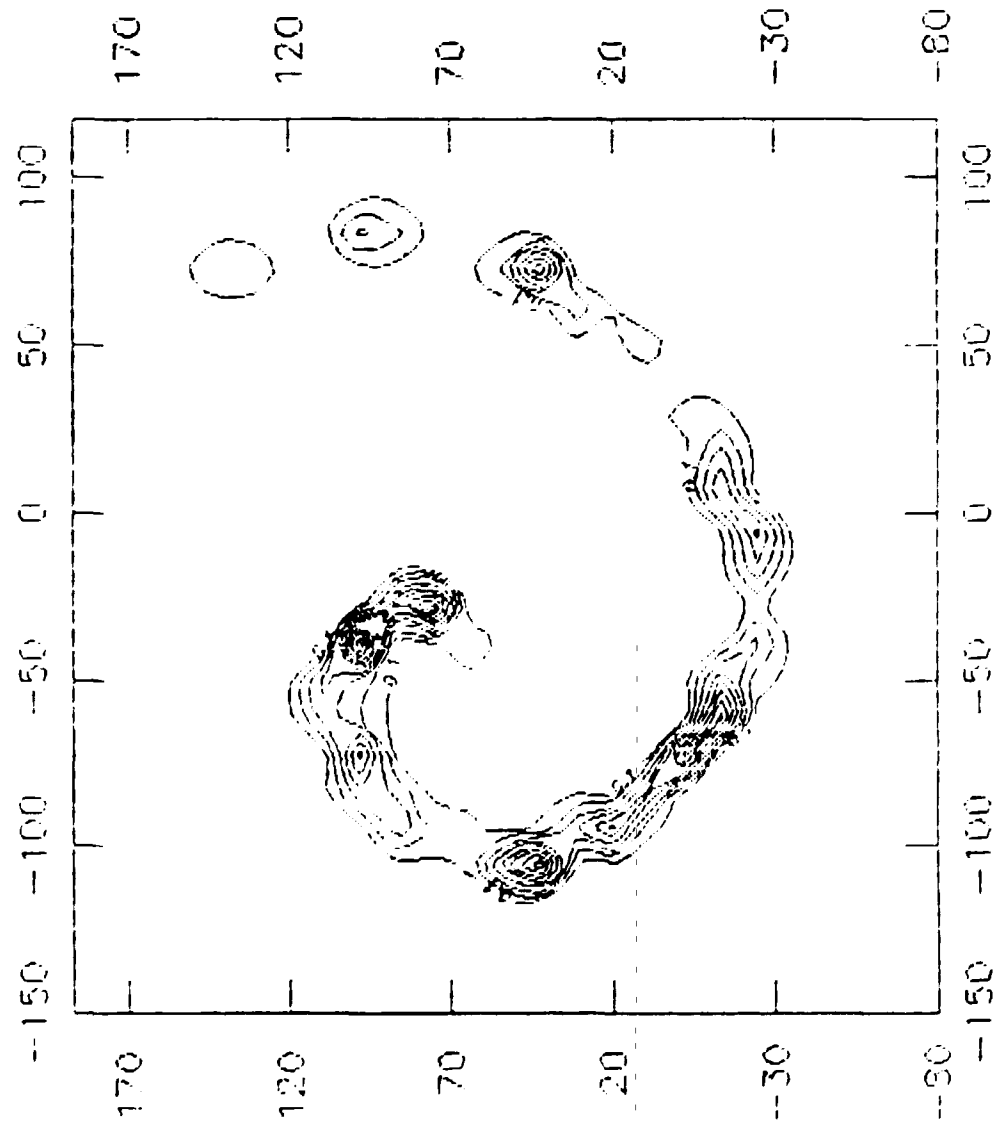
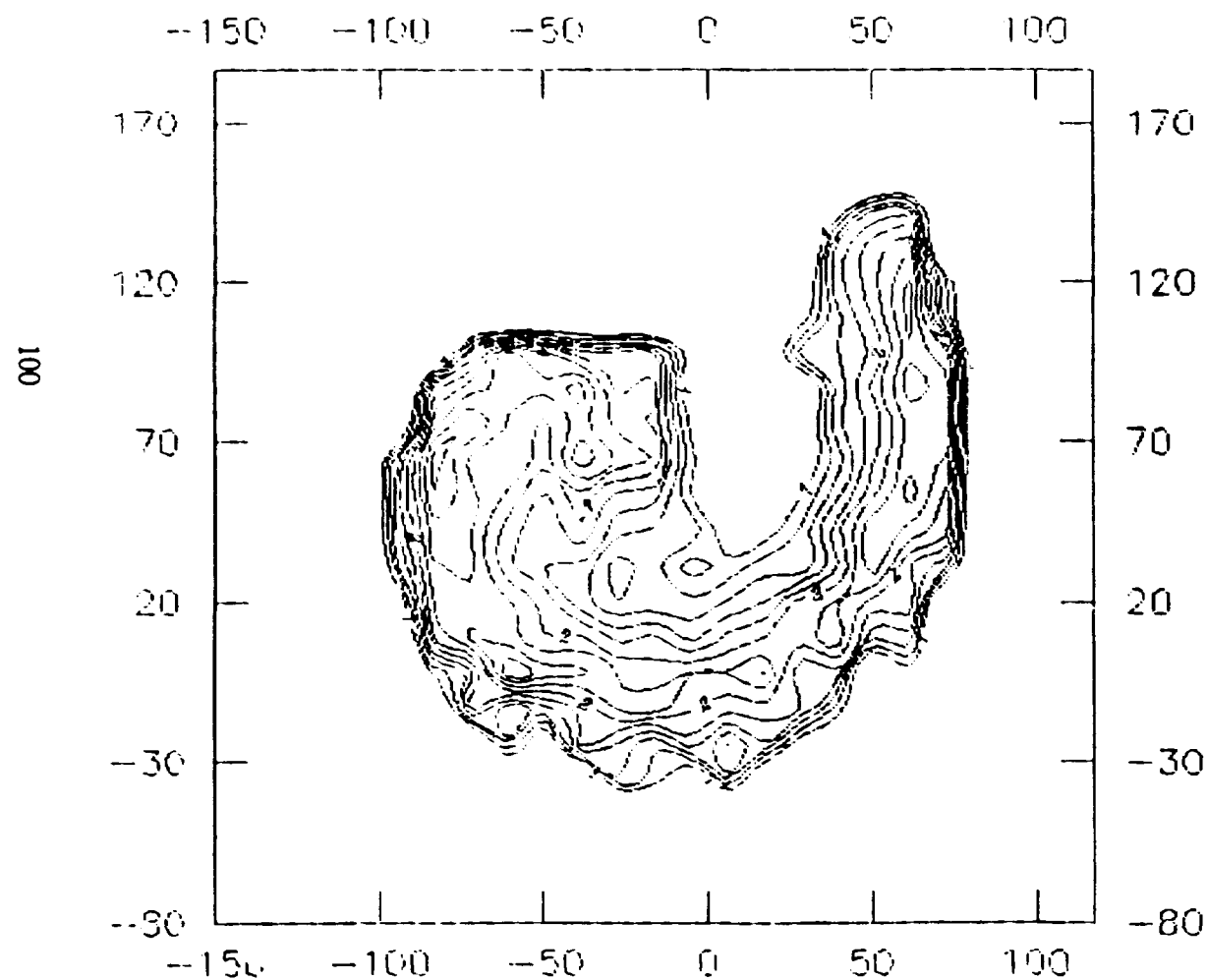


Fig. 4a

RT back-projection reconstruction
model 2
height 105 km

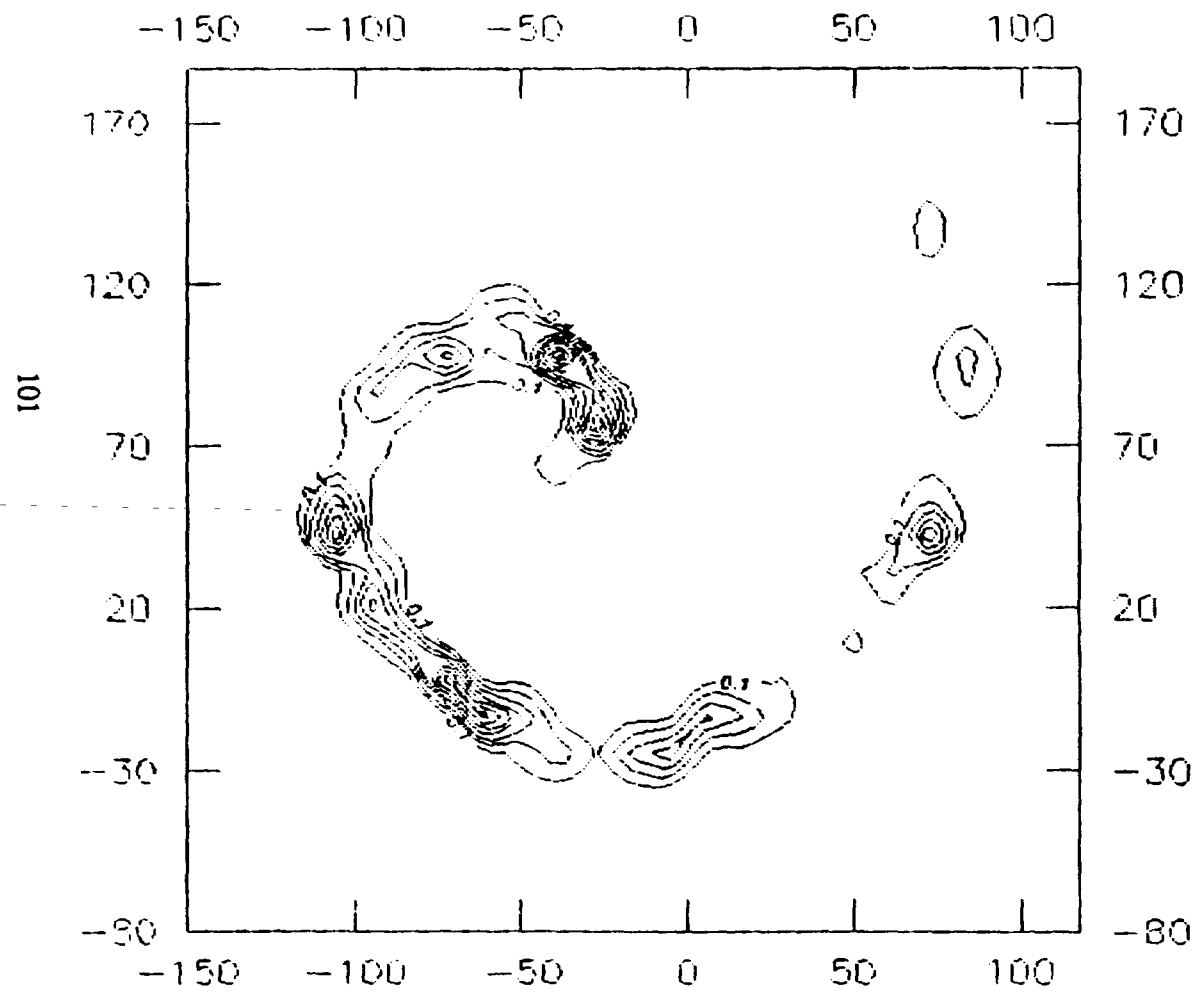


Minimum contour: 1
Maximum contour: 2.935
Contour interval: 0.2

Fig. 4b

The auroral model 2

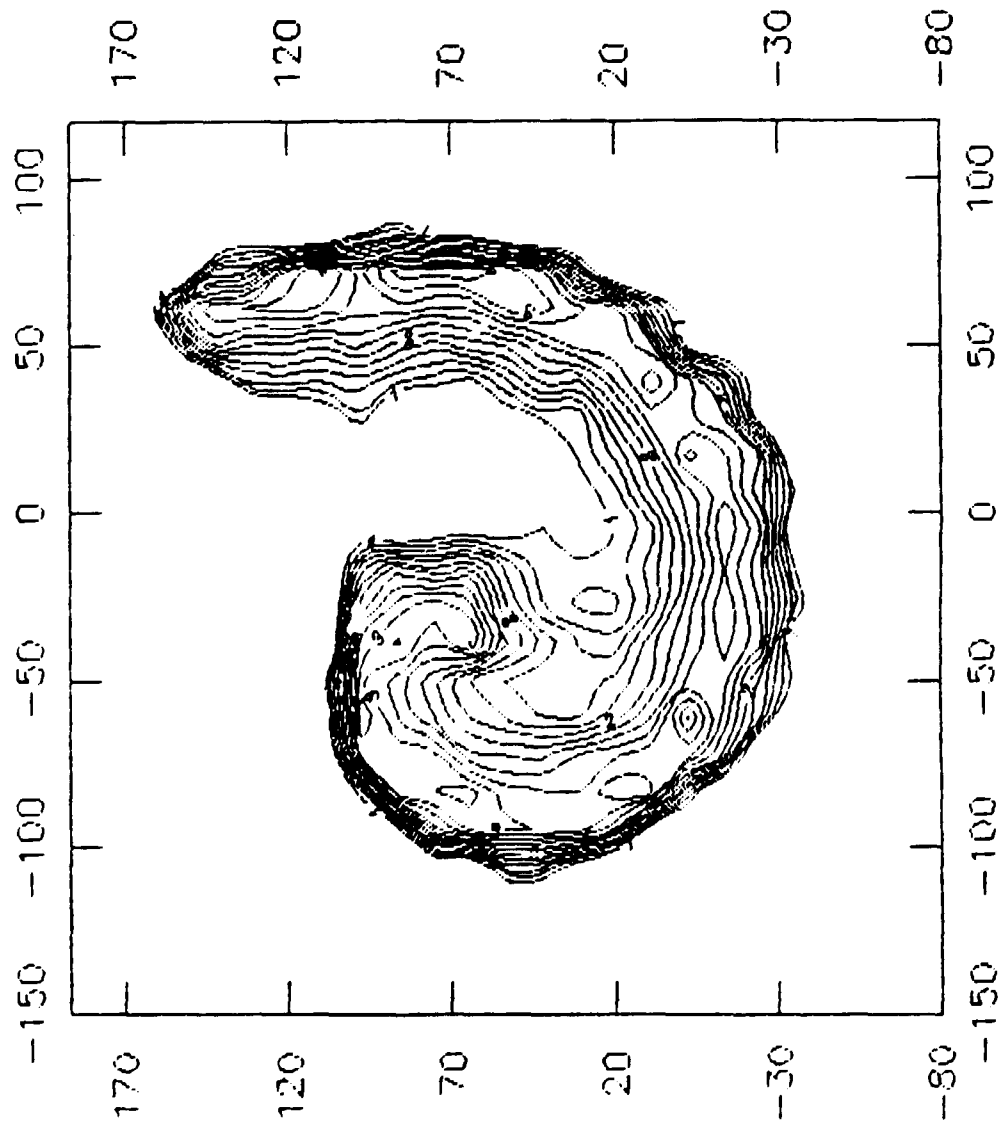
height 120 km



Minimum contour: 0.1
Maximum contour: 2.859
Contour interval: 0.3

Fig.5a

RT back-projection reconstruction
model 2
height 120 km



Minimum contour: 1
Maximum contour: 3.413
Contour interval: 0.2

Fig. 5b

List of participants and addresses

The address list contains names and addresses to participants in the workshop, in addition addresses to colleagues who have indicated interest for inversion techniques with relation to auroral tomography have been included. Non-attendee is marked with *.

NAME	ADDRESS	TEL.	FAX	TELEX E-mail
Alpatov, Victor	Institute of Applied Geophysics, Rostokinskaya st. 9, Moscow 129128, Russia		7-095-288 95 02	<u>411944 ZEMLA SU</u>
Arinin, Vladimir*	All-Russia Research Institute for Experimental Physics in Arzamas-16, P.O. Box 41, Nizhny Novgorod area, 607200, Russia		83130-54-565	<u>151109 ARSA SU</u>
Aso, Takehiko*	Department of Electrical Engineering, Kyoto University, Yoshida Honmachi, Sakyo-ku, Kyoto, 606, Japan	75 7535875	75 751 1576	<u>5422455DEEKYUI</u> aso@abel.kuee.kyoto-u.ac.jp
Brändström, Urban	Swedish Institute of Space Physics, P.O. Box 812, S-981 28 Kiruna, Sweden	980-79126	980-79050	<u>8754 IRFS</u> urban@snake.irf.se
Chemouss, Sergei	Polar Geophysical Institute, Apatity, Murmansk region, 184200, Russia	37135		<u>126150 WL SU</u> root@apgi.murmansk.su
Danielsson, Per-Erik*	Image Processing Lab., Department of Electrical Engineering, Linköping University, S-581 83 Linköping, Sweden	13-281306	13-282599	ped@isy.liu.se
Davydov, V.S.	State Optical Institute, University of St. Petersburg, St. Petersburg, Russia			
Fehmers, Gijs	Technical University Eindhoven, Department of Applied Physics, P.O. Box 513, NL-5600 MB Eindhoven, The Netherlands	3140473461	3140445253	trnigf@urc.tue.nl
Gustavsson, Björn	Swedish Institute of Space Physics, P.O. Box 812, S-981 28 Kiruna, Sweden	980-79000	980-79050	
Kaila, Kari	University of Oulu, Department of Physics, Linnanmaa, SF-90570, Oulu, Finland	358-81-5531367	358-81-5531287	<u>32375 OYLIN SF</u> fys-kk@finou.oulu.fi
Kosarev, Evgeny	P.L. Kapitza Institute for Physical Problems, ul. Kosyigna 2, Moscow 117334, Russia	7-095-1373248	7-095-9382030	kosarev@magnit.msk.su
Oscarsson, Tord	Swedish Institute of Space Physics, Department of Physics, University of Umeå, 901 87 Umeå, Sweden	090-165031	090-165031	oscarsson@tp.umu.se
Pivovarov, Vladimir	Polar Geophysical Institute, Murmansk, Russia			
Pivovarov, Vladimir, V.*	State Optical Institute, University of St. Petersburg, St. Petersburg, Russia		812-3509993	<u>121235 GOI SU</u> vpiv@soi.spb.su
Pudovkin, Mikhail*	Institute of Physics, University of St Petersburg, St. Petersburg, Petrovoret 198904, Russia	812-4287300	812-4286649	<u>121481 LSU SU</u> pudovkin@space.phys.lgu.spb.su
Ryzhikov, G.A.*	Institute of Physics, University of St. Petersburg, St. Petersburg, Petrovoret 198904, Russia			
Steen, Åke	Swedish Institute of Space Physics, P.O. Box 812, S-981 28 Kiruna, Sweden	980-79074	980-79050	<u>8754 IRFS</u> steen@urf.se
Tagirov, Vartan	Polar Geophysical Institute, Apatity, Murmansk region, 184200, Russia	37135		<u>126150 WL SU</u> root@apgi.murmansk.su
Troyan, Vladimir*	Institute of Physics, University of St. Petersburg, St. Petersburg, Petrovoret 198904, Russia	812-4284348	812-4286649	troyan@ldus.phys.lgu.spb.su